

**EVALUATION OF MICELLAR-POLYMER FLOOD PROJECTS IN
A HIGHLY SALINE ENVIRONMENT IN THE EL DORADO FIELD**

**By
Howard H. Ferrell
Robert A. Easterly
Timothy B. Murphy
Jane E. Kennedy**

December 1987

Performed Under Contract No. AC19-85BC10830

**Keplinger Technology Consultants, Inc.
Tulsa, Oklahoma**

**Bartlesville Project Office
U. S. DEPARTMENT OF ENERGY
Bartlesville, Oklahoma**

**FOR THE
FEDERAL
ENERGY
REGULATION
COMMISSION**



DISCLAIMER

This report was prepared as an account of work sponsored by an agency of the United States Government. Neither the United States Government nor any agency thereof, nor any of their employees, makes any warranty, express or implied, or assumes any legal liability or responsibility for the accuracy, completeness, or usefulness of any information, apparatus, product, or process disclosed, or represents that its use would not infringe privately owned rights. Reference herein to any specific commercial product, process, or service by trade name, trademark, manufacturer, or otherwise, does not necessarily constitute or imply its endorsement, recommendation, or favoring by the United States Government or any agency thereof. The views and opinions of authors expressed herein do not necessarily state or reflect those of the United States Government or any agency thereof.

Printed in the United States of America. Available from:
National Technical Information Service
U.S. Department of Commerce
5285 Port Royal Road
Springfield, VA 22161

NTIS price codes
Paper copy: **A07**
Microfiche copy: **A01**

**EVALUATION OF MICELLAR-POLYMER FLOOD PROJECTS IN
A HIGHLY SALINE ENVIRONMENT IN THE EL DORADO FIELD**

By
**Howard H. Ferrell
Robert A. Easterly
Timothy B. Murphy
Jane E. Kennedy**

December 1987

Work Performed Under Contract No. AC19-85BC10830

Prepared for
**U.S. Department of Energy
Assistant Secretary for Fossil Energy**

**James W. Chism, Project Manager
Bartlesville Project Office
P.O. Box 1398
Bartlesville, OK 74005**

Prepared by
**Keplinger Technology Consultants, Inc.
6849 E. 13th Street
Tulsa, OK 74112**

TABLE OF CONTENTS

	<u>Page No.</u>
ABSTRACT	iii
LIST OF TABLES	iv
LIST OF FIGURES	v
SUMMARY	1
INTRODUCTION: OVERVIEW OF PROJECT AND FIELD SETTING	4
MICELLAR-POLYMER PROCESS	7
PROCESS DESCRIPTION, DESIGN, AND PERFORMANCE	9
Aqueous Micellar-Polymer Process - North (Chesney) Pattern	9
Process Description	9
Laboratory Tests for Process Design	10
Field Performance	13
North Pattern Description and Summary of Operations	13
Oil Production from the North Pattern	14
Surfactant Partitioning into Oil Phase	14
Producing Well Responses	15
Analysis of Changes at Observation Wells	16
Log Profiles at Observation Wells	18
A Review of Simulation Studies	18
Oil Soluble Micellar-Polymer Process - South (Hegberg) Pattern	23
Process Description	23
Laboratory Tests for Process Design	24
Field Performance	25
Pattern Description and Summary of Operations	25
Caustic Preflush	26
Micellar Slug and Polymer Drive	27
Effects of Fracturing on Well Performance	28
No Change in Producing Well Oil Cut	28
FIELD FACILITIES	31
RESERVOIR HISTORY AND DESCRIPTION	33
Production History	33

TABLE OF CONTENTS (Continued)

	<u>Page No.</u>
Coring and Core Analysis	35
Cored Wells and Routine Core Tests	35
Special Core Analysis Tests	36
Logging Results	38
Saturation From Logs	38
Mineralogy From Logs	40
Analyses for Calcium Sulfate and Barium	41
Caustic Consumption Tests on Cores	41
Observation of Produced Concentrations	42
Laboratory Tests for Gypsum and Barium	43
Alternate Depositional Model	45
Presence of Barium is Supported by Geological Conditions	47
Pressure Transient Analysis	49
Tracer Tests	50
Fluid Migration	51
Pressure Gradient Across the Pattern	51
Irregular Produced Water Confirms Migration	52
CONCLUSIONS	53
RECOMMENDATIONS	54
REFERENCES	55
TABLES	58
FIGURES	76
APPENDIX A	122

ABSTRACT

Two different micellar processes were conducted in the El Dorado Field in an effort to develop an EOR method for reducing the high oil saturation after waterflooding. Each process was field tested on adjacent 25 acre blocks of four 5-spot patterns. This report reviews the field performance, geology, formation evaluation, and laboratory support tests for the field tests.

Both processes failed to recover additional oil, primarily because of unavoidable exposure to and mixing with divalent ions. An unusual oil saturation distribution also contributed to the failure. Unfortunately, these conditions could have been predicted from study of previous air, water, and steam injection projects in the field.

LIST OF TABLES

	<u>Page No.</u>
TABLE 1 Description of North (Chesney) Pattern Process	58,59
TABLE 2 Chronology of Field Operations, Chesney Lease	60-63
TABLE 3 The Change in Water Resistivity vs. Formation Resistivity	64
TABLE 4 Description of South (Hegberg) Pattern Process	65
TABLE 5 Chronology of Field Operations, Hegberg Lease	66-69
TABLE 6 Analyses of Supply and Injection Waters	70
TABLE 7 Semiquantitative X-Ray Diffraction Analysis	71,72
TABLE 8 Caustic Consumption and Sulfate Liberated by Caustic Solution	73
TABLE 9 Analysis of Caustic Depletion from Selected Core Samples	74
TABLE 10 Eluted Quantities of Selected Ions Following Preflush	75

LIST OF FIGURES

	<u>Page No.</u>
FIGURE 1 Typical Micellar-Polymer Coreflood Response	76
FIGURE 2 Core Flood Results Using Chemical Slug for North Pattern	77
FIGURE 3 Oil Displacement Results in Berea and El Dorado Cores Using Shell Process	78
FIGURE 4 El Dorado Project Layout	79
FIGURE 5 Produced Fluids, Chesney Lease, Project Totals - Oil Rate and Injection Rate	80
FIGURE 6 Produced Fluids, Chesney Lease, Project Totals - Oil Cut	81
FIGURE 7 Produced Fluids, Chesney Lease, Well MP-114 - Oil Rate, Oil Cut, and Surfactant in Water	82
FIGURE 8 Produced Fluids, Chesney Lease, Well MP-114 - Polymer and Secondary Butyl Alcohol Concentrations	83
FIGURE 9 Produced Fluids, Chesney Lease, Well MP-114 - Calcium and Chloride Concentrations	84
FIGURE 10 Produced Fluids, Chesney Lease, Well MP-122 - Oil Rate, Oil Cut, and Surfactant in Water	85
FIGURE 11 Produced Fluids, Chesney Lease, Well MP-122 - Calcium and Chloride Concentrations	86
FIGURE 12 Produced Fluids, Chesney Lease, Well MP-122 - Polymer and Secondary Butyl Alcohol Concentrations	87
FIGURE 13 Produced Fluids, Chesney Lease, Well MP-131 - Calcium and Chloride Concentrations	88
FIGURE 14 Produced Fluids, Chesney Lease, Well MP-131 - Oil Rate, Oil Cut, and Surfactant in Water	89

LIST OF FIGURES (Continued)

	<u>Page No.</u>
FIGURE 15 Produced Fluids, Chesney Lease, Well MP-131 - Polymer and Secondary Butyl Alcohol Concentrations	90
FIGURE 16 Produced Fluids, Chesney Lease, Well MP-132 - Calcium and Chloride Concentrations	91
FIGURE 17 Produced Fluids, Chesney Lease, Well MP-132 - Oil Rate, Oil Cut, and Surfactant in Water	92
FIGURE 18 Produced Fluids, Chesney Lease, Well MP-132 - Polymer and Secondary Butyl Alcohol Concentrations	93
FIGURE 19 Produced Fluids, Chesney Lease, Well MP-124 - Polymer and Secondary Butyl Alcohol Concentrations	94
FIGURE 20 Produced Fluids, Chesney Lease, Well MP-124 - Calcium and Chloride Concentrations	95
FIGURE 21 Produced Fluids, Chesney Lease, Well MP-124 - Oil Rate, Oil Cut, and Surfactant in Water	96
FIGURE 22 Selected Log Responses for Well MP-131	97
FIGURE 23 Selected Log Responses for Well MP-132	98
FIGURE 24 Core Flood Results Using Chemical Slug for South Pattern	99
FIGURE 25 Oil Displacement Results in Berea and El Dorado Cores Using Union Oil Process	100
FIGURE 26 Produced Fluids, Hegberg Lease, Project Totals - Oil Rate and Injection Rate	101
FIGURE 27 Produced Fluids, Hegberg Lease, Project Totals - Oil Cut	102
FIGURE 28 Produced Fluids, Hegberg Lease, Well MP-227 - Oil Rate, Oil Cut, and Surfactant in Water	103

LIST OF FIGURES (Continued)

	<u>Page No.</u>
FIGURE 29 Produced Fluids, Hegberg Lease, Well MP-227 - Polymer and Secondary Butyl Alcohol Concentrations	104
FIGURE 30 Produced Fluids, Hegberg Lease, Well MP-227 - Calcium and Chloride Concentrations	104
FIGURE 31 Produced Fluids, Hegberg Lease, Well MP-228 - Oil Rate, Oil Cut, and Surfactant in Water	106
FIGURE 32 Produced Fluids, Hegberg Lease, Well MP-228 - Polymer and Secondary Butyl Alcohol Concentrations	107
FIGURE 33 Produced Fluids, Hegberg Lease, Well MP-228 - Calcium and Chloride Concentrations	108
FIGURE 34 Produced Fluids, Hegberg Lease, Well MP-219 - Oil Rate, Oil Cut, and Surfactant in Water	109
FIGURE 35 Produced Fluids, Hegberg Lease, Well MP-219 - Polymer and Secondary Butyl Alcohol Concentrations	110
FIGURE 36 Produced Fluids, Hegberg Lease, Well MP-219 - Calcium and Chloride Concentrations	111
FIGURE 37 Produced Fluids, Hegberg Lease, Well MP-229 - Oil Rate, Oil Cut, and Surfactant in Water from Core Analysis Data	112
FIGURE 38 Produced Fluids, Hegberg Lease, Well MP-229 - Polymer and Secondary Butyl Alcohol Concentrations	113
FIGURE 39 Produced Fluids, Hegberg Lease, Well MP-229 - Calcium and Chloride Concentrations	114
FIGURE 40 EOR Projects in the El Dorado Field	115
FIGURE 41 Oil Saturation Distribution from Core Analysis	116
FIGURE 42 Capacity Distribution Using Core Analysis Data	117

LIST OF FIGURES (Continued)

	<u>Page No.</u>
FIGURE 43 Oil Saturation Distribution from Well Logging	118
FIGURE 44 Composite Log Response Well MP-130	119
FIGURE 45 Capacity Distribution Using Pressure Transient Data	120
FIGURE 46 Pressure Distribution Map	121

SUMMARY

Field trials of two micellar processes were performed between 1974 and 1982 in the El Dorado Field, Kansas. The incentive for this project was the high remaining oil saturation - even after years of air, then water injection and, finally, an attempted steam pilot. Two micellar processes were employed on adjacent 25-acre areas consisting of four 5-spot patterns. Although two different methods were used, it can be shown that they are theoretically similar and that both are sensitive to reservoir water salinity and hardness.

Samples taken from observation wells 90 feet from injection wells indicated a change in oil cut; however, a change in either oil rate or oil cut was not observed in any of the producing wells. Since the project did not recover measurable additional oil from either pattern area, the El Dorado project is interpreted as a technical and economical failure.

This study presents an interpretation of the geology, oil saturation distribution, and reservoir flow properties which we believe logically explains the poor performance at El Dorado. The specific causes for the project failure are primarily the following:

1. Gypsum and barium deposits.
2. Unusual vertical oil saturation distribution.
3. Migration of liquids into the test area.
4. High hardness of waterflood injected water.

Although these causes are specific to El Dorado, they point out the sensitivity of the micellar process and lead to broader conclusions which are applicable to most reservoirs:

1. Use of alkyl aryl sulfonates results in good oil displacement only in a narrow range of total salinity and divalent ion concentration. The utility of a preflush to adjust the reservoir water to optimal concentration is questionable, at best, and impractical if the reservoir contains gypsum.
2. A high average oil saturation is not necessarily an attractive target for an EOR process. As demonstrated at El Dorado, the high oil saturation may be contained in strata which cannot be contacted by the micellar slug.
3. An unusual pressure gradient and fluid migration within the reservoir can bring extraneous high salinity, high hardness brine in contact with the micellar slug, greatly reducing the effectiveness of the micellar slug and at the same time causing an inefficient reservoir sweep pattern.

In spite of the disappointment of the El Dorado project, the lessons learned there have made an important contribution to the evolution of the micellar flooding process. El Dorado emphasizes the consequences of overlooking deleterious reservoir properties.

It is recommended that prior to site selection and process specification, the usually available conventional data be thoroughly digested, as shown by this study, to detect, or at least suggest, harmful characteristics before a major technical and financial commitment is made. For example, although the unusual saturation distribution at El Dorado was not obvious from study of the electric logs, there were hints of this condition from the oil saturation observed in core analysis and also a suggestion of the unusual saturation distribution by study of the relatively poor waterflood performance and a lack of additional oil recovery observed during the steam flood pilot. Fluid migration can be detected by observing the pressure gradient prior to project initiation. Further, the presence of gypsum and barium can be diagnosed by one or a combination of the following techniques:

1. Analysis of injected and produced water from previous injection processes.
2. Study of the core and use of special core tests.
3. Lithological determination from logs together with an outcrop study can be used to compliment a depositional environmental study.

If a hostile reservoir environment is suspected, more thorough reservoir measurements and tests, together with laboratory core tests to analyze possible adverse effects and to develop a remedy, are recommended.

INTRODUCTION:
OVERVIEW OF PROJECT AND FIELD SETTING

The El Dorado micellar-polymer demonstration project was a cost-shared project between Cities Service Oil Company and the United States Department of Energy. The project objectives were to evaluate the micellar-polymer process to increase oil recovery, to assess problems that may occur with a micellar-polymer process, and to compare two different micellar-polymer processes. The results of this project were reported in eight annual reports covering the life of the project from 1974 to 1982.¹⁻⁸

This review encompasses the performance of the El Dorado micellar-polymer project during the first eight years of the project's life, the duration of the cost-share agreement. The performance of the project during this period suggests the El Dorado micellar-polymer project was a technical and economic failure.

The Chesney and Hegberg leases of the El Dorado Field, located in Butler County, Kansas, were chosen as the location of the demonstration project. Production in this area of the field is primarily from the Admire (650 feet) sandstone. Primary production began in 1916 and accounted for approximately 14.5 million barrels of oil. In 1924, secondary recovery using air injection was initiated and continued until 1954. Waterflooding was attempted unsuccessfully in the heart of the field near the surfactant test site between 1937 and 1939.

Waterflooding was attempted again in 1947 on the Pierpont Lease near the edge of the field. The operator attributed the success in the Pierpont Lease to the use of salt water injection, whereas the first attempt had used fresh water. The success of the second pilot, however, may have been due to higher oil saturation near the edge of the field where oil recovery by air flooding was poor. Secondary recovery by waterflooding continued field-wide in the early 1950s with peak injection rates occurring in 1955. Waterflooding continued in the project area until 1971, when the injection was discontinued and the producing wells were abandoned.

In spite of the long production history of the El Dorado Field, oil saturation was quite high, and the micellar-polymer project provided potential to recover a large volume of the remaining oil. Two micellar-polymer processes were implemented during the life of the project. An aqueous-phase process developed by Shell Oil Company that included sulfonates, alcohol, and biopolymer in the chemical slug was used in the north pattern. The other process, used in the south pattern, was developed by Union Oil Company and utilized a chemical slug composed of a micellar oil slug consisting of a mixture of sulfonates and crude oil alternately injected with a micellar water chemical slug. Each of these processes is described in this report.

Laboratory tests indicated both processes should recover significant amounts of oil from the project area. This report also provides a summary of the design and operation of the El Dorado project and an evaluation of the performance of both processes.

It will be shown that the reservoir characteristics were particularly unfavorable for the application of both micellar-polymer processes. Laboratory test results indicate the total gypsum concentration is approximately one percent. The sand also contains a high percentage of clays and feldspars which in turn have been shown by outcrop studies to contain high amounts of barium.⁹

The Admire Formation in both pattern areas is composed of sand layers a few inches thick separated by mica. The thin sand layers have permeabilities of several hundred millidarcies, and pressure transient tests demonstrated communication areally for distances greater than well spacing. The average oil saturation is about 40 percent or about 10 to 15 percent above residual oil saturation. Although there is little difference in the average saturation between wells, there are thought to be large saturation differences between layers, with saturation possibly as low as 15 percent in some and as high as 60 percent in other layers. The sand layers are too thin to detect by logs, so the log saturations reflect a running average of several layers.

The type of sulfonates used in both processes as the main building block for the micellar solution will not tolerate contact with water having a salinity in excess of about 1 percent and a total hardness greater than a few parts per million (ppm). The reservoir water at the start of the project was about 7 percent salinity with about 3,000 ppm hardness. Reducing the salinity and hardness by preflushing was totally impractical, particularly because of (1) an influx of extraneous high salinity, high hardness water into the pattern area, and (2) a release of calcium from gypsum and a barium release from clay and feldspars. Therefore, it can be seen that the micellar processes selected for El Dorado were ill advised and were destined for failure from the outset.

This review describes the micellar flood results and is focused on events and tests which directly help to explain the poor performance. It should be kept in mind that this review has the benefit of both hindsight and technical developments subsequent to the initiation of the project.

MICELLAR-POLYMER PROCESS

This section will give a theoretical overview of the micellar process and a basis to interpret specific data and descriptions in the following sections.

Although there are important operational differences between the two processes, Healy and Reed showed that all surfactant processes may be studied from phase relationships on ternary diagrams.¹⁰ The oil external process (Union) begins as a single oil phase but is diluted with brine at both the leading and trailing boundaries to form two phases in the reservoir. Likewise, the water external process (Shell) begins as a single water phase and becomes a multiphase fluid by mixing with oil at the leading boundary. It can be seen that a large fraction of the total oil recovered in either process is by immiscible displacement which is controlled by the capillary number¹¹: $(NC = V\mu/\sigma)$. Therefore, one design criteria is to adjust the salinity and cosurfactant concentration to give the lowest interfacial tension as the micellar slug is diluted.

In both processes, it is desirable to extend the concentration ranges of salt, surfactant, and oil where the micellar fluid exists as a single phase region to prolong the miscible displacement. This is achieved by adjusting the salinity of the mixture. In addition to the shape and size of the single phase boundary, the interfacial tension is greatly affected by the salinity.¹² Another important design parameter for both processes is the amount of surfactant retention, which can be minimized by the adjustment of the total salinity, surfactant concentration, and cosurfactant concentration.¹³

From these brief discussions, it is seen that the salinity of the micellar fluid is the most significant parameter of the micellar-polymer process. Changes in salinity of the micellar fluid change the phase relationship. High salinity causes the surfactant and water to partition into and swell the oil phase, while low salinity causes oil and surfactant to partition into and swell the water phase. Other

studies have shown that mixing of surfactant with multivalent ions has a deleterious effect. The effect of multivalent ions on surfactant phase behavior is equivalent to about ten times that of the sodium ion concentration. High calcium and barium concentration can cause partitioning into the oil phase and precipitation or salting out of the surfactant.¹⁴ Therefore, it is imperative to adjust the reservoir water to the optimum salinity and hardness by preflushing prior to sulfonate-micellar slug injection. Herein lies the futility of the salt and hardness sensitive micellar processes selected for El Dorado. The preflush simply cannot reduce salinity and hardness to tolerable levels and the micellar process simply cannot displace oil in the salinity and hardness environment existing after preflushing.

Extensive laboratory testing using the reservoir water, crude oil, and core samples are needed to design the optimal salinity and slug composition. Typical results of laboratory corefloods after the chemical process has been optimized are shown in Figure 1. Figure 1 is provided so that a comparison can be made between it and laboratory corefloods and field recovery performance of the El Dorado micellar-polymer process as discussed in subsequent sections. Important features of this coreflood are: (1) oil response is shown by an increase in oil cut after about 25 percent pore volume injected, (2) oil cut is increased from near 0 to about 50 percent, and (3) the cumulative oil recovery is in excess of 60 percent of residual oil saturation.

PROCESS DESCRIPTION, DESIGN, AND PERFORMANCE

AQUEOUS MICELLAR-POLYMER PROCESS - NORTH (CHESNEY) PATTERN

The following subsections describe the micellar process, the laboratory tests which formed the basis of the process design, and the actual performance of the process in the Chesney pattern. The computer simulation attempt to match the performance of the Chesney pattern is also discussed.

Process Description

The aqueous micellar-polymer process used in the north (Chesney) pattern included the injection of a two stage preflush followed by injection of a water-soluble micellar solution. A biopolymer was injected during and after micellar injection to provide mobility control. A design change during the project resulted in the substitution of polyacrylamide for biopolymer.

The first stage of the two-stage preflush consisted of a 39.4 percent pore volume slug of 1.4 weight percent sodium chloride in fresh water. The second stage preflush was a 41.8 percent pore volume slug of sodium, calcium, and magnesium chloride in fresh water with concentrations of 2.9, 0.102, and 0.097 weight percent, respectively. Calcium and magnesium were included to minimize the negative effects of cation exchange.¹⁵⁻²⁰

The micellar solution consisted of a mixture of two sodium alkyl aryl sulfonates with an average equivalent weight of 430, alcohol ($C_{12} + C_{15}$ alcohol ethoxysulfate sodium salt) as a co-surfactant, secondary butyl alcohol as a tracer, polysaccharide biopolymer (added to give a viscosity of 32 cp) for mobility control, and sodium chloride to provide optimum salinity, all added to fresh water. The micellar solution volume was 10.6 percent pore volume of the north pattern area. Slug size and chemical compositions were based upon the results of

laboratory tests. A complete description of the micellar process, including composition and volume of preflush slug and polymer drive can be found in Table 1.

Biopolymer was injected following the micellar solution. It is believed that during the biopolymer injection, SBA was added as an antimicrobial agent. Later isobutyl alcohol was substituted at a lower concentration to reduce the cost. In October, 1980, the polymer drive solution was changed to polyacrylamide to provide mobility control. A 42.2 percent pore volume slug of the polysaccharide polymer was injected before switching to polyacrylamide polymer. The polyacrylamide polymer was tapered to decrease chemical costs. The polyacrylamide tapered slug consisted of a 4.3 percent pore volume slug of 30 cp polymer, a 7.0 percent pore volume slug of 20 cp polymer, and a 4.9 percent pore volume slug of 10 cp polymer. Isopropyl alcohol was added to the polymer solution as a tracer. The polymer was followed by drive water.

Laboratory Tests for Process Design

The dependence of micellar process design on laboratory testing to identify and remedy potential problems was previously discussed in this report. Often, the optimal design is a compromise between several complex variables. These variables include salinity, phase behavior, interfacial tension, adsorption, and the presence of co-surfactants. Therefore, the best micellar formulation can only be determined by extensive laboratory testing. The following discussion indicates which laboratory tests were performed and their significance on the design.

Preliminary laboratory design information for the Chesney (North) pattern area was provided to Cities Service in October 1975 by Shell Oil Company. Oil displacement tests were performed in 2-inch diameter cores which were approximately 10 inches in length. An example of one coreflood test is provided in Figure 2. Test results indicate that a 25 percent pore volume slug of micellar solution reduced the residual oil saturation from 29 percent to 20 percent pore volume.

Figure 3 shows the effect of slug size on residual oil saturation in Admire cores. The residual oil saturation for various slug sizes of the same micellar process and fluids, except in Berea cores, is also shown in Figure 3.

The differences in residual oil saturation between chemical floods in Berea and Admire sandstone cores indicate that the micellar-polymer process was not efficient in the Admire Sand. Tests using the Shell chemical formulations in Berea sandstone resulted in virtually zero residual oil for a 10 percent pore volume chemical slug, while tests in Admire sandstone using much larger slugs resulted in only a slight reduction of waterflood residual oil saturation (Figure 3).

The initial oil saturation for the chemical tests is about 40 percent compared to waterflood residual oil saturations of about 26 percent obtained during relative permeability testing. The higher initial oil saturation results in a high apparent oil recovery by chemical flooding, even though the final residual oil saturation after chemical flooding is equal to that of waterflooding. Further investigation into the reasons for these inconsistent test results was not pursued; however, further discussion of inconsistent oil saturation measurements is presented in the discussion of well logging.

Surfactant adsorption tests in Chesney core material indicated a loss of 0.10 to 0.158 meq per 100 grams of rock. This is equivalent to a loss of approximately 1.15 to 1.82 pounds of surfactant per barrel of reservoir pore volume, which is considered to be high for surfactant flooding.

X-ray diffraction studies conducted on rock samples from the 650 Foot Admire Sand indicated clay minerals, predominantly kaolinite, with montmorillonite and chlorite present in lesser amounts. The detrimental effect of cation exchange and clay minerals on enhanced oil recovery processes has been reported.¹⁵⁻²⁶ Cation exchange is a physical process that is related to the quantity of clay minerals within the reservoir rock. The cation exchange capacity (CEC) of El Dorado core material was

experimentally determined on two samples. The results of these tests indicated a cation exchange capacity of 4.4 and 7.1 milligrams of calcium per 100 grams of rock. Due to the presence of clays and a moderate cation exchange capacity, a greater loss of surfactant is expected in El Dorado core material than in fired Berea sandstone.

Other laboratory tests were performed to aid in the evaluation of the El Dorado micellar-polymer flood. An interfacial tension measurement of 10^{-2} dynes per centimeter was obtained with a spinning drop tensionmeter using the Shell surfactant mixture and El Dorado crude oil. A dispersion coefficient of the 650 foot Admire sandstone was measured in the order of 10^{-3} cm² per second.

Calcium sulfate (gypsum) is known to adversely affect caustic and surfactant flooding.²¹ Analyses of produced water suggested the presence of gypsum and barium, yet tests to confirm their presence were not performed until the caustic preflush apparently failed during the field tests. The presence of slightly soluble calcium sulfate was later confirmed in the Admire sand.²²

The Shell micellar-polymer process utilized a biopolymer for mobility control of the micellar slug. The biopolymers tested for this application included the Abbott, Kelco, and Pfizer biopolymers. Based on cost, viscosity, filterability, field injectivity and laboratory injectivity tests, the Abbott biopolymer was selected as the mobility control agent. Laboratory tests also included the testing of biocides and their effects upon polymer stability and optimum salinity of the biopolymer and surfactant slugs.

Field Performance

North Pattern Description and Summary of Operations:

The north pattern area consists of 27 wells: 4 production wells, 9 injection wells, 12 monitoring wells, and 2 observation wells. The pattern area encompasses 25.6 acres with four contiguous five-spot patterns. Figure 4 provides a layout of the project area. Note observation wells MP-131 and MP-132 are 90 feet and 180 feet, respectively, southwest of the central injector. Wells MP-101, 102, 103, 104, and 105 are outside the pattern area and were used as test wells.

The producing wells in the pattern were drilled with air to a coring point 50 feet above the formation. The remainder of the well was drilled and cored with formation water. Five and one-half inch casing was cemented from the bottom of the well to the surface. Fluid production was through 2½-inch-diameter tubing after perforation. The injection wells were drilled in the same manner as the production wells except 4½-inch-diameter casing was set to the top of the producing formation and open hole completions were made.

The first preflush began in November 1975. A second preflush was initiated in December 1976. Both preflushes consisted primarily of sodium chloride and fresh water, while calcium and magnesium were added to the second preflush in small concentrations. Micellar solution injection began in November 1977, followed by biopolymer injection in November 1978. A polyacrylamide polymer was substituted for the biopolymer in October 1980. Water drive was then initiated in March 1982. A summary of the operating events is given in Table 2 and the Chesney project oil production and fluid injection rates to mid-1981 are shown in Figure 5.

Oil Production from the North Pattern:

A graph of the oil cut for the north pattern area is shown in Figure 6. The oil cut varies from 1 to 2 percent, probably because of measurement fluctuations, but there is no indication of an increase in oil cut. Since the oil cut does not increase, the micellar solution was obviously ineffective in reducing the oil saturation for an appreciable distance into the reservoir and thus failed to sustain an oil bank. Typical oil cuts for successful micellar-polymer projects range from 15 to 30 percent.²³

A total of 10,200 barrels of oil and 1,381,802 barrels of water was produced from the Chesney lease during the life of the project. The pore volume of the north pattern area was estimated to be 894,257 barrels with the oil-in-place estimated to be 300,000 barrels.³³ After the start of the preflush, 4,100 barrels of oil were produced before micellar injection and logically can be attributed to waterflooding. During the micellar-polymer flood, 6,100 barrels of oil were produced in the north pattern, which is equivalent to slightly over 2 percent of the oil-in-place.

Surfactant Partitioning into Oil Phase:

A significant quantity of surfactant was detected in the produced oil from Wells MP-114, MP-122, and MP-132. The concentrations ranged from about 3 percent of the initial injected concentration at Wells MP-114 and MP-122 to about 17 percent at Well MP-132. The analysis of surfactant in the aqueous phase indicates a high of 9.5 percent of injected concentration at Well MP-132 and a low of 0.1 percent at Wells MP-114 and MP-122. The high concentrations of surfactant detected in produced oil are due to partitioning of surfactants into the oil phase. Partitioning occurs when the salinity of the reservoir brine is too high and/or the calcium ion concentration is too high, resulting in formation of oil soluble calcium sulfonates. Although analyses specifically for calcium sulfonate in the oil phase were not reported, oil soluble and water insoluble calcium sulfonate will form in the high salinity and

high hardness environment present within the reservoir. Partitioning of surfactant into the oil phase resulted in surfactant slug deterioration and ultimately in the failure of the process to improve oil recovery.

High salinity and the presence of divalent cations in the reservoir brine were well established at the beginning of the project. However, the presence of water soluble calcium sulfate in significant concentrations (1 to 2 weight percent) was not acknowledged until after the project was initiated. Further, a pressure gradient was discovered which introduced brine into the reservoir after preflushing. The calcium sulfate and pressure gradient combined with an initially low oil saturation in zones contacted by the micellar fluid, were the significant causes for the failure of the micellar-polymer process in the north pattern area. These three conditions will be discussed further in the section on Reservoir History and Description.

Producing Well Responses:

It is interesting to note that Well MP-114 produced more than 45 percent of the total oil recovered from the north pattern area. However, chemical analysis of produced fluids suggests Well MP-114 was not affected significantly by the reservoir preflush or the micellar-polymer flood. The oil production, oil cut, and produced ion and tracer concentrations for this well are presented in Figures 7 through 9. Although chloride ion concentrations declined slowly during the project, the reduction in concentrations does not appear to be strongly linked to the preflush or to the micellar-polymer injection. Calcium concentration began to increase shortly after the start of the micellar slug injection. The produced SBA tracer concentrations were very low and IBA was not detected in the produced water. Likewise, polymer was not detected during the life of the project in Well MP-114.

These data do not reflect the arrival of an oil bank at Well MP-114 or, for that matter, the arrival of any injected fluid in significant concentrations during the life of the project. Therefore, the oil

production from Well MP-114 does not appear to be a result of the micellar-polymer project, rather the sustained low oil cut production may have been the result of fluid migration from the western part of the field.

Well MP-122 was the only other producer in the Chesney pattern which produced measurable amounts of oil. Wells MP-114 and MP-122 account for 89 percent of the total production in the north pattern area. Surfactant was only detected in trace quantities in the water phase, but was 30 times higher in concentration in the oil phase at Well MP-122. Although significant tracer was produced, an oil bank was not observed at the well and the percent oil cut does not increase appreciably above 2 percent, as seen in Figures 10 through 12. The chloride ion concentrations in the produced water suggest a limited response to preflushing, but the calcium ion concentrations never decreased to acceptable levels for aqueous phase micellar flood propagation. Polymer was not detected in Well MP-122 during the period of review. For different reasons than Well MP-114, the data for Well MP-122 also do not indicate measurable additional oil recovery by the micellar-polymer process.

Analysis of Changes at Observation Wells:

The chemical analyses of fluids produced from observation Wells MP-131 and MP-132 indicate that preflushing was only effective at Well MP-131. This well is 90 feet away from the central injector, Well MP-118.

The analysis of produced fluids from Wells MP-131 and MP-132 reveals some causes for failure of the process in the north pattern. Well MP-131, which is closest to the central injector MP-118, experienced a decrease in calcium concentration from approximately 2,000 ppm to approximately 300 ppm during the preflush period. The concentration of calcium continued to decrease as polymer was produced (Figure 13). Following the preflush, there was an increase in oil cut preceding an increase in produced surfactant concentrations. The oil cut from MP-131 shown on Figure 14 increases to almost 30 percent. The produced alcohol

tracer concentration varies from 1.5 to 3.75 weight percent (50 to 75 percent of the injected concentration). Polymer is also detected at high concentrations (Figure 15). The increases in oil cut and surfactant concentration were sustained for about 11 months before they decrease to levels near zero. These data are consistent with the passing of mobilized oil and the chemical flood front.

In contrast, the preflush was not effective to MP-132, 180 feet from injection well MP-118, because the concentration of the calcium remained above 900 to 1,000 ppm and the total hardness was near 1,500 ppm which is unacceptably high for this micellar process (Figure 16).

As a result, the concentrations of produced surfactant (Figure 17) and polymer (Figure 18) in the water phase were low even though a significant quantity of alcohol tracers was produced. Instead of being in the water phase, surfactant was found in the oil phase at Well MP-132 indicating that a substantial amount of the surfactant had partitioned into an immobile oil phase. This is consistent with deterioration of a micellar chemical slug due to high salinity or high levels of divalent cations. Well MP-132 shows an increase in oil cut which lasts from August 1980 until May 1982 (Figure 17). This demonstrates that some of the displaced oil reached MP-132; however, the logging surveys, discussed in subsequent paragraphs, showed that the process failed to move the created oil bank beyond MP-132.

The apparent discrepancy between the high oil cut measured at both observation wells and the low oil cut recorded at producing Well MP-124 is further evidence of the deterioration of the micellar slug. Well MP-124, 90 feet from Well MP-132, produced tracer (Figure 19) but maintained a high salinity and calcium concentration (Figure 20) and did not produce even a suggestion of oil or surfactant (Figure 21).

A second explanation for the discrepancy in oil cuts may be the loss of sweep efficiency during the course of micellar-polymer flooding. The absence of polymer in produced samples from observation Well MP-132 suggests the loss of mobility control, hence a decrease in sweep efficiency.

The absence of polymer in produced fluids from observation Well MP-132 suggests either bacterial or chemical degradation of the polymer during sample collection or chemical degradation of the polymer between Wells MP-131 and MP-132. Biodegradation of biopolymers often occurs near the injection wellbore, particularly when a complete kill of bacteria is not achieved before injection. However, this is not believed to be the case because the polymer concentration at Well MP-131 was nearly equal to the injection concentration. Therefore, the deterioration is not believed to be due to biodegradation in the reservoir.

Log Profiles at Observation Wells:

The log profiles of observation Wells MP-131 and MP-132 were studied to better understand the movement of the oil bank. The interpretation of resistivity is complicated by the change in salinity of the injected fluid. The salinity injection history in Well MP-118 and observation well logging dates are given in Table 3. Since the formation factor, F , is a constant for a given depth in an observation well, the water saturation is proportional to the square root of the ratio of formation water resistivity, R_W , to the formation resistivity, R_T . R_T may be used from the log responses shown in Figures 22 and 23. R_W was calculated from chloride concentrations which are shown in Figures 13 and 16. Table 3 shows the change in the value of the square root of R_W/R_T . The change from March 1976 may reflect the change in water saturation due to micellar flooding. At Well MP-131, there is evidence of an oil bank with oil saturation build up of about 7 percent by early 1978. The saturation bank apparently carried to Well MP-132, at least by 1980. The oil bank saturation was reduced at Well MP-131 by mid-1979, but the saturation was not reduced at Well MP-132.

A Review of Simulation Studies

One method of optimizing the design of a surfactant flood is to use observed laboratory data in a chemical flood numerical simulator model. With the computer model, results of micellar-polymer floods can be predicted and the optimum pattern design and chemical slug size can be

estimated more accurately. Unfortunately, at the time the El Dorado project design started, a comprehensive chemical simulator was not available. However, later in the life of the project, simulation studies of the Chesney pattern performance were performed by the operator.

A finite-difference chemical-flood simulator was used to match the results of a coreflood in an Admire Sand core using the Shell high water content process used in the Chesney pattern. With respect to chloride concentration, oil cut, oil breakthrough, and total oil recovery, the calculated results agreed well with experimental data. Using the process characterization data from this coreflood match as a basis, simulations were performed for the quarter five-spot of the Chesney area containing the two observations Wells MP-131 and MP-132.

In general, the observed oil breakthrough time and oil cut behavior of well MP-131 were matched well. A polymer biodegradation effect was included in an attempt to better simulate the polymer concentration behavior at this observation well. However, since the extent of any possible degradation in the reservoir is unknown, the two extreme cases of no polymer degradation and severe polymer degradation, were tested. The actual polymer concentration data of MP-131 are enveloped by the curves of these two biodegradation cases. Measured surfactant concentrations at this well were also compared with simulation results, but the match, especially of the surfactant breakthrough time, was poor.

The fit of simulation results to observed data was much less accurate at the second observation Well MP-132, due to the complexity of the various mechanisms which contributed to the breakthrough of the micellar and polymer slugs. Very high polymer retention was required for even a fair match of the oil breakthrough time at this well. The effect of polymer degradation of the oil cut behavior of MP-132 was investigated. Again, the observed oil cut curve lay between those calculated with minimal polymer biodegradation and severe polymer biodegradation. Graphs of polymer and surfactant concentrations computed at this well were not provided.

The comparisons of actual and calculated sodium ion concentrations for these two observation wells differed dramatically. The fit is extremely good at MP-131, while the simulated sodium concentration is much less than measured at MP-132. This is evidence of an external salt source, which could be caused by an externally caused pressure gradient which produced a drift in the field. This point will be discussed more thoroughly in a subsequent section. Basically, the results of drift would be twofold: (1) if the drift resulted in an influx of a more highly saline brine, the brine would damage the surfactant; and (2) the drift would greatly reduce production from the wells in the direction opposite the drift, but increase production from wells in the direction of the drift from the injector. However, an increase in oil production was not observed at any producer. It is well known that the effectiveness of the micellar solution is dependent upon the salinity.

Attempts to predict the performance of the four producers in the Chesney pattern based upon the results of the history match of this quarter five-spot were unsuccessful. Since breakthrough of oil at producing Well MP-124 had not occurred during the period of review, a history match could not be made for the one producer in the quarter five-spot area. Therefore, an expansion of this history match to oil recovery predictions on a pattern-wide scale would not be justified.

In September 1978, the Department of Energy awarded Gulf Universities Research Consortium (GURC) a contract to establish data requirement guidelines, and to evaluate the adequacy of available data on the El Dorado cost-shared project, for numerical reservoir simulation.²⁴ The Chesney lease and its associated micellar-polymer process were selected for study. One conclusion of this study was that the El Dorado project data available in the public domain were inadequate for accurate characterization of the geology, reservoir, and process required for complex reservoir simulation. Also, field performance predictions based on coreflood simulation matches of a micellar-polymer process could not be definitely justified.

Despite the outcome of the GURC study, attempts were made in the current study to simulate the Chesney quarter five-spot previously discussed with a two-dimensional, three-phase chemical flood simulator. Parameters absent from available data were derived or assumed. Since a better match of the history data of the two observations wells MP-131 and MP-132 than provided by the operator was not obtained, further simulation studies were abandoned. The surfactant loss and the interfacial tension play important roles in oil recovery and are interrelated. Obviously, if the interfacial tension is low but the surfactant loss is excessively high, there would be poor propagation of the micellar bank and consequently poor oil recovery.

Highest oil recovery occurs when the micellar-oil mixture is in the lower phase (water), just at the point of entering the middle phase. In this range, the interfacial tension decreases to a minimum as the salinity increases. However, if the salinity increases beyond the point where the minimum interfacial tension occurs, the surfactant partitions into the oil phase. Therefore, the best recovery results should be obtained if the preflush reduces the reservoir salinity to the optimum concentration, and the surfactant is introduced at this optimum salinity.

In order to assure that the surfactant remains in the lower water phase upon dilution, the chase or polymer slug should have a lower salinity. Cities recognized this point and reduced the polymer drive salinity, but not until after a considerable quantity of high salinity polymer solution had been injected. By this time, the sulfonate partitioned into the oil and adsorption was already very high and there was no micellar bank in front of the lower salinity polymer bank.

Although simulation attempts in this and the GURC study did not match the recovery, they did point out that oil recovery is strongly influenced by surfactant slug size and the salinity of the polymer drive, and that capillary number and relative permeability data are also extremely important in modeling chemical flood performance. High surfactant losses at El Dorado resulted from the following mechanisms:

(1) ineffective preflush due to reservoir heterogeneity, (2) phase separation due to polymer/surfactant interaction, and (3) surfactant partitioning into the oil phase. Partitioning was accelerated by unfavorable cation exchange between the clays and surfactant.

Three additional factors discussed in the current study may individually or in combination, explain the micellar process failure and the difficulty in accurately simulating the performance at El Dorado. They are: (1) a mineral dissolution of calcium sulfate together with an exchange of barium from the rock minerals, (2) an unusual saturation distribution such that even with adequate mobility control the oil saturation would not be contacted by the surfactant, and (3) the very high salinities encountered due to drift and liquid migration within the reservoir. The basis for these interpretations will be discussed in section on Reservoir History and Description.

OIL SOLUBLE MICELLAR-POLYMER PROCESS - SOUTH (HEGBERG) PATTERN

Process Description

The oil soluble micellar-polymer process used in the south (Hegberg) pattern was designed by Union Oil Company of California. The process included injection of a two-stage preflush, a micellar oil or soluble oil slug, a micellar water, and a drive solution of polyacrylamide polymer. The polyacrylamide polymer followed the micellar oil and water to provide mobility control.

The preflush was designed as a two-stage treatment. The first stage consisted of a 14.7 percent pore volume slug of 2.0 weight percent sodium chloride salt in fresh water. This was followed by a second stage preflush consisting of a 16.8 percent pore volume slug of caustic solution. The caustic solution consisted of 0.281 weight percent sodium silicate and 0.418 weight percent sodium hydroxide in softened fresh water. The role of the caustic preflush was to precipitate unwanted calcium and magnesium cations within the formation.^{22,25}

The soluble oil solution consisted of four sodium alkyl aryl sulfonates having an average equivalent weight of 425, ethylene glycol monobutyl ether (a mutual solvent), crude oil, and fresh water. A description of the micellar oil is provided in Table 4. A micellar water was injected alternately with the micellar oil. The micellar water consisted of sodium chloride salt and nitrilotriacetic acid trisodium salt dissolved in fresh water. The nitrilotriacetic acid trisodium salt was provided as a chelating agent for hardness cations.²⁶ A 5.7 percent pore volume slug consisting of micellar oil and micellar water was injected into the south pattern area.

A tapered slug of polyacrylamide was injected after the micellar solution to provide mobility control. The solution viscosity was graded from a 120 cp slug to 20 cp. A 78.8 percent pore volume slug of the graded polymer solution was injected. After polymer injection, a drive water was injected using polyacrylamide polymer (50 ppm) in fresh water.

Laboratory Tests for Process Design

Core flood tests were originally performed using Berea sandstone core and Chesney lease crude oil. The results of these tests indicated the potential of the soluble oil process to recover a significant amount of post-waterflood oil. Further tests in the El Dorado Field cores indicated good oil recovery was possible. Oil recovery was less in the El Dorado cores than in Berea sandstone cores, and larger volumes of the soluble oil micellar solution were required to reduce residual oil saturation to 10 percent. The results of these preliminary tests suggest the composition of the Admire Sandstone core material may be one of the causes for lower recovery efficiency. The results of a laboratory core flood test using a 20 percent slug are presented in Figure 24. The effect of micellar slug size on residual oil saturation is shown in Figure 25.

An effort was made to understand the relatively poor oil recovery by the soluble oil process in laboratory core tests. The results of one core flood study suggested the surfactant loss was approximately 0.47 pounds per barrel of pore volume. This does not appear to account for the low recovery. Additional tests also indicated the pH of the caustic preflush was reduced from 13 to 9.5 after injection into Admire Sandstone core material. This substantial change in pH suggests a significant loss of alkalinity during the preflush. The pretreatment and caustic preflush were used to reduce high levels of divalent cations, such as calcium and magnesium, which have been shown to have detrimental effects on micellar and polymer chemicals. The results of the laboratory tests, including the surfactant floods and caustic preflushes, suggest that rock/fluid and fluid/fluid interactions are adversely affecting the performance of these tests.

Various polyacrylamide polymers were evaluated for mobility control of the soluble oil process. The tests included viscosity and screen factor measurements, mobility tests in laboratory cores, shear degradation tests, polymer aging studies with and without biocide, and optimum polymer salinity tests. Polyacrylamide polymers manufactured by

American Cyanamid and Nalco Chemical were selected as the most favorable polymers. Nalco polymer was eventually selected for use in the south (Hegberg) lease.

Field Performance

Pattern Description and Summary of Operations:

The south pattern area consists of 29 wells: 4 production wells, 10 injection wells, 12 monitoring wells, and 3 observation wells. The pattern area, having the same configuration as the north pattern, encompasses 25.6 acres with four contiguous five-spot patterns.

Figure 4 provides the layout of the project area. Observation Well MP-227 is 90 feet from the two center injectors, Wells MP-213 and MP-216. Observation Well MP-228 is approximately 180 feet from the central injectors. Both wells are located between the center injectors and a producing well, MP-219. Observation Well MP-229 was drilled 200 feet southwest of injection Well MP-203 after the injection of soluble oil was completed. Drilling and completion procedures for the wells were the same as for north (Chesney) pattern.

By the end of the project period, a total of 16,534 barrels of oil were produced from the south pattern area. Approximately 2,594 barrels of oil were produced before micellar-polymer injection began in March 1977 and, consequently, are attributed to waterflooding. An oil volume of 16,000 barrels injected as part of the oil soluble chemical slug was also deducted. Therefore, the project experienced a net loss of 2,060 barrels of oil after micellar injection began. The Hegberg project produced oil rates and injection rates are shown in Figure 26, and the oil cut is shown in Figure 27. Well MP-219, which is discussed in later paragraphs, produced just under half of the total oil from the Hegberg pattern; yet this well showed a decrease in oil cut after micellar slug injection.

The reservoir pretreatment began in November 1975. The pretreatment, which was the first stage of a two-stage preflush, consisted of a 2.0 weight percent sodium chloride solution prepared in fresh water. Approximately 14.7 percent of a pore volume of pretreatment fluid was injected. The pretreatment stage was followed by a caustic preflush in June 1976.

Caustic Preflush:

During the injection of the caustic preflush, an increase in injection pressure and a decrease in injectivity were noted. Several of the wells were stimulated by acidizing during the caustic preflush which may have neutralized the caustic chemicals and reduced their ability to decrease the hardness level of the reservoir brine. The wells were repeatedly stimulated in order to repair the damage sustained during the caustic preflush injection as shown in Table 5.

The caustic preflush was successful in laboratory tests for removing divalent cations.^{22,25} In the El Dorado Field, however, precipitation of insoluble calcium and magnesium silicates probably occurred during flushing possibly blocking some pore throats which could have resulted in a loss of permeability. The caustic solution preflush may also have dissolved clay minerals resulting in the migration of clay fines, leading to additional plugging.²⁷ Silica dissolution as a result of caustic injection may have also contributed to reduced injectivity.²⁸ The use of a chelating agent injected ahead of the caustic slug is recommended to minimize deterioration of the slug and to overcome low injectivity due to the precipitation of silicates which formed after the caustic reacted with calcium and magnesium in the brine.

The pH of produced fluids was measured during the injection of the preflush. Since pH is a measure of the acidity or alkalinity of the produced brine, the pH of the produced fluids would be elevated above pH 7 (neutral) if caustic was present at the observation or production wells. A significant increase in the pH of the produced fluids was not observed. It is concluded that the reservoir pretreatment and caustic

preflush in the south (Hegberg) pattern was ineffective, as evidenced by the absence of an increase in pH and the continued presence of high concentrations of calcium and magnesium in the reservoir brine.

The chemical analyses of produced fluids from the Hegberg producing wells were similar to those of the Chesney Lease. The calcium and magnesium concentrations decreased slowly after start of the preflush, then tended to remain constant at unacceptably high concentrations. Generally, the divalent ion concentrations remained higher than 2,000 ppm during the eight year life of the project. These analyses also indicate the preflush was ineffective in lowering the hardness levels of the reservoir brine.

Micellar Slug and Polymer Drive:

Micellar oil and micellar water injection began in March 1977.

Alternate injection of micellar oil and water continued until the end of March 1978, when 5.7 percent pore volume of micellar fluid was injected. The micellar oil and water solutions were injected in approximately equal volumes.⁴ During the injection of micellar oil, a loss of injectivity was observed. The cause of the low injectivity was found to be the precipitation of wax from the crude oil used to formulate the micellar oil solution. This may have been the result of a loss of light hydrocarbon components in the crude oil due to long storage periods. This problem was remedied by adding a solvent to the crude oil portion of the micellar oil solution before injection.

The injection of a tapered polyacrylamide polymer slug began in April 1978. The viscosity of the slug was reduced from 120 cp to 1 cp between April 1978 and December 1981. The viscosity of the polymer solution was then increased to approximately 20 cp. Injection of polymer continued even after the contract period was over in November 1982. Occasional well plugging was noted during polymer injection, and well stimulation was routinely performed.

Effects of Fracturing on Well Performance:

During fracturing of Well MP-213, the fractures became overextended resulting in communication with Wells MP-227 and MP-228. Premature breakthrough of a radioactive cobalt tracer was observed in Well MP-227, confirming the existence of the fracture. Later, an interpretation of a pressure transient test suggested the fracture may have closed between Wells MP-213 and MP-227; however, still later, a second tracer test using isobutyl alcohol indicated that fracture communication still existed. The presence of the fracture allowed inefficient sweep and bypassing of the micellar slug by polymer, resulting in a loss of mobility control and deterioration of the flood front.

Fracture flow from Well MP-213 past observation Wells MP-227 and MP-228 in the direction of Well MP-219 rules out quantitative analysis of the swept reservoir volumes and recovery efficiency. However, study of the oil cuts and concentrations of injected liquids in Wells MP-227, MP-228, and MP-219 can shed light on the process performance. In Well MP-227, there was a "nail-like" spike of injected oil (Figure 28) followed immediately by arrival of injected concentration polymer (Figure 29). The performance in Well MP-228 is analogous to Well MP-227 if it is considered that the greater distance from MP-213 to MP-228 causes some dispersion of the fronts. The injected oil bank (Figure 30) arrived just a little later than in MP-227 and was followed immediately by the arrival of the polymer bank (Figure 31). The chloride and calcium concentration dropped to near injected levels after the arrival of polymer bank in both Wells MP-227 and MP-228, as shown in Figures 32 and 33, respectively. There was no change in oil cut or evidence of injected fluids at Well MP-219 as shown in Figures 34 through 36.

No Change in Producing Well Oil Cut:

If an oil bank was created ahead of the micellar fluid, it apparently became immobile. The formation of a viscous immobile oil phase due to calcium sulfonate precipitation may be a reason for deterioration of the oil bank. An extended fracture, resulting in bypassing of the oil bank,

is another reason for deterioration. The existence of fracture flow between injection Well MP-213 and observation Well MP-228 as late as May 1981 is demonstrated by the detection of isobutanol tracer at the observation well less than one month after the tracer injection began.⁸

Observation Well MP-229 was drilled and completed in March 1979. Two months later, the injected oil was observed at Well MP-229. The performance curves for Well MP-229 have almost identical characteristics to those of Well MP-227, as shown in Figures 37 through 39. This similarity implies that injection Well MP-203 was also fractured. An oil bank was not created since no change in oil rate or oil cut was observed in any of the Hegberg producing wells.

The results of fluid analyses from the three observation wells suggest the surfactants partitioned into the oil phase. This is due to the low surfactant concentrations in the water phase and the persistent high concentrations of calcium ions.

All four producing wells were acidized in November 1981 and monitoring Wells MP-202 and MP-206 were converted to production wells in May and June 1982, respectively. There was an increase in oil production; however, this oil rate increase is attributed to increased withdrawal rate and not improved recovery since none of the producing wells increased in oil cut.

Although polymer injection into the pattern area was not completed at the end of the project period, an increase in oil cut at the producing wells should have been observed before or during surfactant breakthrough. An increase in oil cut was not observed, however, and is believed unlikely in the future.

The failure of the oil soluble process to recover additional oil from the pattern area is attributed to the failure of the reservoir preflush to remove divalent cations and high salinity reservoir brine from the pattern area. The presence of high salinity and a high concentration of divalent ions resulted in the partitioning of surfactant into the oil

phase due to a higher than optimum salinity environment and the formation of oil soluble calcium sulfonate. The preflush failure was due to the presence of a water soluble calcium sulfate mineral, but the high reservoir brine salinity and a large pressure gradient across the test area contributed to the failure by causing extraneous reservoir brine to migrate into the pattern area.

FIELD FACILITIES

After drilling and completion within the test areas, the wells were placed on production to establish baseline performance. A production facility was constructed to process the produced fluids from the pattern areas. The process design and construction are straightforward and conventional with the addition of a 100-barrel test tank to allow individual well tests on a periodic basis.

El Dorado city water was chosen as the water source for this project. The city water, obtained from Lake El Dorado, required additional treatment before it could be used in this project. An upflow sand filter was used to remove solids; however, the addition of chlorine to the treatment water was found to effect the stability of polymer solutions. As a result, biocides and other polymers were evaluated in the laboratory to solve the incompatibility problem. The water injection facilities were completed by November 1975.

The design of the injection facilities allowed for versatility and ease of operation. Sampling of injected fluids was facilitated by the addition of sample taps at advantageous locations. Two buildings were constructed on location to house the injection facilities. Injection pumps, mixing controls, and an on-site field laboratory were contained in one building. The header building contained distribution headers and polymer mixing equipment.

Some difficulties were experienced during the preflush injection when sodium chloride precipitated in the piping from a supersaturated solution, causing the plugging of the lines. A change in the chemical delivery procedures resulted in a satisfactory solution to the problem. Due to the waxy nature of the Green County crude oil used in the south (Hegberg) pattern, wax precipitation and injection problems developed during the project. A diatomaceous earth filter system was developed to filter the soluble-oil micellar solution. Heated lines and tanks were

also employed (to maintain enough temperature) to keep the waxy solids in solution, so that the micellar could be injected into the reservoir before cooling to the wax temperature. As a safeguard, it would have been desirable to have filtered the waxy oil at a temperature lower than the reservoir temperature.

The startup of polymer flooding resulted in some liquid polyacrylamide plugging the flow lines before mixing with injection water. The cause of this problem was found to be injection water contacting the concentrated polymer solution without adequate mixing. Additional problems due to undissolved or partially hydrated polymer resulted in the plugging of small restrictions in the flow system. Installation of additional filtering, mixing, and heating equipment helped to overcome this problem.

The review of field facilities was based solely on information provided in annual technical reports and publicly available literature.³⁴ The results of this review indicate that the facilities were planned, constructed, and operated in a manner consistent with current technology. However, several modifications to the injection facilities are recommended. These recommendations include replacement of throttling valves on the injection manifold, which may shear and degrade the injected polymer, with pinch type valves as used by Conoco or possibly a length of small diameter tubing as used by Phillips and Marathon. The upflow sand filter cannot usually achieve the quality of preflush filtration desired unless a flocculent is used in conjunction with the filter. In addition, filtration is also desirable after mixing and dilution of the surfactant and polymer solution for both pattern areas. Also, note that a considerable effort was made to maintain the performance of injection wells by acidizing. This suggests plugging due to inadequate filtration of the injection fluids. Installation of a downstream filter may have helped to eliminate injection well plugging during the project period.

RESERVOIR HISTORY AND DESCRIPTION

A thorough description of the Chesney and Hegberg leases is necessary in order to understand the behavior of the micellar-polymer floods conducted in the El Dorado Field. A brief reservoir description was given in the introduction. The following section provides an historical, geological, and engineering background of the El Dorado Field with emphasis on the pattern area.

The unsuccessful results of this micellar-polymer flood may have been expected after a review of previous injection and production operations, core analysis, logging, pressure transient tests, and geology. The interpretation of these data is different from those published by Cities,¹⁻⁸ and we believe provides a more consistent explanation of the process behavior. Because Cities' interpretation, particularly the geological interpretation, formed the basis for the design and operation of the project, a summary of Cities' conceptual geological model is given in Appendix A.

PRODUCTION HISTORY

The El Dorado Field is located in Township 25 South, Range 5 East, Butler County, Kansas. Most of the field is operated by Cities Service and some smaller portions were operated by Skelly, Texaco, and Sohio.³⁶ The Admire Sand (650 foot sand) was discovered in September 1915. Most of the wells were drilled between 1910 and 1920 and continued to produce into the early 1950s. Initially, the production rate was 40 to 80 barrels of oil per day per well, although a few wells produced oil in excess of 100 barrels per day. During primary recovery, the wells flowed for a short time before declining rapidly, requiring the wells to be equipped with pumps. Primary recovery was essentially complete by 1924; at which time, about 14.5 million barrels of oil had been produced.²⁹ Figure 40 shows the major units in the field and also locates the sites of the pilot tests discussed in the following paragraphs.

During 1924 and 1925, a pilot air injection test began in Section 29 using one air injection well and eight oil producing wells. Good results were obtained, and the air flood commenced full-scale operation in 1926. The first development included approximately 110 air injection wells and 500 producing wells. Later, the project was gradually expanded to include a total of about 770 wells. The air flood was continued, at least in parts of the field, until about 1954. Recovery by air injection accounted for 12.2 million barrels of oil.²⁹

In 1937, while the air flood process was still in operation, a pilot waterflood using fresh water was initiated on the Hegberg lease. The injectivity of the well dropped off rapidly. After the well developed injectivity problems, a second injection well was added. During the period from 1937 to 1939, a total of 190,000 barrels of water was injected into the two wells. An increase in the rate of oil production was not observed. The poor injectivity was attributed to formation sensitivity to fresh water injection. A second waterflood pilot using salt water began in 1947 on the Pierpont lease with four injection wells drilled between existing producing wells to give a spacing of about six acres per well. The Pierpont lease (in the southeast part of the field) is on the fringes of the El Dorado Field, and was not located in a portion of the field where air injection response was previously observed.

The waterflood increased production to about 230 barrels per day from the Pierpont lease. Production in surrounding wells averaged about 7 to 8 barrels per day. The waterflood pilot was expanded slowly through the early 1950s. By 1955, nearly 4,000 acres were included in the project, with over 200 injection wells and about 448 producing wells. Water for the Pierpont waterflood pilot was obtained from the Arbuckle Limestone. Table 6 shows the composition of the supply water, produced water, and mixed water, as typically injected in the El Dorado shallow waterflood. Note the high sulfate ion concentration in the supply water.

The most common completion method for the water injection wells was to set casing on the formation top, drill, and underream through the

producing interval. Wells which did not have an adequate injection rate were explosively stimulated with nitroglycerin followed by cleaning of the well bore. Old wells were used as production wells unless there were severe casing leaks which could not be repaired. Overall, it was necessary to redrill about 25 percent of the production wells. The new production wells were also stimulated using nitroglycerin.

The peak water injection rate occurred in 1955, with about 11.5 million barrels of water injected per year. In 1955, water production was approximately 5.4 million barrels per year and oil production was approximately 1.42 million barrels per year. The oil production climbed slowly to about 1.6 million barrels per year from 1955 to 1959.²⁹

A steam injection pilot project was initiated in 1964 due to the high oil saturation thought to remain after the waterflood project. The Hegberg lease, Section 28, was the site of the steam pilot (Figure 37) which consisted of four inverted 5-spot patterns, with nine injection wells and four producing wells. Prior to the initiation of the steam project, the oil cut average of the four producing wells was about 1 percent. During the peak response to steam injection, which occurred after a positive temperature rise and a drop in chloride concentration was observed in the producing wells, the maximum oil cut was only 2.75 percent.³⁰

CORING AND CORE ANALYSIS

Cored Wells and Routine Core Tests

A total of 35 wells were cored for the El Dorado micellar-polymer project. Nine of the 35 wells were cored with formation water and sodium sulfite to obtain "native-state" cores. One core was obtained using a low loss emulsion mud, and 25 wells were cored using formation water as the coring fluid. Oriented cores from Wells MP-112, MP-126, and MP-211 were obtained for directional permeability measurements.

Routine air permeability, porosity, and fluid saturation measurements were performed using core plug samples from 31 of the 35 cored wells. Air permeability measurements were used to obtain variance factors using the Dykstra-Parsons analysis technique. Porosity and fluid measurements were correlated with log analysis results and used in volumetric calculations. The capacity (Kah) was calculated for each cored well from air permeability and plotted on the capacity distribution map, Figure 42. An oil saturation distribution map derived from core analysis is shown in Figure 41.

Oriented whole-core air permeability measurements were performed on cores obtained from Wells MP-112, MP-126, and MP-211. The north-south air permeabilities are typically higher than east-west air permeabilities. The differences in directional permeabilities are usually less than 10 percent. However, when core plug samples are used to measure directional permeability instead of whole-core samples, the differences in directional permeability usually exceed 20 percent and are as high as 70 percent.

Special Core Analysis Tests

Additional core analysis tests include mercury injection capillary pressure tests, wettability tests, fresh water injectivity tests, and relative permeability tests. The results of these tests are described below.

Mercury injection capillary pressure tests were performed on core samples from Wells MP-106, MP-110, and MP-122. The samples were cleaned, dried, and used to obtain routine core analysis data before mercury injection tests were performed. Mercury injection tests indicated that more than 70 percent of the pore throat radii are greater than 1.0 micron in size.

Wettability tests were performed on "native-state" core samples from Wells MP-114, MP-124, MP-209, and MP-217 were performed. Test results indicated an intermediate to slightly oil-wet nature of the core material. However, tests performed on heated test samples indicated rock wettability could be altered as unheated core samples displayed an increased oil-wetting tendency.

Fresh water sensitivity tests were performed using core material from several wells. Some of the samples used in these tests displayed a sensitivity to fresh water with a liquid permeability reduction averaging 28 percent. It is unclear if the sensitivity observed during some of these tests is a widespread problem that affected chemical injection in the project area or if the sensitivity was limited. The results of analyses of the Admire 650 foot sand by X-ray diffraction (XRD) techniques are provided in Table 7. The results of these analyses show that the Admire sandstone contains a significant quantity of clay minerals. Clay minerals such as kaolinite, illite, and montmorillonite exhibit flow rate and fresh water sensitivity as well as an increased cation exchange capacity which may explain the fresh water sensitivity observed in some of the El Dorado samples which were tested.

The predominant clay minerals appear to be kaolinite and illite. Illite was reported in the X-ray diffraction test results. However, the responses observed for illite and mica when analyzed by X-ray diffraction are identical. A visual inspection of the core material indicates that mica is abundant in El Dorado core material and is probably present in the core material instead of illite.

Relative permeability tests were performed using core plug samples from Wells MP-104, MP-124, and MP-217 and included steady-state drainage and imbibition, unsteady-state drainage and imbibition, and end-point drainage and imbibition tests. The results of these tests suggest also that the Admire sand has an intermediate to slightly oil-wet nature. The results of these tests were used to calculate relative mobilities of the oil and water phases for the project.³¹

LOGGING RESULTS

Saturation From Logs

Formation evaluation was implemented using well logs from almost all of the wells drilled in the project area. Open-hole logging was performed using dual-induction-laterologs, compensated neutron and density, spontaneous potential, caliper, and gamma ray logs. The epilog analysis method was used to evaluate logging results.

Results of well logging indicated the oil saturation in the region of the wellbore of some wells was higher than suggested by core analysis. The geometric mean oil saturation for each well as calculated in Reference 1 is plotted on the oil saturation distribution map, Figure 43. Several wells have average oil saturations of 35 to 45 percent. However, a study of the relative permeability data indicates the residual oil saturation after waterflooding is about 26 percent. Therefore, wells with oil saturations of 10 to 20 percent above residual oil saturation should exhibit a high oil cut during additional waterflooding. Initially, Wells MP-207 and MP-214 produced at only about 4 percent oil cut. All other wells had immeasurably low oil cuts at the start of the preflush. This suggests that although well logs indicate high oil saturation, the oil saturation pattern-wide may be near residual oil saturation.

The response to steam flooding initiated in 1964 is also difficult to explain in light of the postulated 40 percent oil saturation. The response observed during the steam pilot suggested a very low oil saturation which is contradictory to log interpretation and to the material balance of the field based on the assumed initial saturation.

The apparent discrepancy between laboratory test results and log analyses prompted a review of the log analysis in more detail. Several core plug samples were supplied by the project operator, Cities Service Oil Company, for additional laboratory study. Briefly summarized, the laboratory measurements of formation factor, resistivity index, and

grain density of selected samples were measured and compared to reported test results. Some discrepancy was observed between grain density measurements reported by Cities Service and those reported by Keplinger Laboratories, but they are probably due to differences in extraction and cleaning techniques. Otherwise, the formation factor and resistivity indexes obtained experimentally were similar to values reported earlier, indicating that the saturation values are correct. With the saturation data verified, the question still remains as to how oil saturation can be significantly above residual values and still produce at such low oil cuts.

One possible explanation for the high oil saturations interpreted from the logging calculation, stems from the presence of numerous thin mica-rich laminae scattered throughout the producing intervals of the reservoir. The micaceous laminae may serve as vertical permeability barriers separating discrete lenses and layers of sandstone, with an average spacing estimated to range from one to four inches. This spacing is smaller than the vertical resolution of the logging tools employed in the analysis, resulting in a vertically averaged log response of multiple layers and beds within the reservoir interval. The net effect of this microstratification is best illustrated by an example. Assume the presence of three discrete sandstone layers separated by micaceous laminae within a given foot of reservoir interval having permeabilities of approximately 1,000, 700, and 300 millidarcies, respectively. The microstratification could result in a poor sweep efficiency during secondary and tertiary recovery projects. For example, the air flood may have reduced the oil saturation within the highest permeability strata to approximately 15 percent, while the waterflood may have reduced the oil saturation within the second interval to approximately 30 percent. The injected water may have contacted additional oil after air injection because of its improved mobility ratio, but waterflooding failed to sweep the third zone which was depleted only by primary production. This zone may have in excess of 50 percent oil saturation. The resulting average oil saturation for the three sandstone layers is 37 percent, which agrees with the calculated value from electric logs and may explain the high oil saturation values interpreted from log analysis at the El Dorado Field.

A review of core analysis results provides further insight into the nature of the oil saturation anomaly. Core analysis data for Wells MP-106 and MP-205 indicate the presence of permeable zones with oil saturations of 15 percent or less, deep within the reservoir interval.¹ It is postulated that these low oil saturation values deep within the sand body correspond to laminar zones which were preferentially swept in the course of air injection of the reservoir.

The microstratified reservoir model described above may also help to explain the poor performance of the steam flood attempted at El Dorado. It is probable that the injected steam preferentially channeled into layers which had been previously swept by air injection. Since the air flood was probably very efficient in reducing the oil saturation in layers contacted, there was very little additional oil available for recovery by the steam drive.

Mineralogy From Logs

The basic logs for Wells MP-130, MP-208, and MP-228 were studied to review mineralogy and the sedimentary interpretation. The basic logs for Well MP-130 were supplied by Cities Service and logs for Wells MP-208 and MP-228 were printed in References 1 and 2, respectively. It will be helpful in the following discussion to recall that the typical sonic travel time for gypsum is about 52 to 56 msec/ft and its bulk density is 2.32 to 2.35 gm/cc.

Figure 41 is a section of the gamma ray-caliper, induction, resistivity, and sonic logs for Well MP-130. A gypsum layer is identified at a depth of about 593 feet. This zone has the following characteristics: sonic travel time is approximately 60 seconds; gamma count increases from shale line; the resistivity increases and the density decreases approaching 2.3 gm/cc.

With these characteristics in mind, the 10 foot interval just above the main sand which begins at 625 feet was examined. This interval is composed of three beds: lime, shale, and gypsum. Each of these beds is

about three feet thick. It is seen that the gypsum layer at a depth of 623 feet has similar characteristics as the interval at 593 feet. The sonic travel time is about the same in both the gypsum and lime layers, but the density log response decreased to nearly 2.3 gm/cc for the gypsum, and increased to about 2.7 gm/cc in the lime layer. Similar interpretation can be made for Wells MP-208 and MP-228.

The interpretation of gypsum at the top of the sand suggests the possibility of interbedded gypsum and random gypsum intrusion throughout the sand body. This view is consistent with the finding of gypsum in core floods and with the performance discussed earlier. It also represents an alternative geological interpretation of the sedimentary nature of the beds from that given in the annual project reports and summarized in Appendix A.

ANALYSES FOR CALCIUM SULFATE AND BARIUM

Caustic Consumption Tests on Cores

The presence of calcium sulfate within the Admire Sandstones has been cited as a factor which may influence the consumption of caustic preflush components and the chemical degradation of the micellar slug.⁵ Calcium sulfate was not detected in the initial analysis of El Dorado core material. However, after the poor performance of reservoir preflushing, the laboratory core tests were re-examined, resulting in the discovery of calcium sulfate.

Caustic consumption tests were performed on crushed core material from five wells within the northeast quadrant of the Hegberg pilot area using an equivalent concentration of caustic silicate solution as was present within the preflush solution. The weight percent of sulfate present within the spent caustic solution was determined from the addition of barium chloride and the subsequent precipitation of barium sulfate. This procedure serves as an indirect measure of the weight percent of calcium sulfate present within the crushed core sample. Table 8 summarizes the caustic consumption, sulfate liberated by the caustic

solution, and calculated weight percent of calcium sulfate determined from these analyses. Tests performed by Holm and Robertson²² on core samples of Admire Sandstone revealed very high consumption values of sodium orthosilicate (approximately 9 lb/bbl PV), as well as high sulfate concentrations within the circulating preflush solutions. Chemical analysis of core fragments from the same interval which were not flushed with the orthosilicate solution revealed the presence of 0.23 weight percent calcium sulfate. Other tests showed that this concentration of calcium sulfate can account for the high caustic consumption values observed in core flood tests.

Observation of Produced Concentrations

Additional data suggesting the occurrence of calcium sulfate within the Admire Sandstone is present in the form of produced fluid analyses from the south (Hegberg) pattern of the project area. Brines containing variable amounts of sulfate have been produced from several of the production and observation wells, providing an indirect indication that a soluble, sulfate bearing mineral (probably gypsum) is present within the reservoir interval.

Table 9 provides an analysis of caustic depletion for five wells from the northeast quadrant of the Hegberg pilot area.⁸ These data indicate that (1) the caustic solution was depleted prior to reaching the adjacent observation and/or production wells within this portion of the pilot area, and (2) a correlation exists between the caustic consumption values and the volume of calcium sulfate present within the reservoirs.

The occurrence of gypsum in the formation in sufficient quantities to destroy the effectiveness of both micellar processes was proven in References 21 and 22. In light of studies and tests after start of the project, the occurrence of gypsum is now obvious. In order to sharpen the interpretation of El Dorado results and to more easily recognize gypsum in other reservoirs, we ask why was the presence of gypsum overlooked at El Dorado? A possible explanation is that gypsum was disguised by the presence of barium.

An observation of particular importance is that during the waterflood there was a small concentration of sulfate produced in most wells and an absence of the barium ion. After the preflush started, however, there was a continuous production of barium at a concentration of approximately 250 ppm in most wells and an absence of the sulfate ion. These observations may be explained by noting that during the normal waterflood operation, the injection water contained approximately 1,700 ppm sulfate, while during the preflush and micellar slug injection, there was no sulfate except the low concentration inherent to the sulfonate. Further, it may be inferred that there was a continual release of barium from the rock of about 1,500 ppm, since during the waterflood operation there was a small excess of sulfate, but no barium was produced. This means that the barium was precipitated as barium sulfate. After the waterflood, sulfate was not injected but was released at a constant 1,100 ppm by dissolution of calcium sulfate. Since barium continued to be released at approximately 1,500 ppm there was now an excess of barium and the sulfate was precipitated.

Laboratory Tests for Gypsum and Barium

The presence of gypsum was conclusively demonstrated in laboratory tests and the presence of barium is logically implied from geological considerations discussed in the next subsection. However, the presence of barium had not been shown by laboratory tests; therefore, an experiment was performed by Keplinger Laboratories, Inc. to substantiate the presence of barium, calcium, strontium, and sulfate by elution from the Admire Sand with water or diluted hydrochloric acid. The results of this test are presented in Table 10.

The cleaned and crushed rock was soaked and eluted in a series of deionized water washes followed by a final elution of hydrochloric acid. The results of Table 10 show the total quantity of the ions analyzed removed after the first wash of about 15 PV. Considering that a large amount of material must have been removed with the first wash, we interpret Table 10 to corroborate Reference 6 which demonstrated that at

least 0.3 weight percent gypsum is present in the formation. Table 10 also confirms that barium and strontium are in sufficient quantities to support the postulated mechanism and to corroborate the existence of 0.16 weight percent barium from geologic considerations discussed in a subsequent section.

The presence of the gypsum can be explained by the tidal flat deposition discussed in the next subsection. Gypsum can also be produced by the reaction of the sulfate ion and calcite to form sodium bicarbonate and gypsum if there is water movement and the water is slightly acidic.

ALTERNATE DEPOSITIONAL MODEL

It is evident from the above discussion that the presence of calcium sulfate within the Admire Sandstones constitutes a major factor in the failure of both the micellar and polymer processes. However, the presence of calcium sulfate within the reservoir interval is incompatible with the interpretation of a deltaic sequence given in Reference 7. An alternative interpretation is presented which we believe logically explains the occurrence of gypsum and also better explains the logging interpretations and flow properties.

The in situ presence of calcium sulfate within the Admire Sandstone requires a modification of the environmental interpretation proposed by Jordan and Tillman.⁷ Their depositional model characterized the Admire reservoir interval as an interbedded sequence of deltaic sandstones and mudstones deposited within interdistributary bay, splay channel, beach, and distributary channel environments. This package of deltaic sediments is overlain by fine grained levee and swamp deposits which were subsequently submerged and transgressed by marine bay claystones and limestones followed by open marine limestones.⁷

An alternative depositional model which may explain the origin of the reservoir sandstones within the Admire Formation involves deposition of these sediments within a migrating complex of tidal channels. This hypothesis is supported by the presence of an abundance of thin microlaminae of mica distributed throughout the reservoir sandstone facies sediments. The micaceous laminae are evenly distributed and spaced at intervals of approximately 1 to 3 centimeters, occurring as sheet-like drapes capping interlaminated, generally ripple-bedded, sandstone layers. The presence of the micaceous laminae throughout the reservoir sandstone facies suggests the predominance of laminar flow conditions within a depositional environment characterized by periodic fallout of suspended material - possibly during periods of reduced current flow, such as high or low tide. Similar characteristics have been described from recent subtidal and channel-fill deposits from the North Sea coast of Europe³³ and from estuary-tidal channel sandstones of

the Cretaceous Dakota Group in Colorado.³³ Although a detailed examination of core material from the El Dorado project area is beyond the scope of this review, the abundance of the interbedded micaceous laminae which dominates the reservoir sandstone facies with the Admire Formation seems to preclude a deltaic distributary channel depositional environment for these sandstones. Fluvially dominated distributary channel sandstones are not characterized by regular fluctuations in current velocity which would allow for deposition of the sheet-like micaceous laminae present within the Admire sandstones. It should be emphasized that given the presence of turbulent flow conditions, mica flakes (with crystal diameters in the very-fine to fine sand size range) would be transported as suspended sediment and would only be deposited in the event of a decrease in current velocity and the transition to laminar flow conditions.

Overlying the reservoir sandstones of the Admire Formation within the El Dorado project area is a sequence of very-fine-grained sandstones, silts, clays, and limestones which are variously interpreted by Jordan and Tillman⁷ as deposits formed within levee, swamp, and protected bay sub environments characterizing the abandonment and subsequent transgression of the deltaic distributary channel. The transitional sequence of sediments separating the underlying reservoir sandstones and the open marine limestones could represent deposits formed within a tidal flat setting which would locally favor the precipitation of evaporite minerals. The transitional facies recognized by Jordan and Tillman⁷ include the protected bay biomicrite facies with local lagoonal shale and the protected bay claystone and shale facies. The lithologic descriptions provided for these units are analogous in many respects to both modern and ancient tidal flat sediments.³³ The precipitation of evaporite deposits is very common within the lower and upper intertidal facies, in addition to occurring within salt marsh deposits. Lower intertidal facies sediments are characterized by extensively bioturbated silty clays which commonly contain laminar concentrations of sand and shell debris near the boundary with the overlying upper intertidal facies sediments. The upper intertidal facies is dominated by laminated silt which is commonly disturbed due to bioturbation, shrinkage, and the

crystallization of evaporites. The dessication features present within this facies are commonly mistaken for burrows and root structures within cores penetrating this facies. Salt marsh deposits closely resemble the upper intertidal facies sediments with the exception that burrow mottling is much less common. Salt marsh deposits are commonly characterized by an erosional base, abundant root structures (which may be infilled with sand or iron hydroxide), irregularly distributed evaporite minerals, and abundant organic detritus derived from the marsh vegetation. The characteristics of the facies described above are similar to descriptions of the protected bay biomicrite facies with local lagoonal shale and the protected bay claystone and shale facies deposits from the El Dorado project area.⁷ Localized lagoonal sedimentation may have occurred in the course of the marine transgression which ultimately submerged the deltaic sediments within the pilot area; however, the presence of tidal flat deposits characterized by the localized precipitation of evaporite minerals cannot be ruled out based upon the available geologic data.

Presence of Barium is Supported by Geological Conditions

The presence of anomalously large amounts of barium and strontium within the pore waters of the Admire Sandstone is believed to have contributed to the degradation of the micellar-polymer solutions injected at the El Dorado project area. Resident water compositions within the eight production wells analyzed prior to the injection of preflush fluids indicate concentrations of barium and strontium which average 240 and 473 meq/L, respectively. These cations may be expected to readily combine with sulfonate ions present within the injected fluids and either partition into the oil phase or precipitate within the pore spaces of the reservoir rock. Interbedded shale laminae, mica, and authigenic clay constitute the most probable source for the barium and strontium present within the produced fluids of the Admire reservoir. Cubitt's⁹ analysis of the geochemistry of Upper Paleozoic shales of Kansas listed average barium and strontium concentrations of 300 and 225 ppm, respectively, for outcrop samples of Admire shales north of the project area. In the absence of geochemical analyses of Admire shales

within the El Dorado Field, these data constitute a first order approximation of the barium and strontium content within clays and mica present within the reservoir. Barium and strontium occupying cation sites on the surface of clay and micaceous minerals would be prone to exchange with available sodium and calcium present within the pore fluids of the reservoir. The large volume of mica and clay contained within these sandstones, especially within the interbedded interdistributary bay, splay channel, and beach facies and the inactive channel fill facies sandstones essentially provide an unlimited number of surface exchange sites.

PRESSURE TRANSIENT ANALYSIS

Extensive pressure transient tests were completed in the project area during 1975 and 1976. Tests were conducted involving 17 injectors and 8 producers in the Chesney and Hegberg patterns, and the testing procedures and analyses were reported by Swift and Brown.³³ These tests included interference testing, pressure build-up, and pressure falloff tests.

The results of these tests were used to evaluate the condition of the wells before chemical injection began. In addition, interference tests were used to aid in choosing the well spacing within the project area. The results of these tests indicated a 6.4 acre, 5-spot pattern was more suitable than a 3.2 acre, 5-spot pattern.

The results of these tests were used to calculate formation flow capacity. The resulting capacity (K_{eh}) data are presented in Figure 45. A capacity contour map was also generated using air permeability (K_a) data from core analyses, as shown in Figure 42. A comparison of the two capacity contour maps demonstrates good agreement. K_e , the water permeability at existing residual oil saturation, is adjusted to air permeability (K_e is approximately ten percent of K_a).

Discrepancies exist between the pressure transient tests described above and tests performed later in the life of the project. For instance, the latter transient testing suggested a barrier between Well MP-226 (replacement twin to Well MP-213) and observation Well MP-227. This finding is contradictory to the results of the first series of field tests. In addition, the second series of pressure transient tests indicated the closure of a fracture which existed between Well MP-213 and Well MP-227 which contradicts the results of chemical tracer response between these wells. Possible causes for these discrepancies include damage from scaling and inadequate perforation data in the test wells.

TRACER TESTS

During 1975 and 1976, six chemical tracers were used to detect gross channeling in the project area. The chemical tracers were injected using the 18 injection wells within the Chesney and Hegberg leases. Sampling and analysis of fluids from the 8 producing wells was performed on a regular basis for 7 weeks. The tracers were not detected during this time, indicating there was no gross channeling between wells in the pattern area. Tracer chemicals were produced at several of the production wells after the 7-week test period. Analysis of chemical tracers after the 7-week test period was performed sporadically and interpretation of these data was not attempted.

A second chemical tracer program was initiated in October 1978. The chemical tracers included ammonium thiocyanate, methanol, radioactive cobalt 57, cobalt 60, and tritiated water. A review of the data obtained during the tracer tests revealed that chemical analysis of the produced fluids was initiated after tracer breakthrough had already occurred. For example, Well MP-207 produced 100 pci/liter of cobalt 57 beginning in January 1980 and 150 pci/liter of cobalt 60 beginning in February 1980. The concentration of these tracers continuously decreases over a period of time. An increase in tracer concentration was not observed. Typically, tracer breakthrough is followed by an increase to some maximum tracer concentration. After reaching a maximum value, the tracer concentration should slowly decline over a period of time. The results indicate the analysis of the chemical tracers began too late to detect tracer breakthrough and the production of the maximum concentration of tracer. Therefore, no further attempts were made to evaluate the second tracer program.

Additional chemical tracers were used to monitor the progress of the chemical flood. Secondary butyl alcohol and isobutyl alcohol were used as tracers and were included in the micellar-polymer chemical slugs. These tracers were detected at the production wells just prior to oil and surfactant breakthrough. The results of these tracer tests were used in the interpretation of project performance.

FLUID MIGRATION

Pressure Gradient Across the Pattern

Reservoir pressure was measured at the monitor wells in the pattern area (Figure 4). Pressure changes were monitored and used to aid reservoir description. The reservoir pressure at the start of the pre flood was approximately 215 psi in the southwest quadrant of the project area. In northeast test Well MP-102, reservoir pressure was approximately 130 psi. A pressure gradient of 100 psi was uniformly distributed across the reservoir, as shown in Figure 46.

Due to over-injection, pressure in the monitor wells increased until August 1977. After August 1977, the monitor well pressures dropped rather drastically. Coincidentally, the injection pressures began to increase during this time. These events raise the question of pressure parting at the injection wells. Step rates for Wells MP-103 and MP-104 are given in Reference 1. A study of the step rate tests suggest parting may occur at a surface pressure of 100 psi injection pressure.

Although the pressure observed in the monitor wells does not agree well with pressures predicted by computer simulation, better agreement between observed and predicted pressures occurred when an extraneous source located northwest and a sink located southeast of the project area were included in the reservoir model. However, observed and predicted pressures did not follow a trend and the differences were not predictable, suggesting that the extraneous source and sink were not constant. The extraneous source is consistent with the observation that both pressure and chloride concentrations were higher than predicted. Other possible explanations for these observations fail to explain this behavior. The effects of heterogeneity, for example, would result in a decrease in salinity but maintain a relatively constant pressure.

Extraneous sources and sinks are expected in old fields like El Dorado. There are offset operators in the same zone and in other producing intervals, as shown in Figure 40. It is sometimes difficult to know the

nature of other nearby field projects or what other operators are doing in nearby wells. There is the possibility of fluid movement behind the pipe of old shut-in or abandoned wells. There was also considerable down time during the pilot project. All of these factors make predictions of fluid movement and the effect of pressure extremely difficult.

Irregular Produced Water Confirms Migration

Changes in the ion concentrations in water from observation wells were previously discussed and it was suggested that variations in concentrations may have been due to extraneous entry of water into the project area. For example, the concentration of calcium at observations Wells MP-131 and MP-132 and produced at Well MP-124 are shown in Figures 13, 16, and 19, respectively. The concentrations of these ions in the injected brine are shown in Table 7. The hardness and salinity levels in produced water from Well MP-131 approached injected levels after about 300 days. Well MP-131 is located 90 feet away from the central water injection well. After the injected hardness and salinity levels were reduced, Well MP-131 responded with lower hardness and salinity levels. However, Well MP-132 located 190 feet from the same injector, did not respond to changes in injected fluid compositions. In fact, calcium and magnesium concentrations in observation well MP-132 actually increased above injected levels on some occasions during the project period. Minimum levels of hardness were observed during the project and occurred sooner than expected when reservoir and injected volumes are compared. Chloride concentrations demonstrate similar anomalous behavior. The discrepancy in concentration profiles of Well MP-132 and other wells within the project area suggests an influx of high salinity water into both patterns. This influx is believed to be the result of the pressure gradient across the project area.

The movement of mobile oil into the project area due to the presence of a pressure gradient is also a possibility. However, additional information would be required to evaluate the possibility of migrating oil from a source outside of the project area. If mobile oil was discovered to be entering the project area, this would help to explain the higher oil production from wells such as Well MP-114 which showed little response to the micellar-polymer project.

CONCLUSIONS

The study of the field test results of an oil soluble and a water phase micellar process in the El Dorado Field lead to the following conclusions:

1. Both micellar processes failed to recover measurable additional oil; therefore, they are interpreted to be economic and technical failures. The failure of both processes was attributed to a combination of the following causes:
 - a. Gypsum deposits in the reservoir.
 - b. Contact of the micellar fluids with extraneous high salinity, high hardness brine.
 - c. The irregular oil saturation distribution caused by mica sandstone lamina.
2. When the reservoir water has high salinity and high hardness, preflushing to adjust the ionic concentration is questionable, at best, but in reservoirs containing gypsum deposits, preflushing is probably futile.
3. Both micellar processes attempted at El Dorado can be shown to be theoretically similar; therefore, micellar degradation will occur if the surfactant is salt sensitive whether the surfactant is injected in the oil or water phase. Since a similar salt sensitive surfactant was used for both processes, their failures at El Dorado are interpreted to confirm the theoretical principle.
4. The El Dorado Field was a poor choice to test micellar processes using salt intolerant surfactants. Danger signs of an impending tragic failure should have been evident from study of previous injection projects and core flood tests.

RECOMMENDATIONS

In order to increase the probability of success for the micellar process, the following recommendations were drawn from the El Dorado study:

1. Since preflushing is probably futile and the method of injection does not overcome the basic problem of salt intolerance for common surfactants, it is recommended that further work be done to develop surfactants which are salt tolerant.
2. Thorough knowledge of the geological and reservoir engineering properties of the reservoir should be obtained before committing to a process and surfactant type. A detailed performance analysis of previous injection projects together with lithological studies from cores and electric logs should be incorporated in the geological deposition and reservoir flow properties studies.
3. Laboratory studies should be made in a systematic manner for two purposes: to recognize harmful conditions in the reservoir and to supply input data for a simulator model.

REFERENCES

1. "El Dorado Micellar-Polymer Demonstration Project", First Annual Report, Report No. BERC/TPR-75/1, U.S. ERDA, Oak Ridge, Tennessee, October 1975.
2. "El Dorado Micellar-Polymer Demonstration Project", Second Annual Report, Report No. BERC/TPR-76/4, U.S. ERDA, Oak Ridge, Tennessee, November 1976.
3. "El Dorado Micellar-Polymer Demonstration Project", Third Annual Report, Report No. BERC/TPR-77/12, U.S. DOE, Oak Ridge, Tennessee, February 1978.
4. "El Dorado Micellar-Polymer Demonstration Project", Fourth Annual Report, Report No. BETC-1800-40, U.S. DOE, Oak Ridge, Tennessee, April 1979.
5. "El Dorado Micellar-Polymer Demonstration Project", Fifth Annual Report, Report No. DOE/ET/13070-53, U.S. DOE, Oak Ridge, Tennessee, February 1980.
6. "El Dorado Micellar-Polymer Demonstration Project", Sixth Annual Report, Report No. DOE/ET/13070-63, U.S. DOE, Oak Ridge, Tennessee, April 1981.
7. "El Dorado Micellar-Polymer Demonstration Project", Seventh Annual Report, Report No. DOE/ET/13070-79, U.S. DOE, Bartlesville, Oklahoma, June 1982.
8. "El Dorado Micellar-Polymer Demonstration Project", Eighth Annual Report, Report No. DOE/ET/13070-92, U.S. DOE, Bartlesville, Oklahoma, September 1983.
9. Cubitt, J. M., "The Geochemistry, Mineralogy and Petrology of Upper Paleozoic Shales of Kansas", Kansas Geological Survey Bulletin 217, 1979.
10. Healy, R. N., Reed, R. L., and Carpenter, C. W., "A Laboratory Study of Microemulsion Flooding", SPEJ, February 1975, pp. 87-103.
11. Chatzis, I. and Morrow, N. R., "Correlation of Capillary Number Relationships for Sandstone", SPEJ, October 1984, pp. 555-562.
12. Reed, R. L. and Healy, Robert N., "Physicochemical Aspects of Microemulsion Flooding", SPEJ, October 1974, pp. 491-501.
13. Hirasaki, G. J., van Domselaar, H. R., and Nelson, R. C., "Evaluation of the Salinity Gradient Concept in Surfactant Flooding", SPEJ, June 1983, pp. 486-500.
14. Somasundaran, P., et al., "A Thermodynamic Model of Redissolution of Calcium Sulfonate Precipitates in NaCl Solutions", SPEJ, December 1984, pp. 667-676.

15. Lake, L. W. and Helfferich, F., "Cation Exchange in Chemical Flooding: Part 2 - The Effect of Dispersion, Cation Exchange, and Polymer-Surfactant Adsorption on Chemical Flood Environments", SPEJ, December 1978, pp. 435-444.
16. Hill, H. J. and Lake, L. W., "Cation Exchange in Chemical Flooding: Part 3 - Experimental", SPEJ, December 1978, pp. 445-456.
17. Hill H. J., et al., " Cation Exchange and Chemical Flooding", JPT, October 1977, pp. 1336-1338.
18. Smith, F. W., "Ion-Exchange Conditioning of Sandstones for Chemical Flooding", JPT, June 1978, pp. 959-968.
19. Griffith, T. David, "Application of the Ion Exchange Process to Reservoir Preflushes", SPE Paper 7587 presented at the 53rd Annual Fall Technical Conference and Exhibition, Houston, Texas, October 1-3, 1978.
20. Hirasaki, George J., "Ion Exchange with Clays in the Presence of Surfactant", SPEJ, April 1982, pp. 181-192.
21. Bernard, George G., "Effect of Clays, Limestone, and Gypsum on Soluble Oil Flooding", JPT, February 1975, pp. 179-180.
22. Holm, L. W. and Robertson, Steven D., "Improved Micellar/Polymer Flooding with High-pH Chemicals", JPT, January 1981, pp. 161-171.
23. Chan, Albert F. and Gupta, Surendra P., "The Propagation of Oil Moving and Solubilizing Components of Broad Equivalent Weight Sulfonate Systems in Micellar Floods", SPE Paper 10200 presented at the 56th Annual Technical Conference and Exhibition, San Antonio, Texas, October 5-7, 1981.
24. Claridge, E. L. and Lohse, A., "Data Requirements for EOR Surfactant-Polymer Process Simulation and Analysis of El Dorado Pilot Project Simulation, Butler County, Kansas", Report No. ET/10145-74, Volumes I and II, U.S. DOE, Bartlesville, Oklahoma, January 1983.
25. Holm, L. W., "Correlation of Oleic and Aqueous Micellar Processes for Tertiary Oil Recovery", SPE Paper 7066 presented at the Fifth Symposium on Improved Methods for Oil Recovery, Tulsa, Oklahoma, April 16-19, 1978.
26. Holm, L. W., "Use of Soluble Oils for Oil Recovery", JPT, December 1971, pp. 1475-1483.
27. Mohnot, S. M., Bae, J. H., and Foley, W. L., "A Study of Mineral-Alkali Reactions", SPE Paper 13032 presented at the 59th Annual Technical Conference and Exhibition, Houston, Texas, September 16-19, 1984.

28. Sydansk, Robert D., "Elevated-Temperature Caustic/Sandstone Interaction: Implications for Improving Oil Recovery", SPEJ, August 1982, pp. 453-462.
29. Powell, J. P., Waterflooding of Oil Sands in Butler and Greenwood Counties, Kansas, Bureau of Mines Information Circular 7750, United States Department of the Interior, May 1980.
30. Hearn, C. L., "The El Dorado Steam Drive - A Pilot Tertiary Recovery Test", SPE Paper 3780 presented at the Improved Oil Recovery Symposium of the Society of Petroleum Engineers of AIME, Tulsa, Oklahoma, April 16-19, 1972.
31. Chang, H. L., et al., "Determination of Oil/Water Bank Mobility in Micellar-Polymer Flooding", JPT, July 1978, pp. 1055-1060.
32. Weimer, R. J., Howard, J. D., and Lindsay, D. R., "Tidal Flats", in Scholle, P. A. and Spearing, D. (eds.), Sandstone Depositional Environments, AAPG Memoir No. 31, April 1982.
33. Swift, S. C. and Brown, Larry, "Interference Testing for Reservoir Definition - The State of the Art", SPE Paper 5809 presented at the Improved Oil Recovery Symposium of the SPE, Tulsa, Oklahoma, March 22-24, 1976.
34. Miller, R. J. and Richmond, C. N., "El Dorado Micellar-Polymer Project Facility", JPT, January 1978, pp. 26-32.
35. State Geological Survey of Kansas, "Data on Secondary Recovery Projects in Kansas", Bulletin 103, Table 1, 1952.

TABLE 1
DESCRIPTION OF NORTH (CHESNEY) PATTERN PROCESS

<u>Event</u>	<u>Composition</u>	<u>Date</u>	<u>Volume Injected (bbl)</u>	<u>Pore Volume*</u>
<u>Begin Preflood I (1 cp)</u>		11-22-75	352,735	0.394
Sodium Chloride	1.4 wt%			
Fresh Water	98.6 wt%			
<u>Begin Preflood II (1 cp)</u>		12-21-76	374,126	0.418
Sodium Chloride	2.9 wt%			
Calcium Chloride	0.102 wt%			
Magnesium Chloride	0.097 wt%			
Fresh Water	96.901 wt%			
<u>Begin Micellar Solution (32 cp)</u>		11-16-77	94,480	0.106
Surfactant	4.69 wt% of 56% active			
High equivalent weight sulfonate				
Low equivalent weight sulfonate				
Alcohol Ethoxysulfate	1.13 wt%			
Secondary Butyl Alcohol	4.13 wt%			
Bipolymer (Xanthan gum)	900 ppm			
Sodium Chloride	0.70 wt%			
Fresh Water	89.26 wt%			
<u>Begin Biopolymer (40 cp)</u>		11-17-78	84,026	0.094
Biopolymer	1,125 ppm			
Sodium Chloride	1.00 wt%			
Secondary Butyl Alcohol	2.00 wt%			
Fresh Water	96.89 wt%			
Cease SBA component of biopolymer		5-15-79	115,730	0.129
Reinitiate 2% SBA component of biopolymer and		12-19-79	10,930	0.012
Reduce salinity to 0.5 wt%				
Reduce salinity to 0.2 wt%		1-05-80	7,186	0.008
Reduce salinity to 0.05 wt%		1-16-80	14,911	0.017
Reduce salinity to 0.025 wt%		2-08-80	6,416	0.007
Reduce SBA to 1.5 wt%		2-18-80	12,021	0.013
Cease SBA and initiate isobutyl alcohol		3-08-80	19,601	0.022
Biopolymer	1,125 ppm			
Sodium Chloride	0.025 wt%			
Isobutyl Alcohol	1.00 wt%			
Fresh Water	98.86 wt%			
Reduce salinity to fresh lake water		4-09-80	1,165	0.001
Increase IBA component to 1.2 wt%		4-11-80	105,015	0.117

TABLE 1 (Continued)

DESCRIPTION OF NORTH (CHESNEY) PATTERN PROCESS

<u>Event</u>	<u>Composition</u>	<u>Date</u>	<u>Volume Injected (bbl)</u>	<u>Pore Volume*</u>
<u>Begin Polyacrylamide</u> (40 cp)		10-25-80	130,562	0.146
Nalflo-F Fresh Water	690 ppm active 99.93 wt%			
Initiate formaldehyde as biocide		11-29-80		
Polyacrylamide Slug 2 (30 cp)		6-22-81	38,619	0.043
Initiate Kathon WT as biocide		6-28-81		
Polyacrylamide Slug 3 (20 cp)		9-22-81	62,443	0.070
Polyacrylamide Slug 4 (10 cp)		1-07-82	43,498	0.049
Test Onyxide as Biocide		3-31-82		
<u>Begin Drive Water</u> (1 cp)		3-12-82		

* Effective confined Pore Volume = 894,257 bbl.

TABLE 2
CHRONOLOGY OF FIELD OPERATIONS
CHESNEY LEASE

<u>Event</u>	<u>Wells</u>	<u>Date</u>
Test wells drilled		Jun 1974
Breakdown tests	MP-103, 104	Dec 1974
Pattern wells completed		May 1975
Pressure transient tests finished	MP-124,114,112,122	Jun 1975
Acid stimulation, solvent stimulation	MP-114	Jun 1975
Final pattern configuration chosen		Jul 1975
Pressure falloff tests	MP-106,108,116,118 120,126,,28,130	Jul-Aug 1975
Fluids swabbed and analyzed	MP-120	Jul 1975
Injection plant completed		Aug 1975
Injection well profiles	MP-106,108,110,116, 118,120,126,182,130	Sep 1975
EDTA and fresh water treatment	MP-114	Sep 1975
Explosive/fracture and proppant stimulation	MP-110/114	Nov 1975
"Phased" fluid pretreatment (4 days)	all injection wells	Nov 1975
Begin Preflood I		Nov 1975
Acid stimulation	MP-120	Dec 1975
Monitoring well bottomhole pressures (BHP)	MP-101,104,109,115.127	Dec 1975
Acid stimulation	MP-106,116/116	Feb/Apr 1976
Acid stimulation	MP-108,110,118,120, 128,130	Mar 1976
Chlorine gas injected into fresh water lines for bacteria control		Mar 1976
Trichlorinated phenol with amine acetate added at injection plant		Apr 1976
Induction logs	MP-131	May-Jun 1976
Acid stimulation	MP-106,108,118,120, 126,128,130	May 1976
Injectivity test	MP-109,121	Aug 76-May 77
Induction logs	MP-131,132	Nov 1976
Monitoring well BHP	MP-107,109,111,113, 115,117,119,121,123 125,127,129	Dec 1976
Begin Preflood II		Dec 1976

TABLE 2 (Continued)

CHRONOLOGY OF FIELD OPERATIONS
CHESNEY LEASE

Event	Wells	Date
Monitoring wells BHP	MP-101,103,104,107, 109,111,113,115,117, 119,121,123,125,127,129	Feb, Apr 1977
Induction logs	MP-131,132	Mar 1977
Pressure falloff tests	all injection wells	Mar 1977
Buildup tests	MP-114,122	Mar 1977
Interference tests	MP-110,112	Apr 1977
Acid stimulation	MP-108,110	Apr 1977
Induction logs	MP-131,132	Jun 1977
Acid stimulation	MP-106,116	Aug 1977
Scale squeeze and fracture stimulation	MP-114	Oct 1977
Stop Preflood II	all injection wells	Oct 10, 1977
Restart Preflood II (8 days)		Nov 5, 1977
Begin micellar solution		Nov 15, 1977
Induction logs	MP-131,132	Jan 1978
Acid stimulation and jetted sandface	MP-116,118,130	Jan 1978
Monitoring wells BHP	MP-101,103,104,107, 109,111,113,115,117, 119,121,123,125,127, 129	Feb, Mar, Jun, Jul, Aug, Oct 1978
Acid stimulation and jetted sandface	MP-108,118,128/130	Apr/May 1978
Fracture and proppant stimulation	MP-114	Jun 1978
Five biocides tested in injection water	all producing wells contaminated	Jul 1978
Jetted sandface	MP-106,118/110,118, 120,126	Jul/Aug 1978
Acid stimulation	MP-118	Aug 1978
Induction logs	MP-131/131,132	Sep/Oct 1978
First oil movement	MP-131	Sep 1978
Tracer program initiated	all injection wells	Oct 1978
Begin biopolymer injection		Nov 1978
Acid stimulation	MP-108,130/106	Oct/Nov 1978
Acid stimulation	MP-118/108,114/ 106,114	Jan/Feb/ Mar 1979
Fracture and proppant stimulation and perforate	MP-114	Feb 1979
Monitoring well BHP	MP-101,102,103,104, 105,107,109,111,113, 115,117,119,121,123, 125,127,129	Mar, Jul, Nov 1979

TABLE 2 (Continued)

CHRONOLOGY OF FIELD OPERATIONS
CHESNEY LEASE

Event	Wells	Date
Biocide in biopolymer changed to glutaraldehyde/also in injection water		May 1979
Induction logs	MP-131	Jun 1979
Fracture and proppant stimulation	MP-114	Jun 1979
Perforated @ 652'/644'-648' and 652-658'	MP-132	Jun/Oct 1979
Jetted sandface and acidize	MP-118	Jul 1979
Injectivity up	pattern wide	Sep 1979
Viscosity decrease/biopolymer degraded by bacteria	MP-131	Sep 1979
Re-initiate SBA in biopolymer		Dec 1979
Induction logs	MP-132	Feb, Aug 1980
Reduce SBA in biopolymer		Feb 1980
Substitute isobutyl alcohol for SBA in biopolymer		Mar 1980
Five treatments of glutaraldehyde, 2,000 ppm	all producing wells	Apr-Jul 1980
Monitoring well BHP	MP-101,102,103,104, 105,107,109,111,113, 115,117,119,121,123, 125,127,129	May 1980
Glutaraldehyde, 250 ppm as biocide	all injection wells	Aug & Sep 80
First oil observed	MP-132	Sep 1980
Injection rates lowered/formation breakdown	MP-110,126,128,130	Sep 1980
Begin polyacrylamide Slug 1	all injection wells	Oct 1980
Begin Visco 3991 (DBNPA) as biocide	all injector wells	Oct 1980
Begin formaldehyde as biocide	all injector wells	Nov 1980
Polyacrylamide breakthrough	MP-131	Dec 1980
Monitoring wells swabbed	MP-107,109,111,113, 115,117,119,121,123, 125,127,129	Feb 1981
Screen factors measured	at all injector wellheads	Apr-Aug 1981
Perforated at lower zone	MP-131	May 1981
Injection profiles	MP-106,118,126,130	May 1981
Begin polyacrylamide Slug 2		Jun 1981
Begin Kathon WT as biocide	all injection wells	Jun 1981
Begin polyacrylamide Slug 3		Sep 1981
Install water softener and vacuum deaeration unit		Oct 1981
Discontinue biocide (only chlorine gas in use)	all injection wells	Oct 1981
Acid stimulation	MP-112,114,122,124	Nov 1981

TABLE 2 (Continued)

CHRONOLOGY OF FIELD OPERATIONS
CHESNEY LEASE

<u>Event</u>	<u>Wells</u>	<u>Date</u>
Begin polyacrylamide Slug 4	all injection wells	Jan 1982
Monitoring well BHP	MP-101,102,103,104, 105,107,109,111,113, 115,117,119,121,123, 125,127,129	Feb 1982
Begin drive water injection	all injection wells	Mar 1982
Test Onyxide 200	MP-118 to 131	Mar 1982
Monitoring wells swabbed	MP-111,113,115,117,119	Mar 1982
Monitoring wells pumped	MP-111,113,115,117,119	Apr-May 1982
Monitoring wells put on production	MP-111,115	May 1982
Induction logs	MP-132	Sep 1982
End contract		Nov 1982

TABLE 3

THE CHANGE IN WATER RESISTIVITY vs. FORMATION RESISTIVITY

<u>Date</u>	<u>Well MP-131</u> <u>$\sqrt{R_w/R_t}$</u>	<u>Well MP-132</u> <u>$\sqrt{R_w/R_t}$</u>
3-76	0.24	0.21
9-78	0.17	-
6-79	0.27	-
2-80	-	0.17
8-80	-	0.18

TABLE 4
DESCRIPTION OF SOUTH (HEGBERG) PATTERN PROCESS

<u>Event</u>	<u>Composition</u>	<u>Date</u>	<u>Volume Injected (bbl)</u>	<u>Pore Volume*</u>
<u>Begin Pretreatment (1 cp)</u>		11-18-75	118,500	0.147
Sodium Chloride	2.0 wt%			
Fresh Water	98.0 wt%			
<u>Begin Caustic Preflush (1 cp)</u>		6-20-76	134,776	0.168
Sodium Silicate	0.281 wt%			
Sodium Hydroxide	0.418 wt%			
Fresh Water	99.301 wt%			
<u>Begin Micellar Solution</u>		3-24-77	45,673	0.057
<u>Micellar Oil</u>				
Four Sodium Alkylaryl Sulfonates (equivalent weight 250-650, avg. 425)	23.85 wt%			
Ethylene Glycol Monobutyl Ether	2.63 wt%			
Greenwood County Crude Oil	66.78 wt%			
Fresh Water	6.74 wt%			
Micellar Water				
Sodium Chloride	0.25 wt%			
Nitritotriacetic Acid				
Trisodium Salt	0.65 wt%			
Fresh Water	99.10 wt%			
<u>Begin Polyacrylamide Polymer</u>				
<u>Slug 1 (120 cp)</u>		4-06-78	54,666	0.068
Nal-Flo-F G-6342	870 ppm			
TOL K-470 oxygen scavenger	80 ppm			
Visco 3991 (DBNPA) biocide	60 ppm			
<u>Slug 2 (80 cp)</u>		8-16-78	75,968	0.094
<u>Slug 3 (65 cp)</u>		2-21-79	104,191	0.130
<u>Slug 4 (50 cp)</u>		10-14-79	204,327	0.254
<u>Slug 4a (20 cp)</u>		6-08-81	1,951	0.002
<u>Slug 4a (10 cp)</u>		6-16-81	869	0.001
<u>Slug 4a (5 cp)</u>		6-19-81	2,055	0.003
<u>Slug 4a (1 cp)</u>		6-26-81	62,017	0.077
<u>Slug 4b (20 cp)</u>		12-19-81	195,231	0.242

* Effective confined Pore Volume = 804,500 bbl.

n = Reference number, Third annual report, pg. I-8.

TABLE 5
CHRONOLOGY OF FIELD OPERATIONS
HEGBERG LEASE

<u>Event</u>	<u>Wells</u>	<u>Date</u>
Test wells drilled		Jun 1974
Injectivity test	MP-104	Jun 1974
Acid stimulation	MP-221,225	Jul 1974
Breakdown tests	MP-103,104	Dec 1974
Pattern wells completed		May 1975
Pressure transient tests finished	MP-207,209,217,219	Jul 1975
Final pattern configuration chosen		Jul 1975
Acid stimulation	MP-213	Aug 1975
Pressure falloff tests	MP-201,203,205,211, 213,215,221,223,225	Jul-Aug 1975
Injection plant completed		Aug 1975
Injection well profiles	MP-201,203,205,211, 213,215,221,223,225	Sep 1975
Perforated 673'-679'	MP-213	Sep 1975
Explosive stimulation	MP-213,223,226	Nov 1975
"Phased" fluid pretreatment (4 days)	all injection wells	Nov 1975
Fracture/surfactant stimulation	MP-207	Nov 1975
Begin pretreatment		Nov 1975
Monitoring well bottomhole pressures (BHP)	MP-216,220,224	Dec 1975
Observation wells completed	MP-227,228	Feb 1976
Acid stimulation	MP-203,205/201,211	Feb/Apr 1976
Acid stimulation	MP-213,215,221,223, 225,226	Mar 1976
Chlorine gas injected into fresh water lines for bacteria control		Mar 1976
Induction logs	MP-227/228	Mar/Apr 1976
Trichlorinated phenol with amine acetate added at injection plant		Apr 1976
Injectivity tests	MP-211,225	May 1976
Acid stimulation	MP-203,213/203/215	May/Jul/Aug 1976
Induction logs	MP-227/227,228	May/Nov 1976
Begin caustic preflush		Jun 1976
Acid stimulate/injectivity test	MP-202	Nov 1976
Monitoring wells BHP	MP-202,204,206,208, 210,212,214,216,218, 220,222,224	Dec 1976

TABLE 5 (Continued)

CHRONOLOGY OF FIELD OPERATIONS
HEGBERG LEASE

Event	Wells	Date
Pressure falloff tests	MP-201,203,205,211, 213/226,215,221,223,225	Jan/Feb 1977
Pressure buildup tests	MP-207,219	Feb 1977
Monitoring wells BHP	MP-202,204,206,208, 210,212,214,216,218, 220,222,224	Feb, Apr, Sep 1977
Acid stimulation	MP-203,215,223/205,223	Feb/May 1977
Finish caustic preflush		Mar 1977
Begin micellar solution		Mar 1977
Perforated lower zone	MP-227,228	Apr 1977
Acid stimulation	MP-203,221,225/ 205,221,225/221	Jun/Jul/Sep 1977
Interference test	MP-213/226 to 227	Jul 1977
Circulate hot micellar water to stimulate	MP-211,213,226,215, 221,223,225	Oct 1977
Acid stimulation	MP-203,205,213,226,223	Oct 1977
Addition of 15 volume percent solvent to crude oil of micellar oil	all injection wells	Oct 1977
Explosive stimulation-jet formation- acidize	MP-223	Nov 1977
Fracture and proppant stimulation	MP-207,223	Dec 1977
Perforated @ 666', 668', 675', 677'-680	MP-227	Dec 1977
Induction logs	MP-227,228/228	Jan, Sep, Oct/Dec 1978
Acid stimulation	MP-221	Jan 1978
Monitoring wells BHP	MP-202,204,206,208, 210,212,214,216,218, 220,222,224	Feb, Mar, Jun, Jul, Aug, Oct 1978
Circulate hot micellar water/ acid stimulate	MP-213,226	Mar 1978
Begin polyacrylamide (PAM)	all injection wells	Apr 1978
Globs in PAM reducing injectivity	all injection wells	Apr 1978
Jetted formation face with saline/acid	MP-213,226	May 1978
Fracture and proppant stimulation	MP-226	Jun 1978
Begin PAM Slug 2	all injection wells	Aug 1978
First oil observed	MP-227/228	Aug/Oct 1978
Acid stimulation	MP-209/219,225	Aug/Sep 1978
Fracture and proppant stimulation	MP-213	Sep 1978
Peak oil cut	MP-227	Sep 1978
Tracer program initiated	all injection wells	Oct 1978
Fracture over extension discovered	MP-213 to 227	Nov-Dec 1978

TABLE 5 (Continued)

CHRONOLOGY OF FIELD OPERATIONS
HEGBERG LEASE

<u>Event</u>	<u>Wells</u>	<u>Date</u>
Fracture and proppant stimulation	MP-207	Jan 1979
Acid stimulation	MP-223/226	Jan/Feb 1979
Induction logs	MP-228/229	Jan, Mar/ Jun 1979
Begin PAM Slug 3		Feb 1979
Pressure buildup tests	MP-207,209,217,219	Feb 1979
Monitoring wells BHP	MP-202,204,206,208, 210,212,214,216,218, 220,222,224	Mar, Jul, Nov 1979
Third observation well drilled and completed	MP-229	Mar 1979
First oil observed	MP-229	May 1979
Fracture and proppant stimulation	MP-223	Jun 1979
Begin PAM Slug 4		Oct 1979
Calcium sulfate discovered in south pattern	MP-203,205,207,213,215	Oct 1979
Injection rate decrease - higher molecular weight polymer		Feb 1980
Induction logs	MP-229/228	Feb/Aug 1980
Monitoring wells BHP	MP-202,204,206,208, 210,212,214,216,218, 220,222,224	May 1980
Jetted formation face with sodium hypochlorite	MP-223,225	Jun 1980
Original polymer reinstated	all injection wells	Jul 1980
Perforated @ 660'-670'	MP-228	Aug 1980
Glutaraldehyde as biocide	all injection wells	Aug-Sep 1980
Polymer mixing equipment modified	at injection plant	Sep 1980
Back to Visco 3991 (DBNPA) as biocide	all injection wells	Oct 1980
Begin formaldehyde as biocide	all injection wells	Nov 1980
Begin activator for polymer at 1,000 ppm	all injection wells	Jan 1981
Sampled, found iron sulfide	MP-227	Feb 1981
Acid/sodium hypochlorite stimulation	MP-227	Feb 1981
Monitoring wells sampled	MP-202,204,206,208, 210,212,214,216,218, 220,222,224	Feb 1981
Induction logs	MP-228,229/228	Feb, Jul/ Aug 1981
Change oxygen scavenger to sodium hydrosulfite	all injection wells	Mar 1981
Sodium hypochlorite stimulation	MP-221,223,225	Mar 1981

TABLE 5 (Continued)

CHRONOLOGY OF FIELD OPERATIONS
HEGBERG LEASE

<u>Event</u>	<u>Wells</u>	<u>Date</u>
Pressure falloff tests	MP-201,203	Apr-May 1981
Acid stimulation	MP-225	Apr 1981
Monitoring well BHP	MP-202,204,206,208, 210,212,214,216,218, 220,222	May 1981
Reduced viscosity of PAM to 1 cp (50 ppm)		Jun 1981
Begin Kathon WT as biocide	all injection wells	Jun 1981
Perforated	MP-228	Aug 1981
Redesigned polymer injection equipment installed	at injection plant	Sep 1981
Vacuum deaeration unit and water softener installed	at injection plant	Oct 1981
Discontinue biocides (only chlorine gas in use)	all injection wells	Oct 1981
Acid stimulation	MP-207,209,217,219	Nov 1981
Begin PAM Slug 4b (20 cp)		Dec 1981
Monitoring well BHP	MP-202,204,206,208, 210,212,214,216,218, 220,222,224	Feb 1982
Monitor wells swabbed	a.a.	Mar 1982
Perforated two shots per foot	MP-207	Mar 1982
Monitor wells pumped	MP-202/206	Jun/May 1982
Monitor wells put on production	MP-202,206	Jun 1982
End contract		Nov 1982

TABLE 6

ANALYSES OF SUPPLY AND INJECTION WATERS
 CITIES SERVICE OIL COMPANY
 EL DORADO SHALLOW-SAND PROJECT
 BUTLER COUNTY, KANSAS

Radical	Supply Well Concentration, mg/liter	Produced Brine Concentration, mg/liter	Mixed Brine, Untreated Concentration, mg/liter	Clear Water Concentration, mg/liter
Calcium (Ca)	1,580	5,800	2,260	2,370
Magnesium (Mg)	418	1,750	1,220	1,180
Sodium (Na)	9,080	33,300	19,000	19,400
Carbonate (CO ₃)	0	0	0	0
Bicarbonate (HCO ₃)	232	635	537	605
Sulfate (SO ₄)	2,130	174	1,820	1,760
Chloride (Cl)	16,840	64,700	35,300	36,200
TOTAL SOLIDS	29,840	105,359	60,137	61,515
Hydrogen Sulfide (H ₂ S)	Yes	None	None	None
Barium (Ba)	None	None	None	None
Specific Gravity	1.023	1.077	1.045	1.044

TABLE 7

SEMIQUANTITATIVE X-RAY DIFFRACTION ANALYSIS FOR
CORE FRAGMENTS OF THE LESS-THAN FIVE MICRON SIZE FRACTION

Depth, feet	Percent less than 5	Illite- Montmorillonite					Chlorite	Kaolinite	Calcite	Quartz
		Illite								
<u>Well MP-201</u>										
657	9.1	11	3	4	17	-	17	-	65	
665	8.1	18	3	5	17	-	17	-	57	
673	9.5	16	2	6	15	-	15	-	62	
<u>Well MP-211</u>										
660	8.9	17	2	4	19	-	19	-	57	
667	7.7	20	4	6	18	-	18	-	51	
674	8.0	20	3	6	17	-	17	-	54	
<u>Well MP-213</u>										
674.5	10.2	26	4	6	20	1	20	1	43	
677	8.0	15	3	5	14	-	14	-	63	
680	12.1	30	4	10	19	-	19	-	37	
<u>Well MP-215</u>										
650	9.2	18	3	7	12	-	12	-	60	
656	9.1	21	4	7	17	-	17	-	51	
664	7.3	14	2	5	14	-	14	-	65	
<u>Well MP-221</u>										
662	7.8	40	5	1	39	10	39	10	10	
663	30.0	30	10	15	40	-	40	-	5	
664-667	5.9	35	-	10	45	5	45	5	5	
668-672	6.6	25	5	15	40	5	40	5	10	
673-674	8.4	30	-	10	50	-	50	-	10	
675	7.0	30	-	15	45	-	45	-	10	
677-680	8.9	35	-	-	45	5	45	5	10	
<u>Well MP-223</u>										
672	9.7	19	2	6	15	-	15	-	59	
679	7.7	20	3	7	17	-	17	-	53	
684	9.4	16	2	6	15	-	15	-	62	

TABLE 7 (Continued)

SEMIQUANTITATIVE X-RAY DIFFRACTION ANALYSIS FOR
CORE FRAGMENTS OF THE LESS-THAN FIVE MICRON SIZE FRACTION

Depth, feet	Percent less than 5	Illite	Illite-Montmorillonite	Chlorite	Kaolinite	Calcite	Quartz
Well MP-225							
657-658	13.6	45	5	10	20	10	10
659	6.8	40	15	10	20	-	15
660	16.2	55	15	10	10	-	10
660.4-662.0	7.4	45	10	10	20	5	10
664	7.1	40	15	10	25	-	10
665-666	8.7	50	10	10	25	-	5
667	6.1	40	10	15	20	-	5
668-669	11.0	50	10	15	20	-	5
669.8	5.8	40	10	15	25	-	10
670-671	6.3	35	15	15	20	-	15
672-673	5.7	40	10	15	20	-	15
675-677	15.2	50	10	20	15	-	5
678	23.0	45	5	25	20	-	5

TABLE 8

CAUSTIC CONSUMPTION AND SULFATE LIBERATED BY CAUSTIC SOLUTION

<u>Well</u> <u>Number</u>	<u>Caustic Consumption</u> <u>From Caustic Silicate,</u> <u>meq/100 grams rock</u>	<u>Sulfate Liberated,</u> <u>meq 100 grams rock</u>	<u>Sulfate Liberated-</u> <u>Calculated as</u> <u>Calcium Sulfate,</u> <u>weight percent</u>
MP-203	6.0	3.3	0.23
MP-205	24.6	19.1	1.30
MP-207	3.4	0.0	0.0
MP-213	3.6	0.7	0.05
MP-215	2.0	0.3	0.02

TABLE 9

ANALYSIS OF CAUSTIC DEPLETION
FROM SELECTED CORE SAMPLES

<u>No.</u>	<u>Core Sample</u>	<u>Calcium Sulfate, Wt.%</u>	<u>Caustic Consumption, meq/mL PV</u>	<u>Radius of Depletion, ft.</u>
1	MP-203	0.23	0.51	54
2	MP-205	1.30	2.10	27
3	MP-207	0	0.29	72
4	MP-213	0.05	0.31	69
5	MP-215	0.02	0.17	94
	Average		0.68	63.2

NOTE

1. Formation data for the area between MP-213/226 and MP-228 assumes porosity = 24 percent, grain density = 2.7, thickness = 11 feet average.
2. 14,728 barrels of caustic preflush was injected into MP-213/226 with a concentration of 0.15 meq/mL.
3. No. 1 for example, 14,728 bbl x 158,990 mL/bbl x 0.51 meq/mL = 3.5×10^8 meq (total caustic injection).

$$\frac{3.14 \times (R)^2 \times 11 \times 0.24 \times 158,990 \times 0.51}{5.6} = 3.5 \times 10^8$$

R = 54 feet

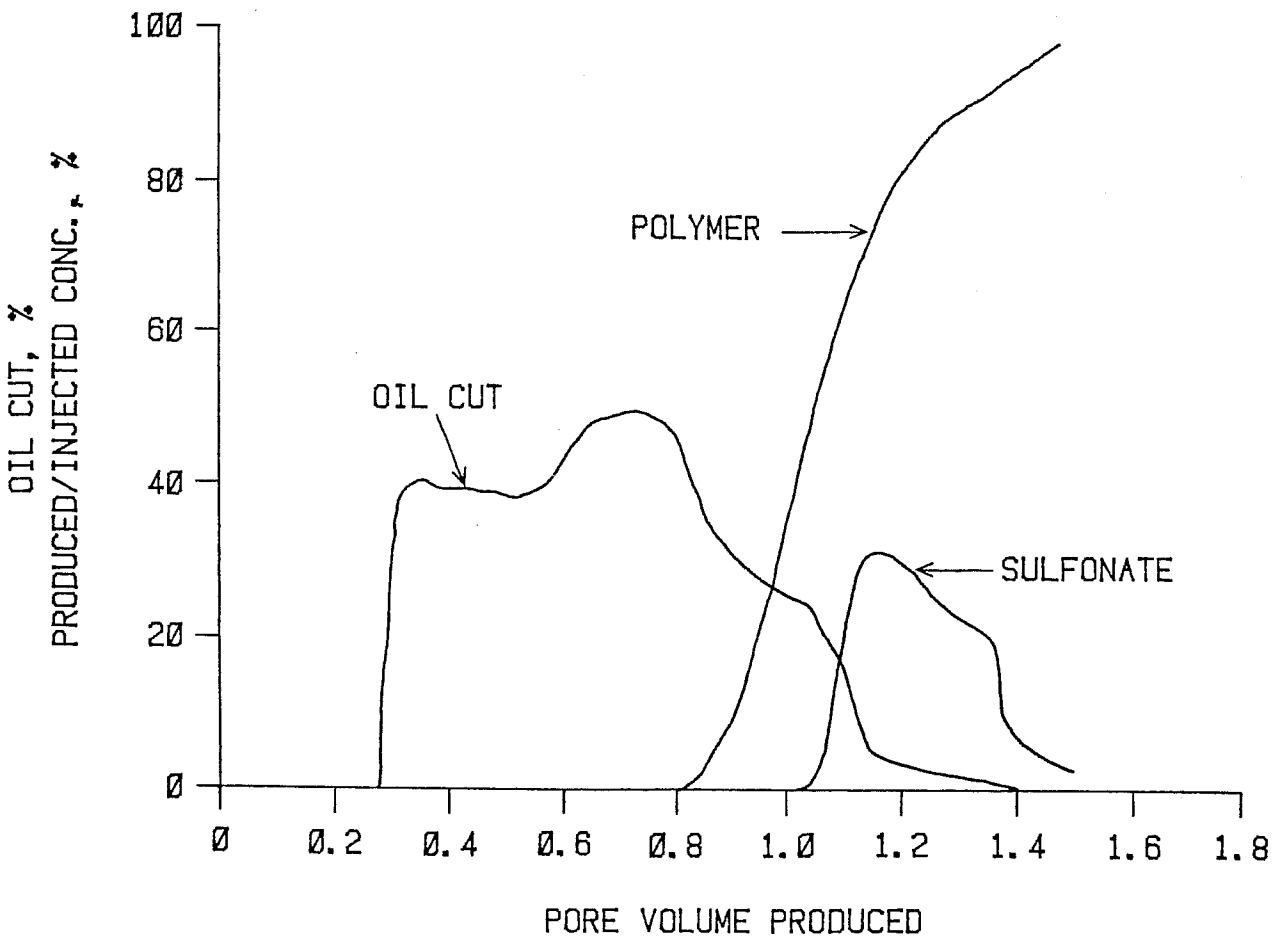
TABLE 10

ELUTED QUANTITIES OF SELECTED IONS
FOLLOWING PREFLUSH*

<u>Ion</u>	<u>Concentration of Ion in Weight Percent</u>
Calcium	0.095
Barium	0.016
Strontium	0.002
Sulfate	0.07

* After a preflush of 15 PV of deionized water.

TYPICAL MICELLAR-POLYMER COREFLOOD RESPONSE



Adapted from Reference 23

FIGURE 1

CORE FLOOD RESULTS USING CHEMICAL
SLUG FOR NORTH PATTERN

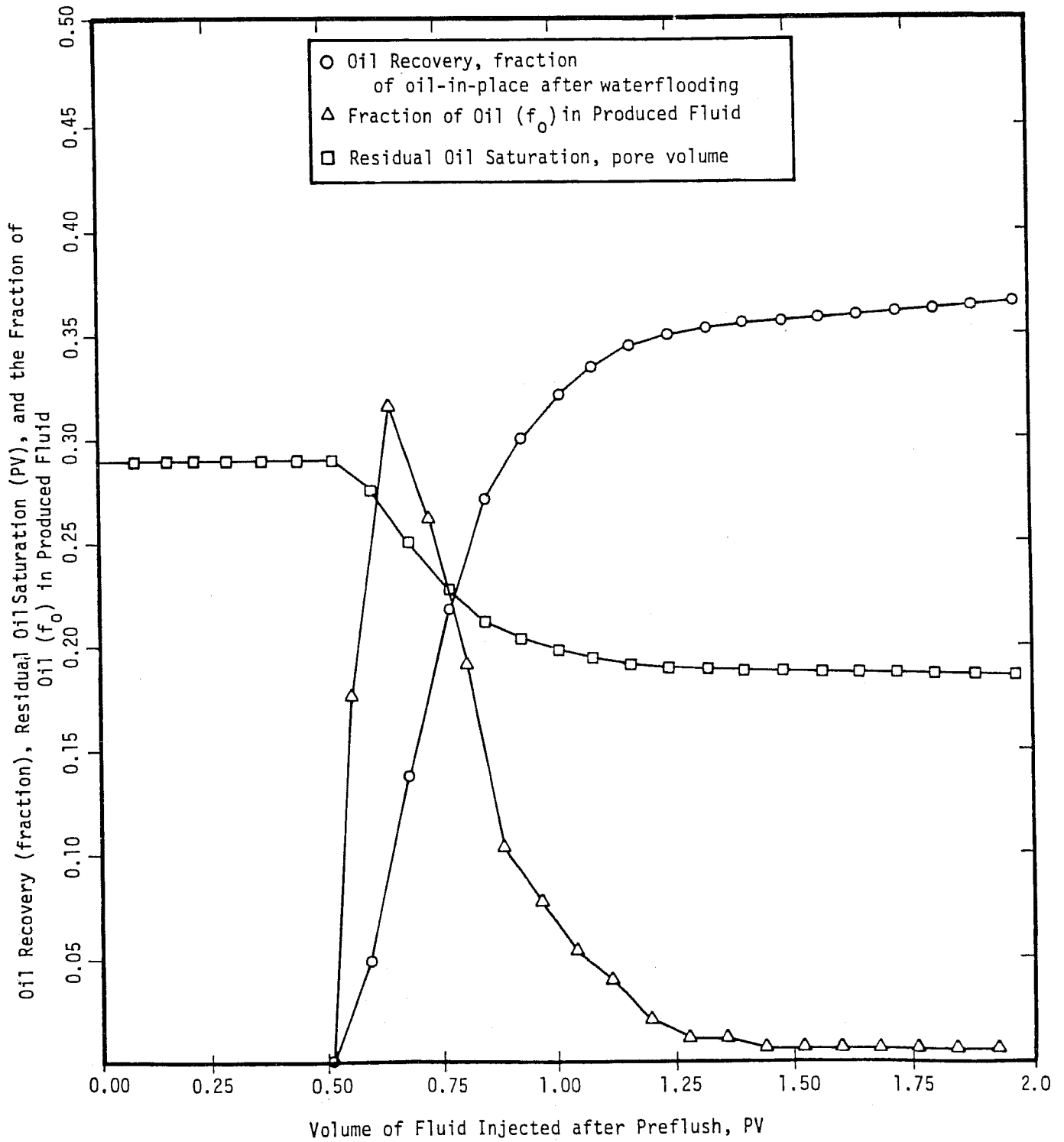
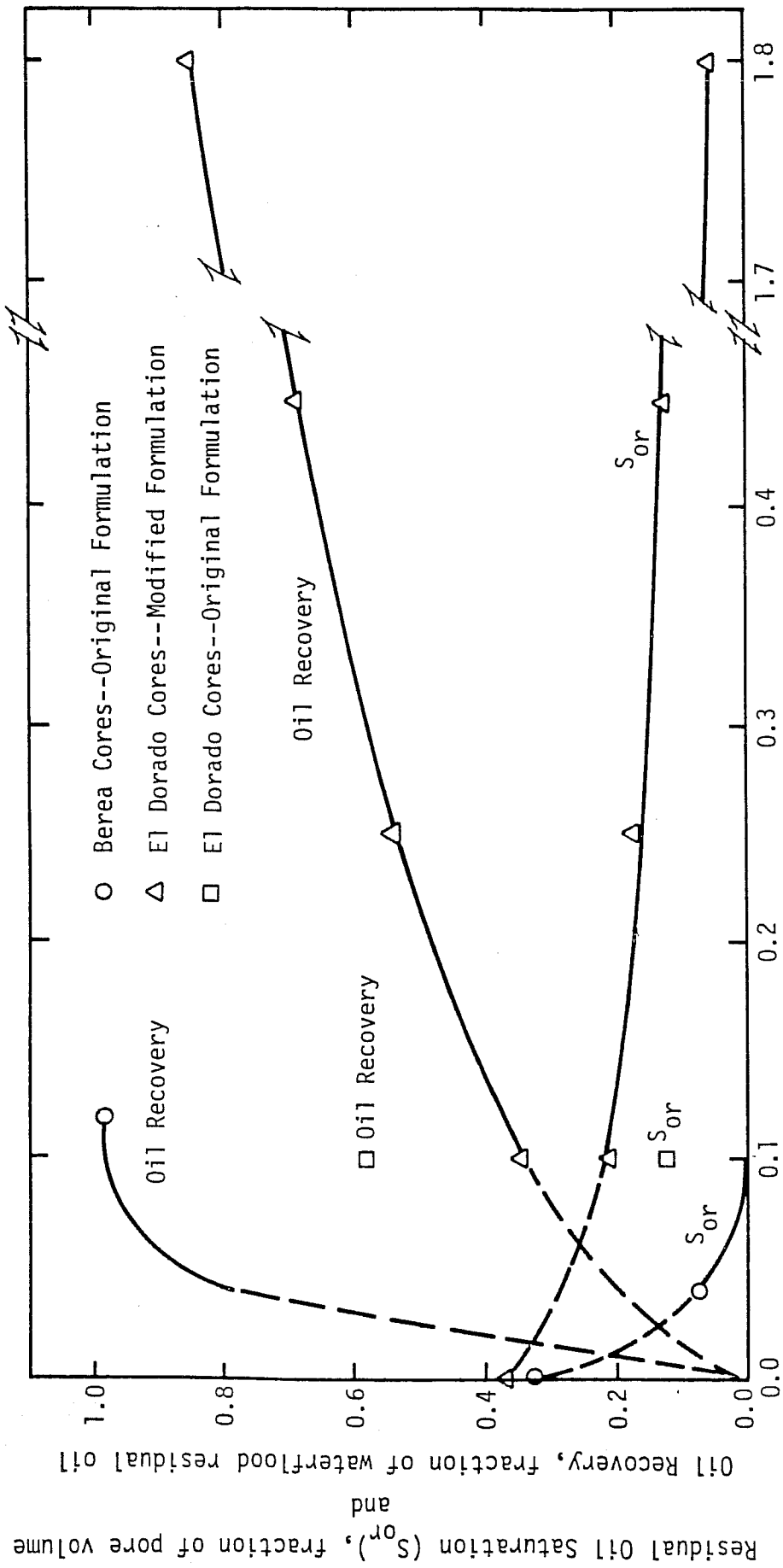


FIGURE 2

OIL DISPLACEMENT RESULTS IN BEREA AND
EL DORADO CORES USING SHELL PROCESS



Chemical Slug Size, fraction of pore volume

EL DORADO PROJECT LAYOUT

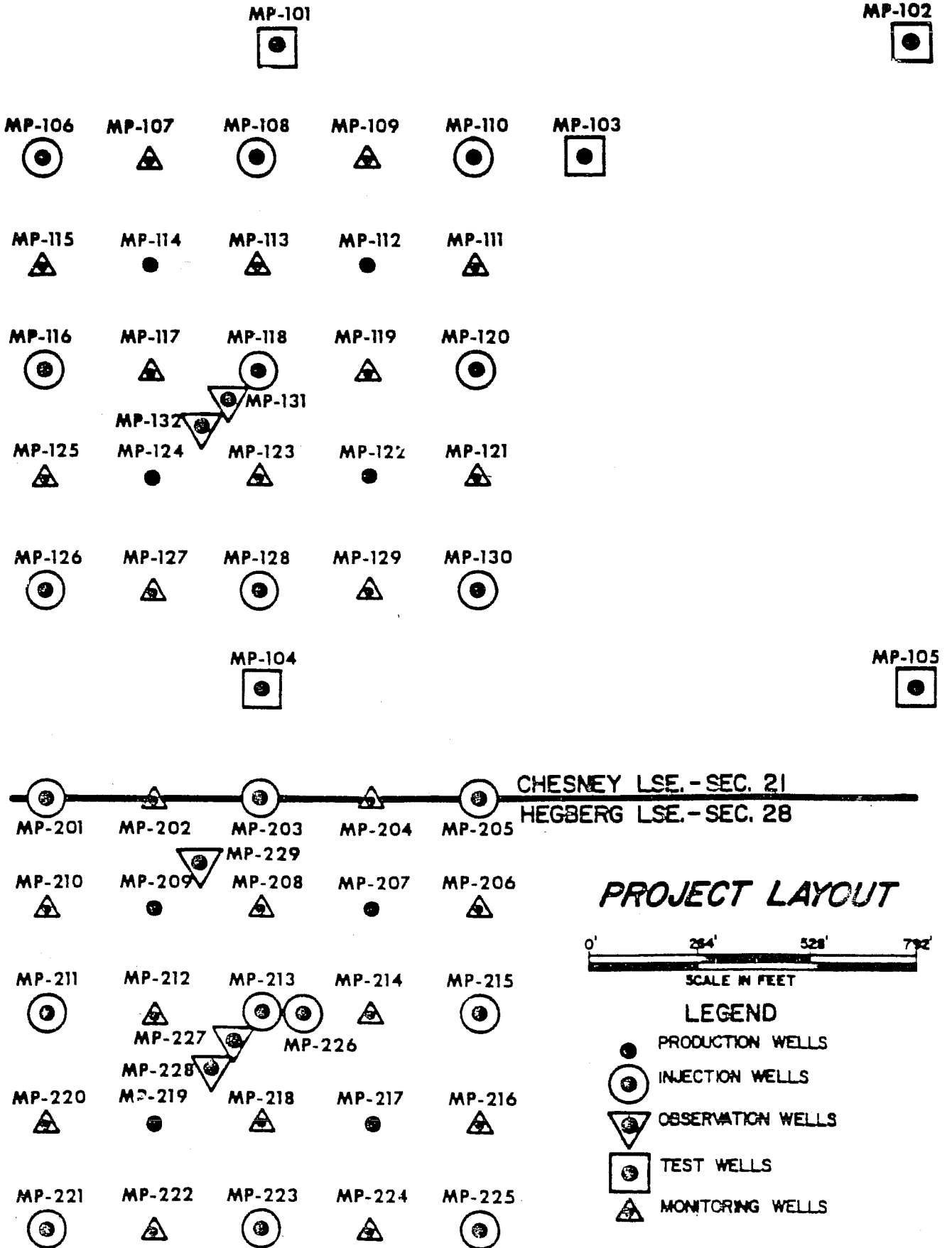


FIGURE 4

PRODUCED FLUIDS
 CHESNEY LEASE
 PROJECT TOTALS

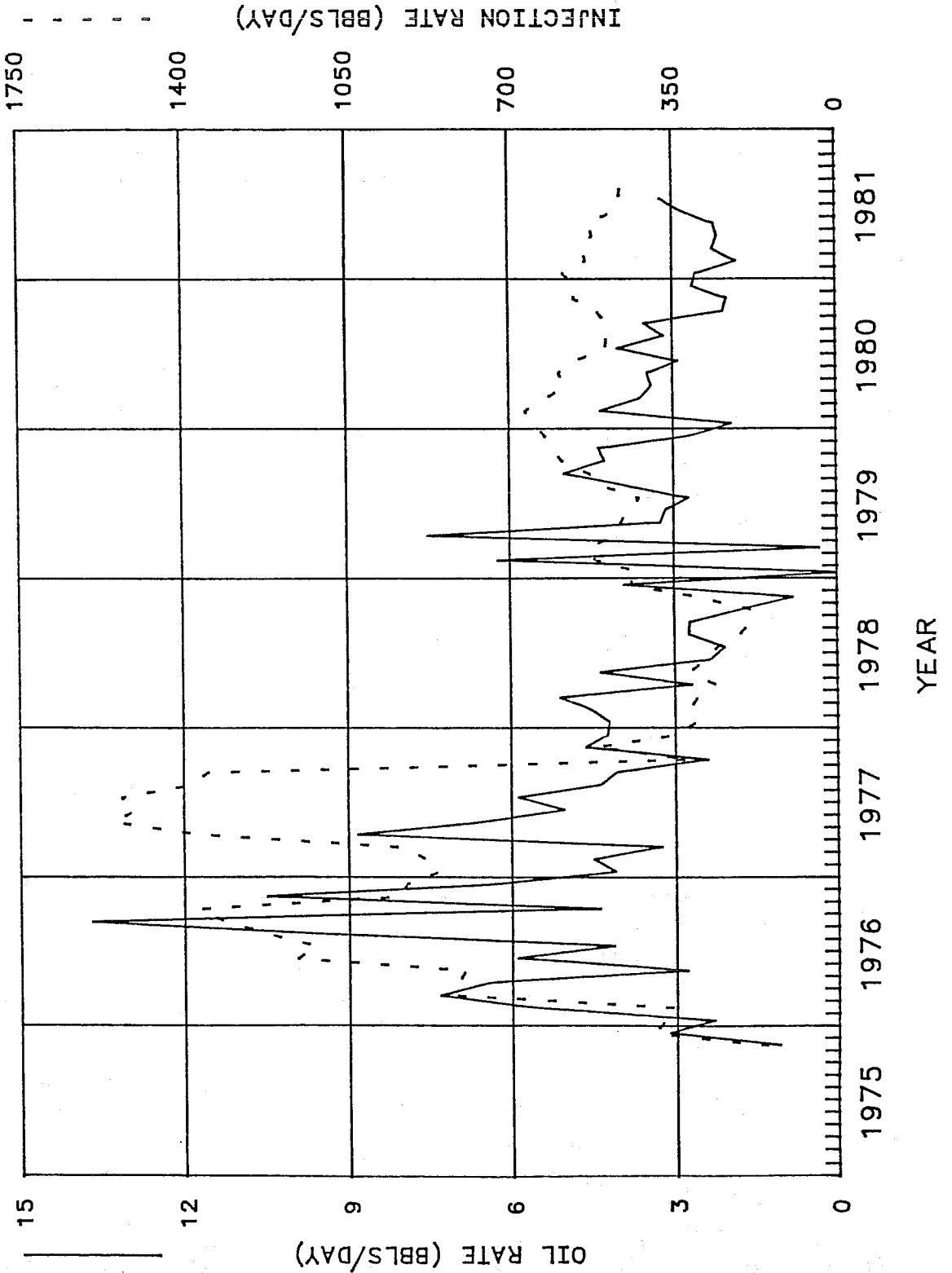


FIGURE 5

PRODUCED FLUIDS
CHESNEY LEASE
PROJECT TOTALS

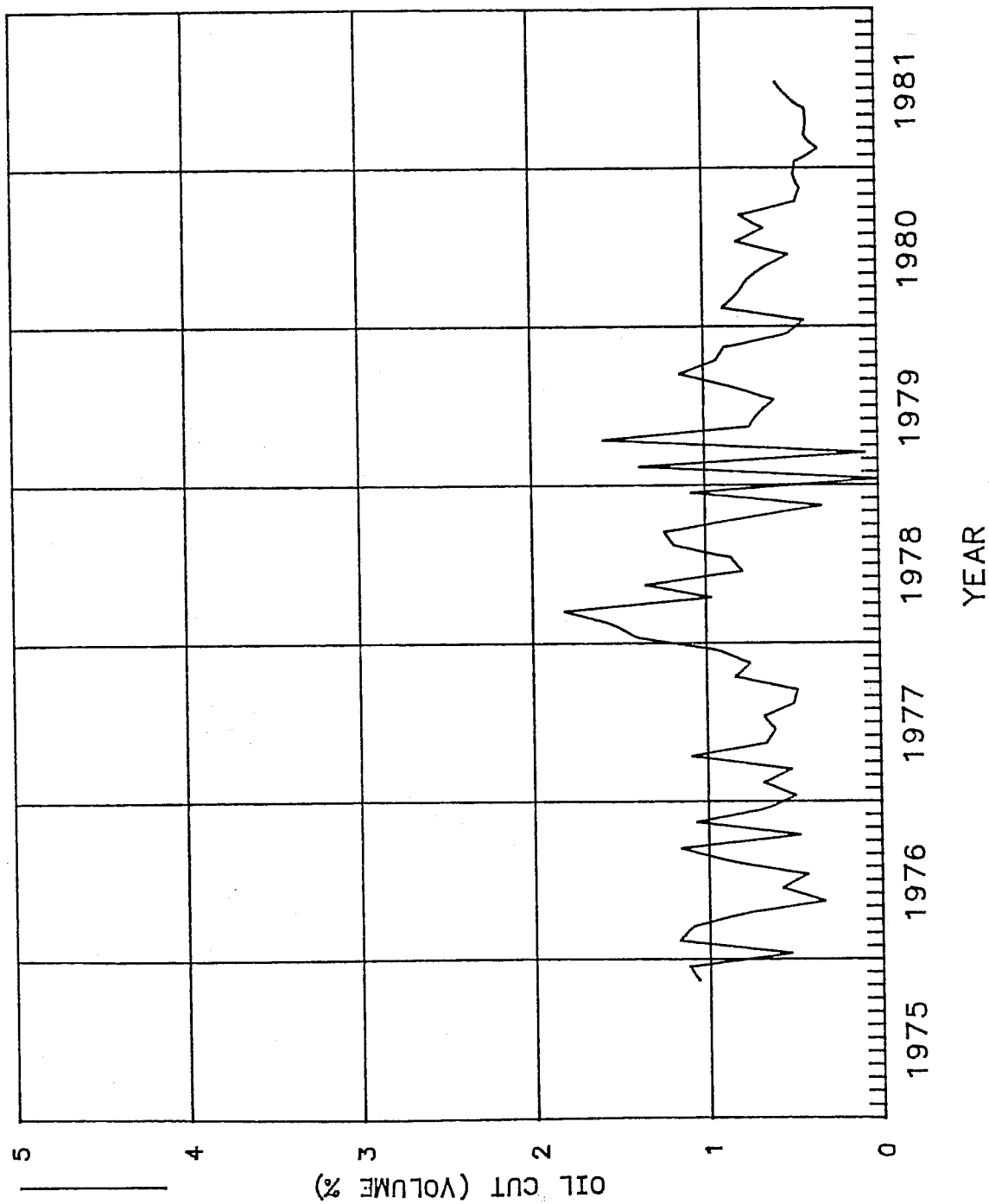
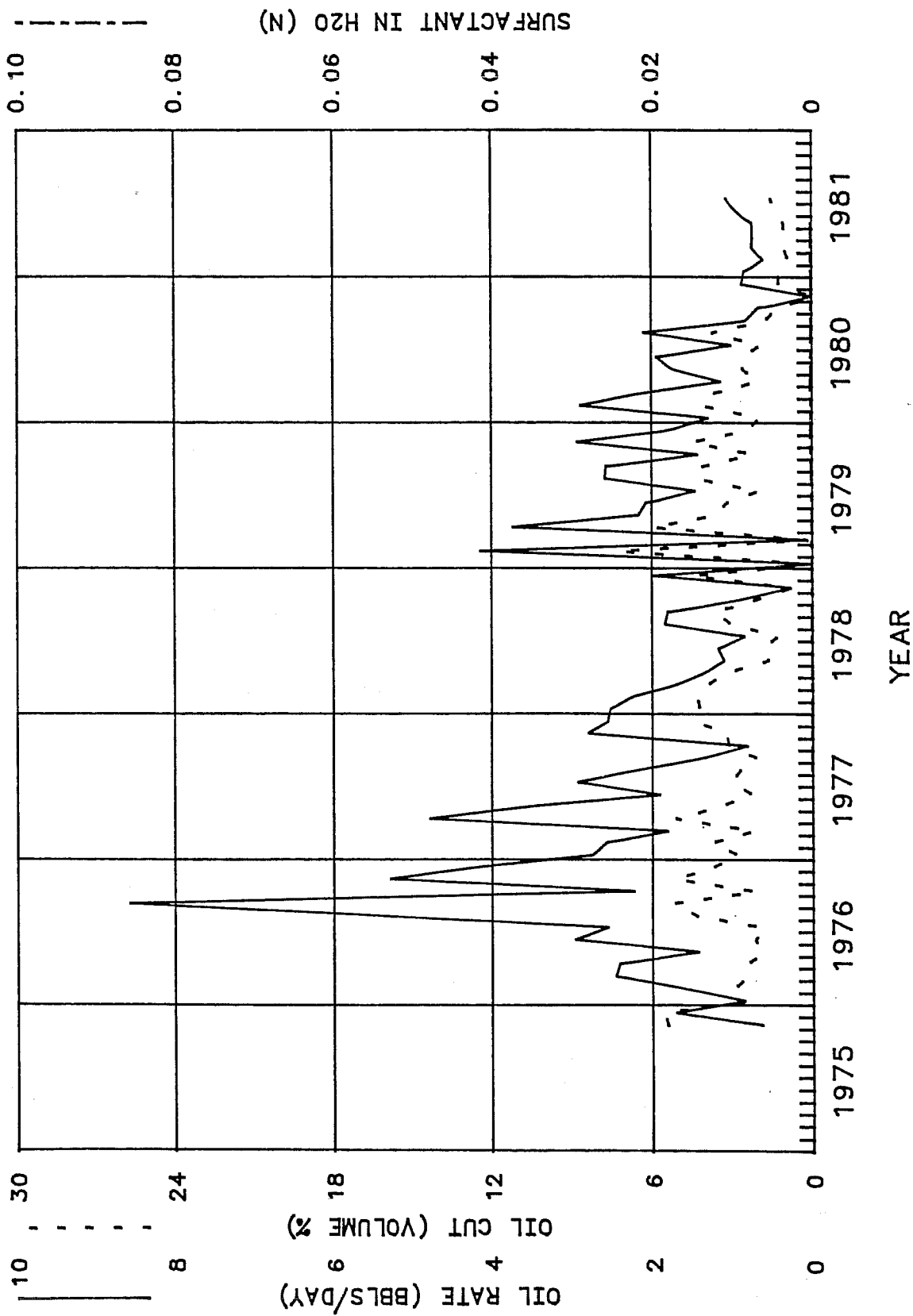


FIGURE 6

PRODUCED FLUIDS
 CHESNEY LEASE
 WELL MP-114



PRODUCED FLUIDS
 CHESNEY LEASE
 WELL MP-1114

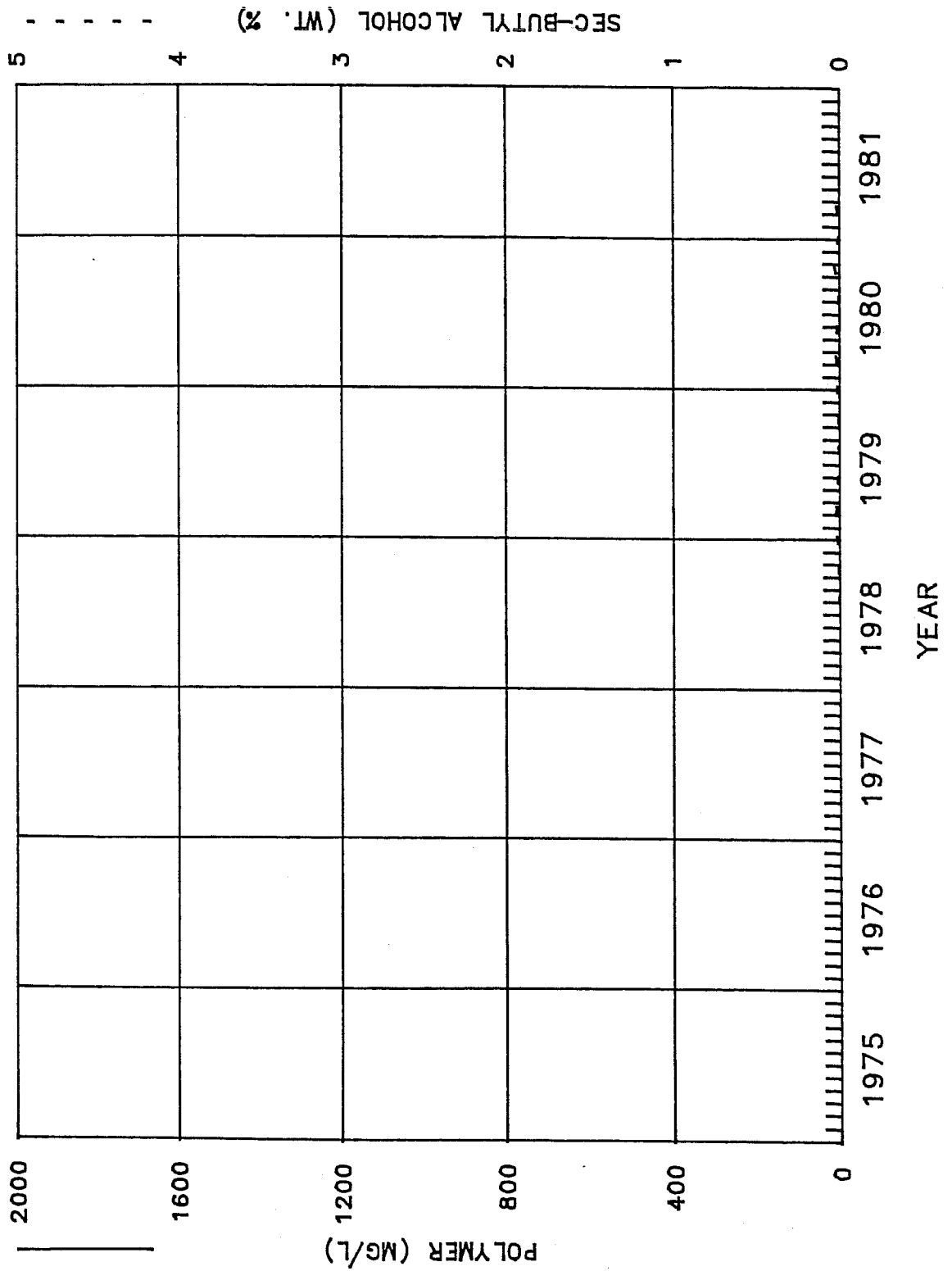


FIGURE 8

PRODUCED FLUIDS
 CHESNEY LEASE
 WELL MP-114

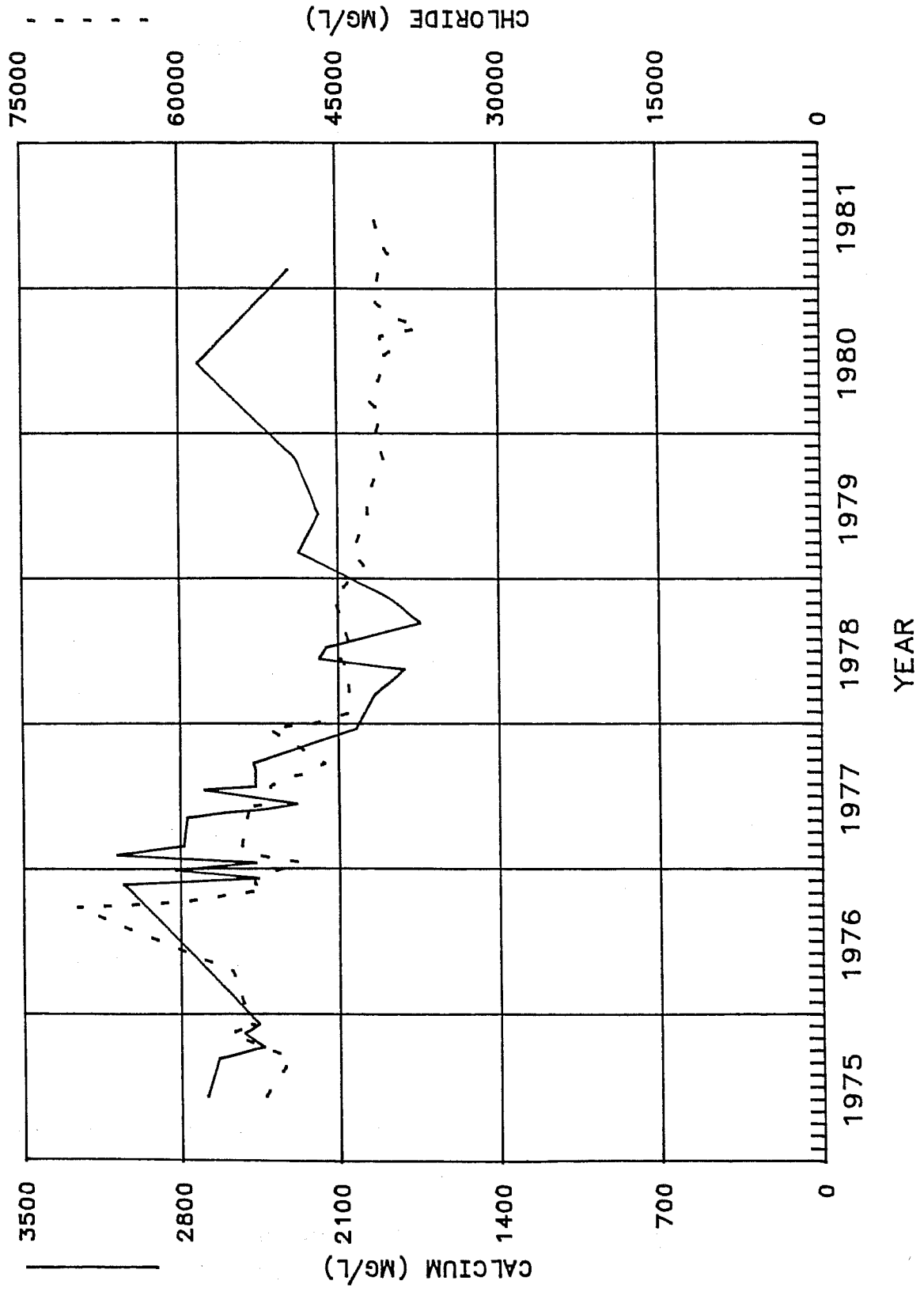


FIGURE 9

PRODUCED FLUIDS
 CHESNEY LEASE
 WELL MP-122

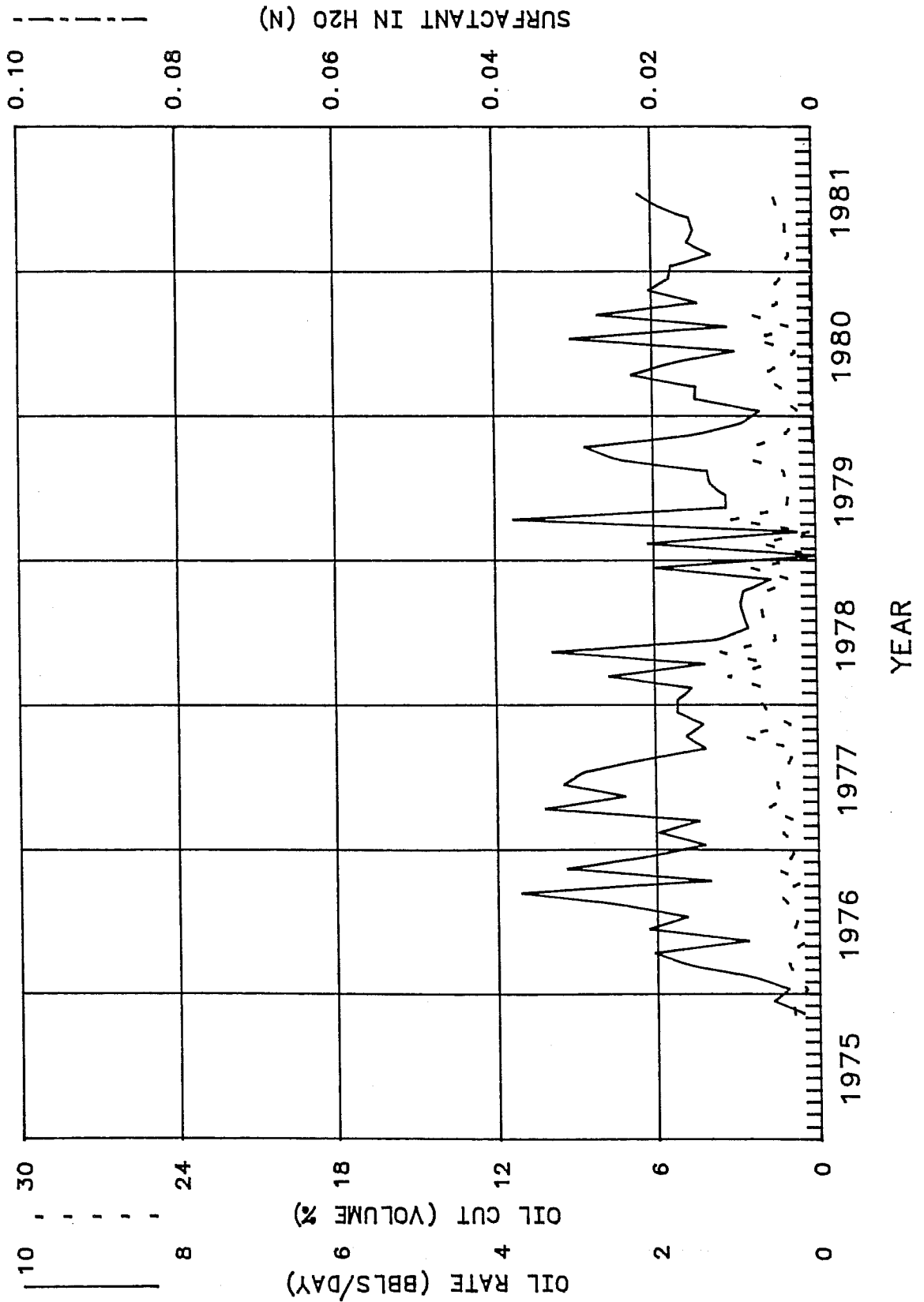


FIGURE 10

PRODUCED FLUIDS
 CHESNEY LEASE
 WELL MP-122

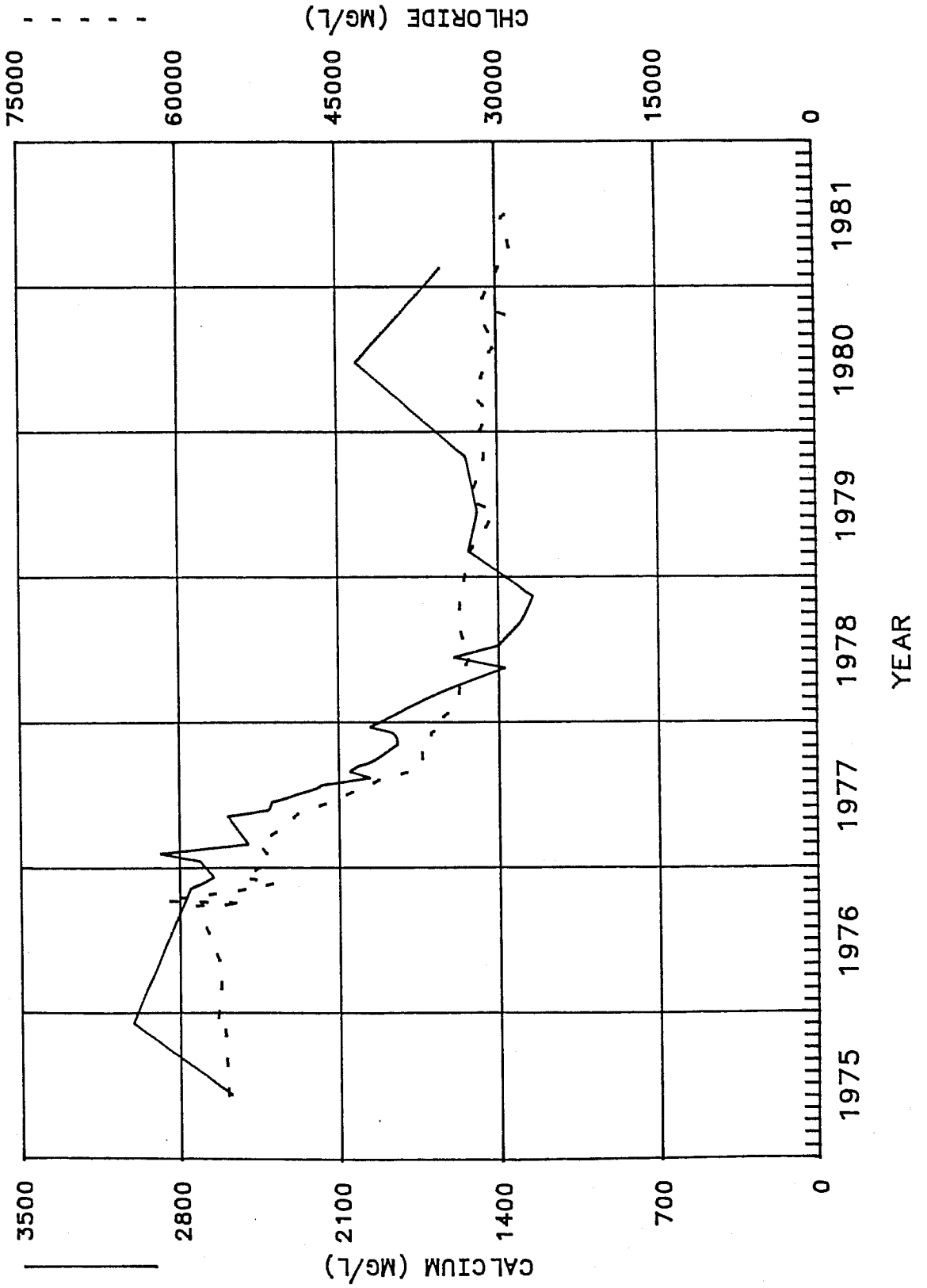


FIGURE 11

PRODUCED FLUIDS
 CHESNEY LEASE
 WELL MP-122

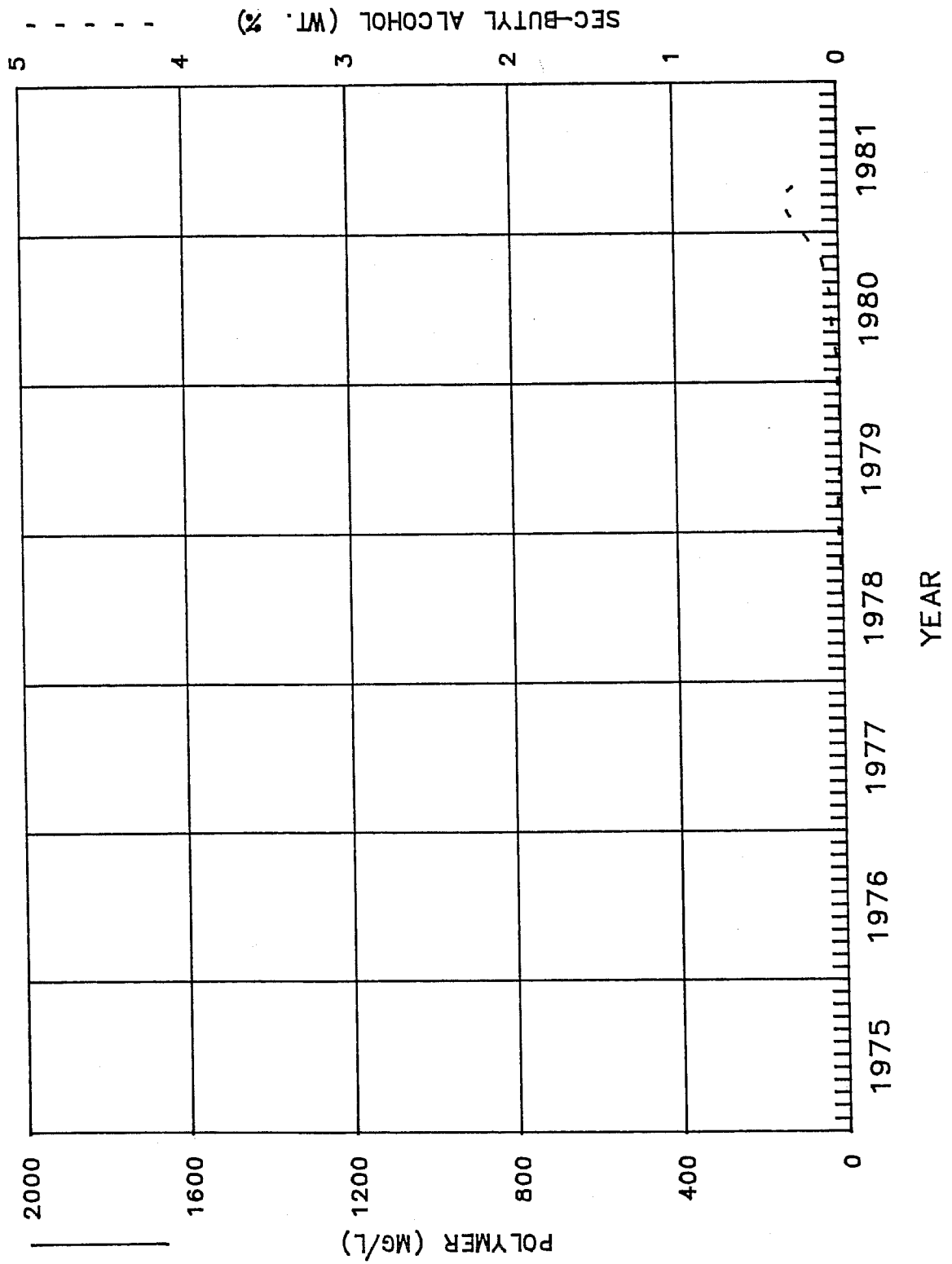


FIGURE 12

PRODUCED FLUIDS
 CHESNEY LEASE
 WELL MP-131

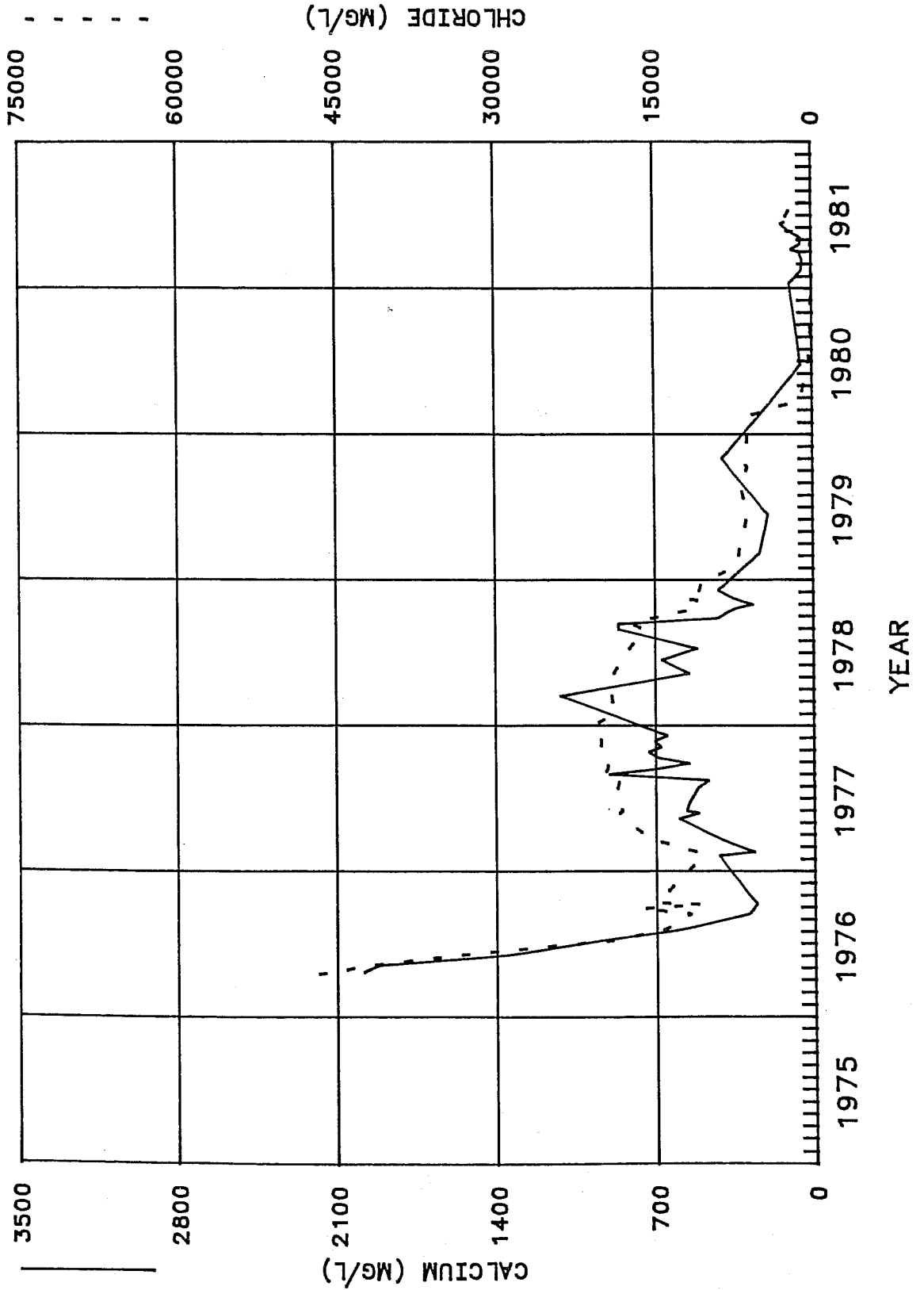


FIGURE 13

PRODUCED FLUIDS
 CHESNEY LEASE
 WELL MP-131

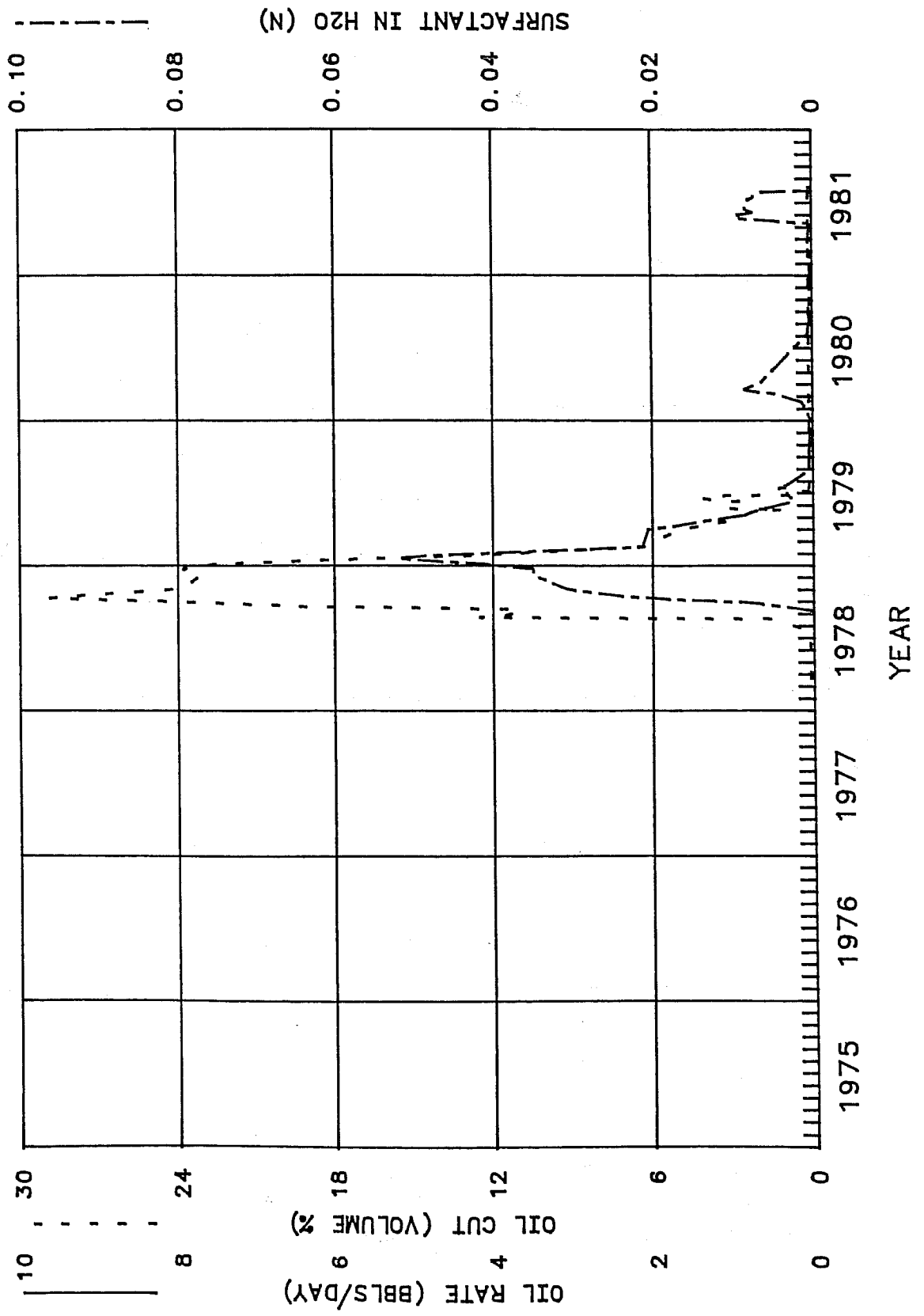


FIGURE 14

PRODUCED FLUIDS
 CHESNEY LEASE
 WELL MP-131

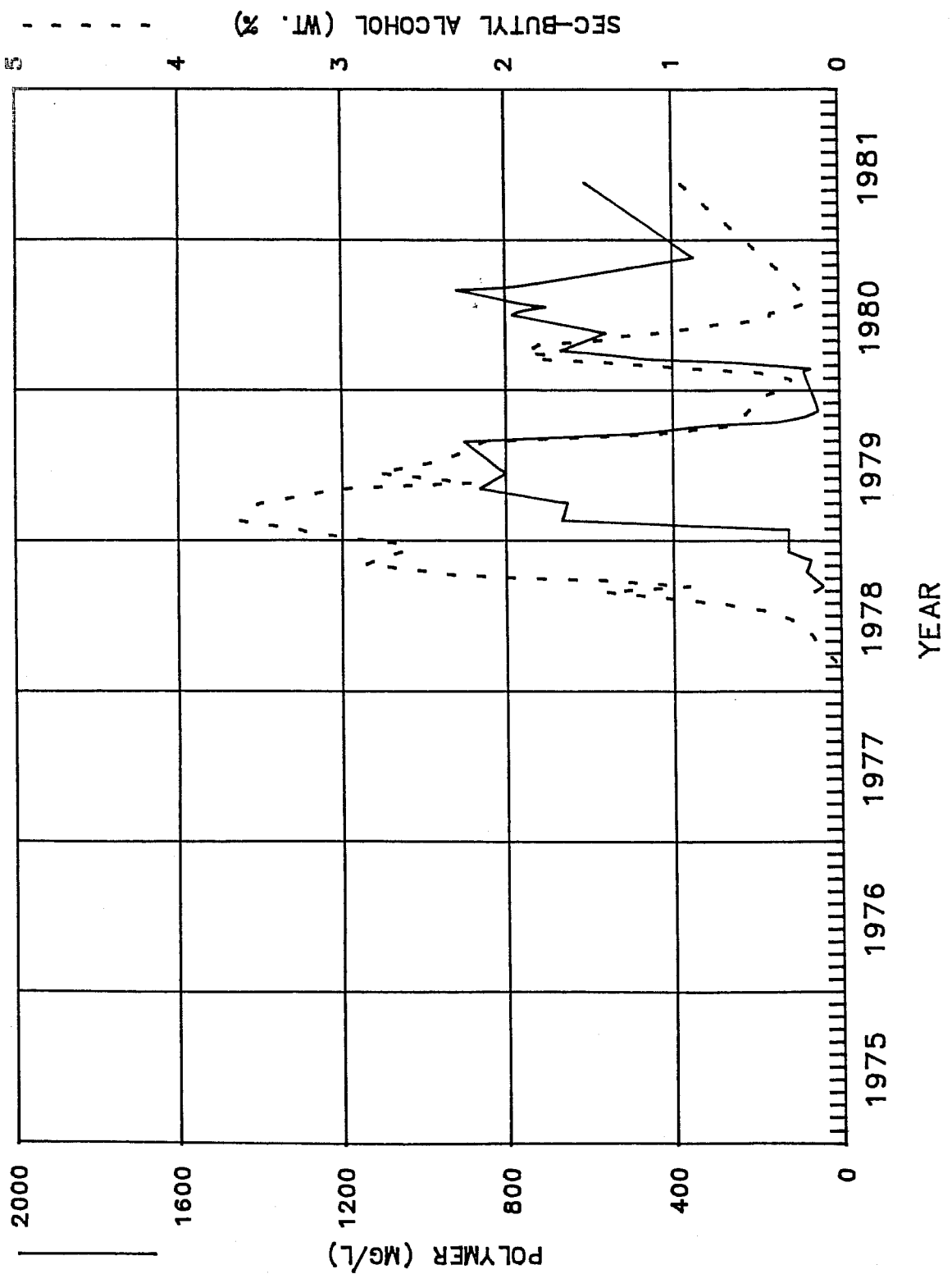


FIGURE 15

PRODUCED FLUIDS
 CHESNEY LEASE
 WELL MP-132

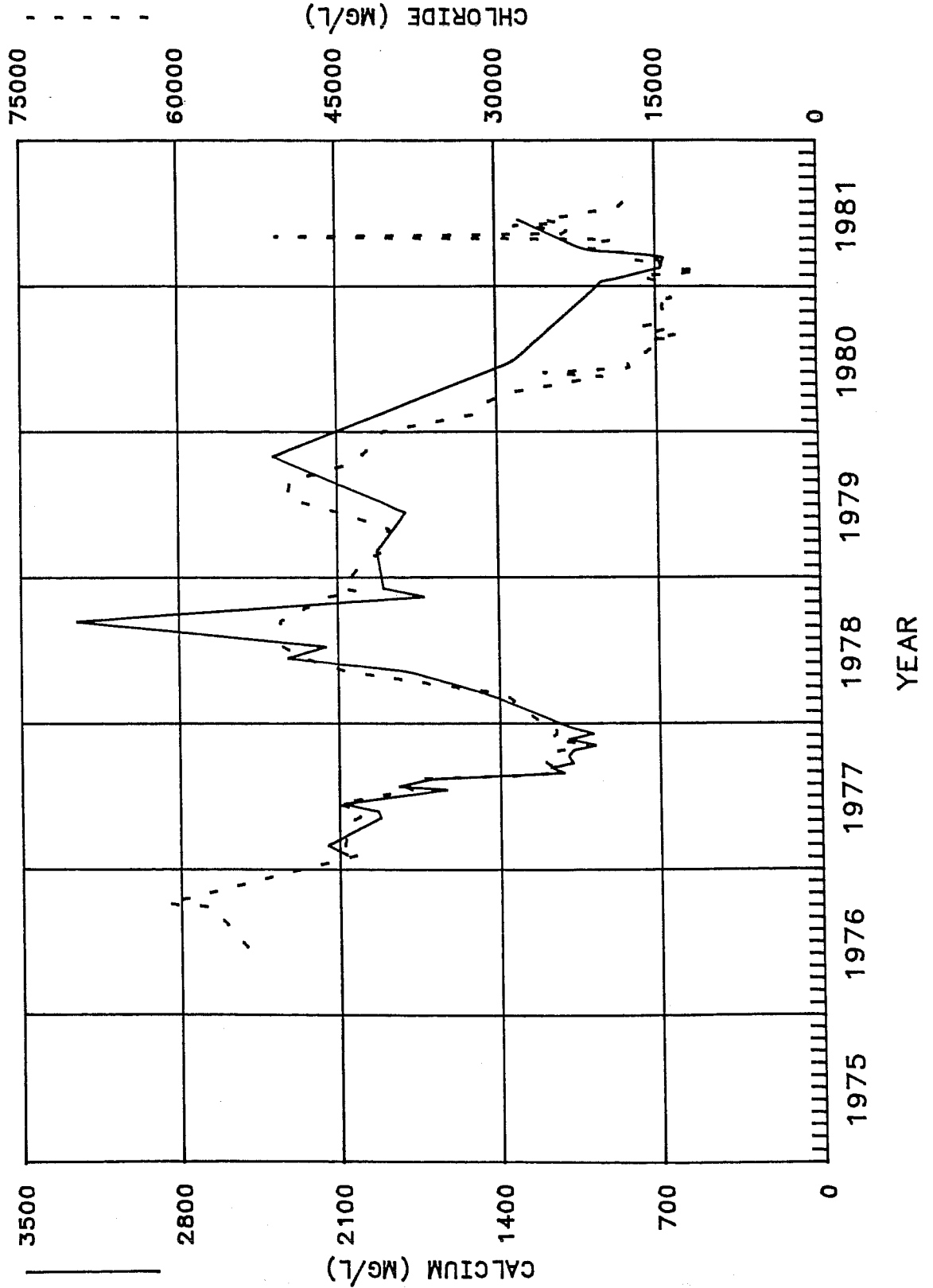


FIGURE 16

PRODUCED FLUIDS
 CHESNEY LEASE
 WELL MP--132

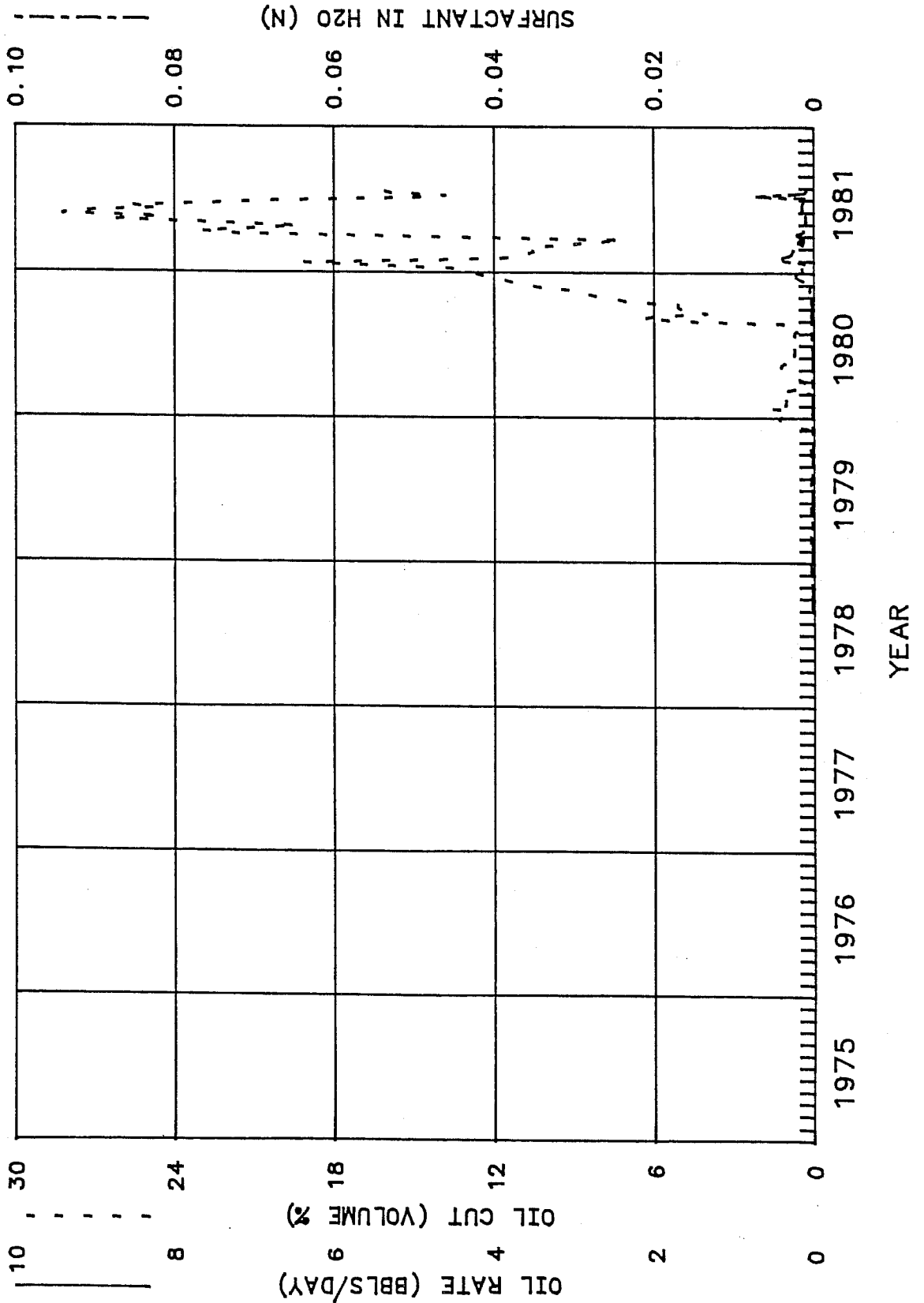


FIGURE 17

PRODUCED FLUIDS
 CHESNEY LEASE
 WELL MP-132

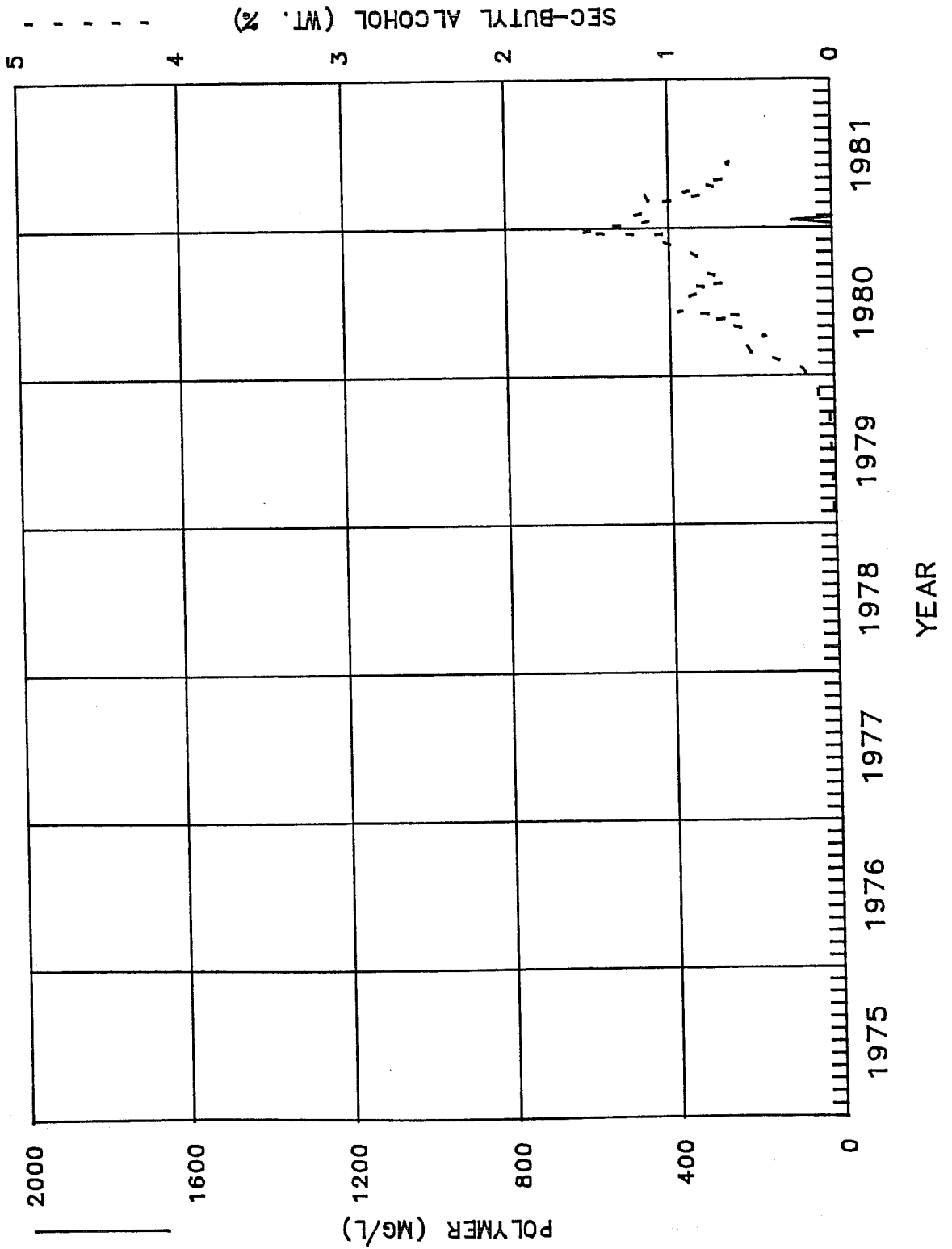


FIGURE 18

PRODUCED FLUIDS
 CHESNEY LEASE
 WELL MP-124

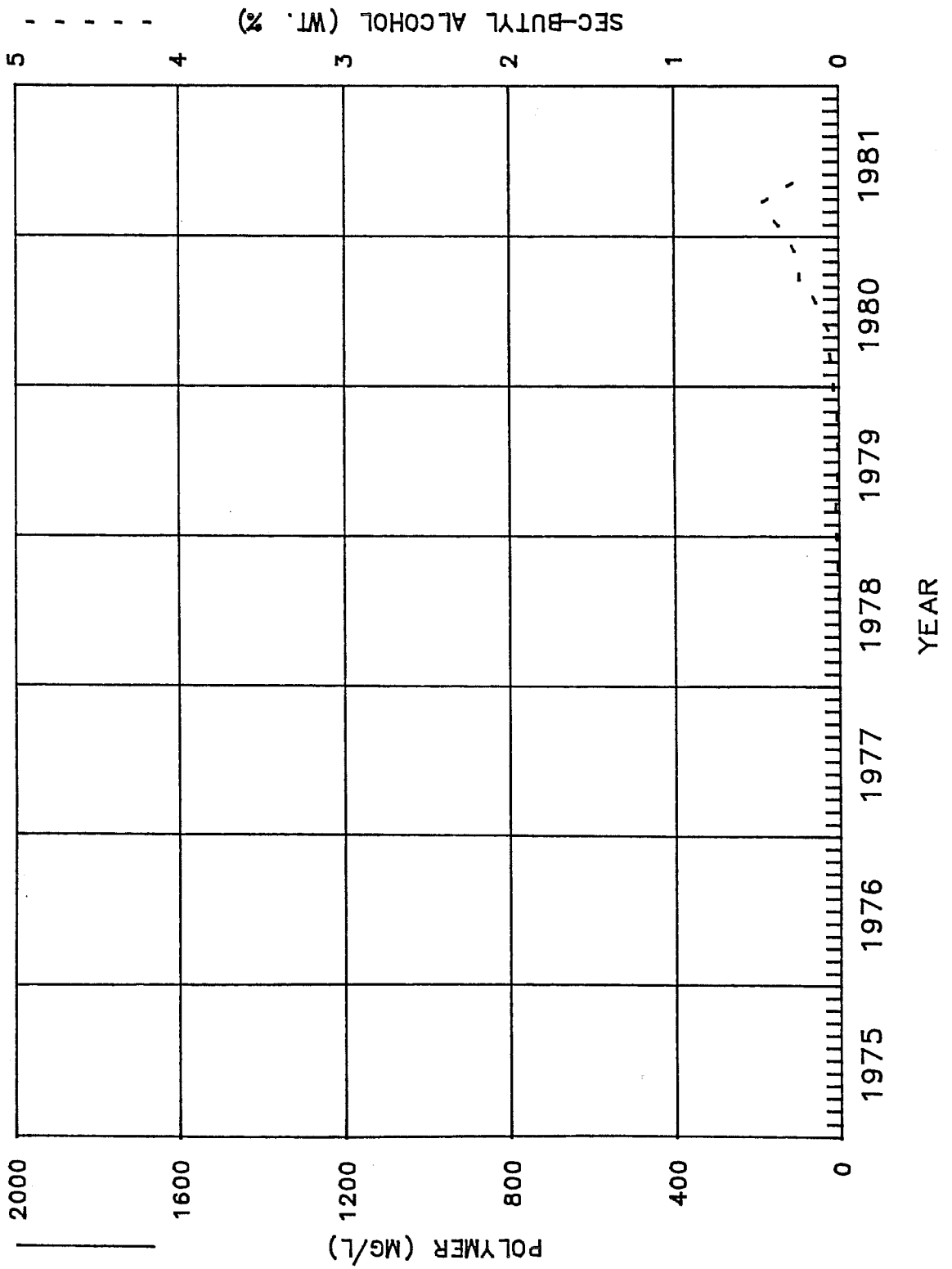


FIGURE 19

PRODUCED FLUIDS
 CHESNEY LEASE
 WELL MP-124

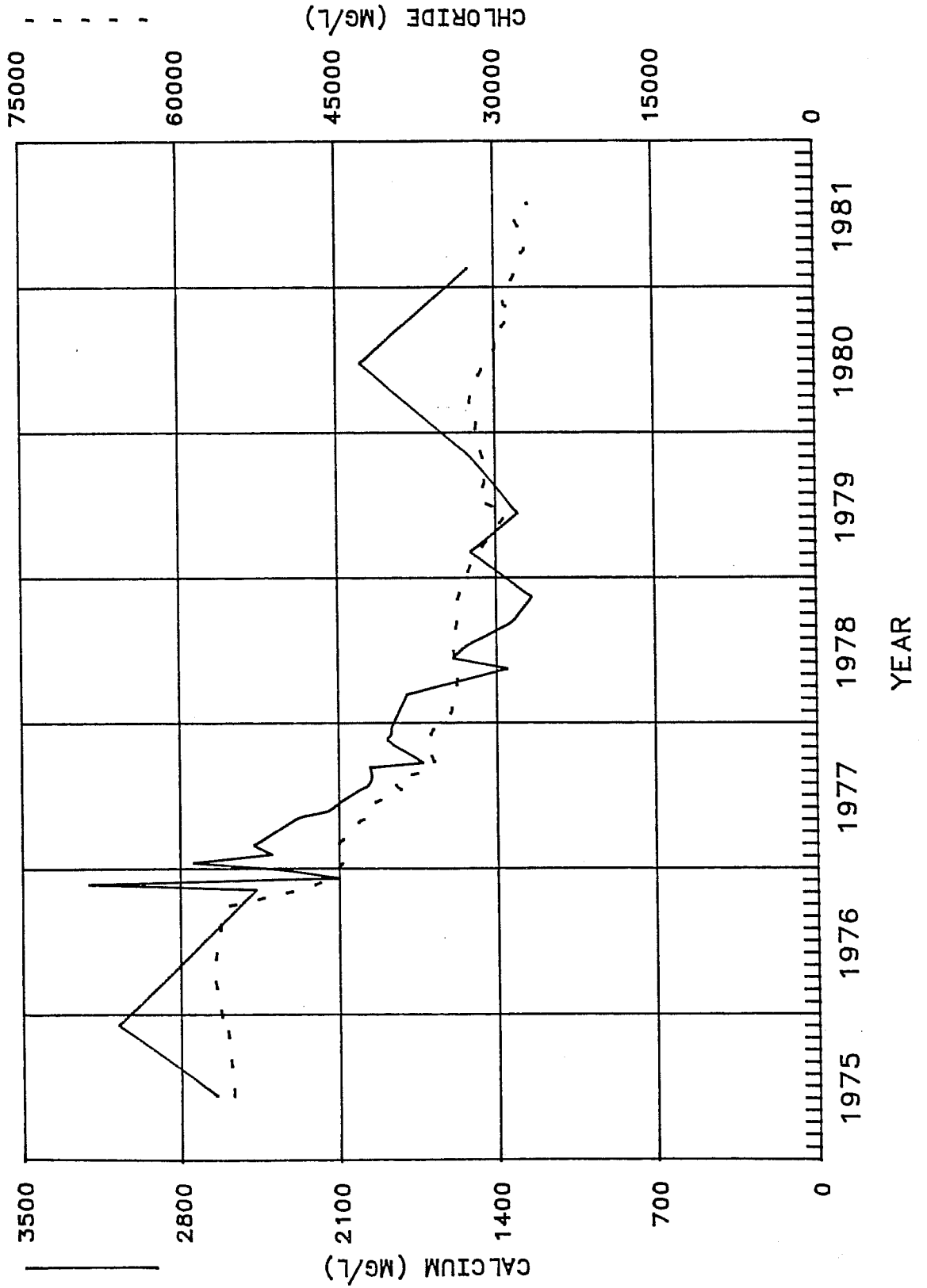


FIGURE 20

PRODUCED FLUIDS
 CHESNEY LEASE
 WELL MP-124

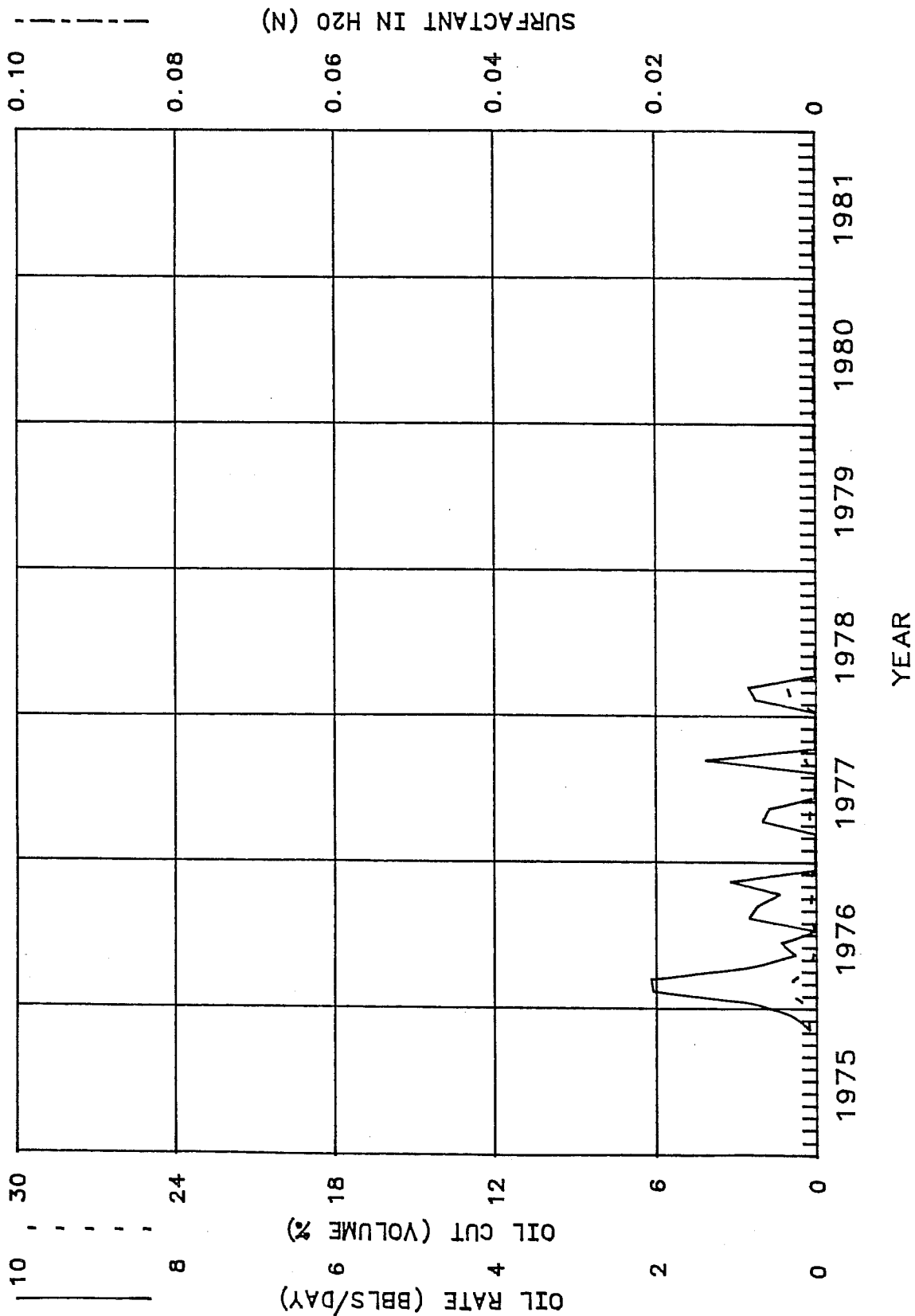


FIGURE 21

SELECTED LOG RESPONSES FOR WELL MP-131

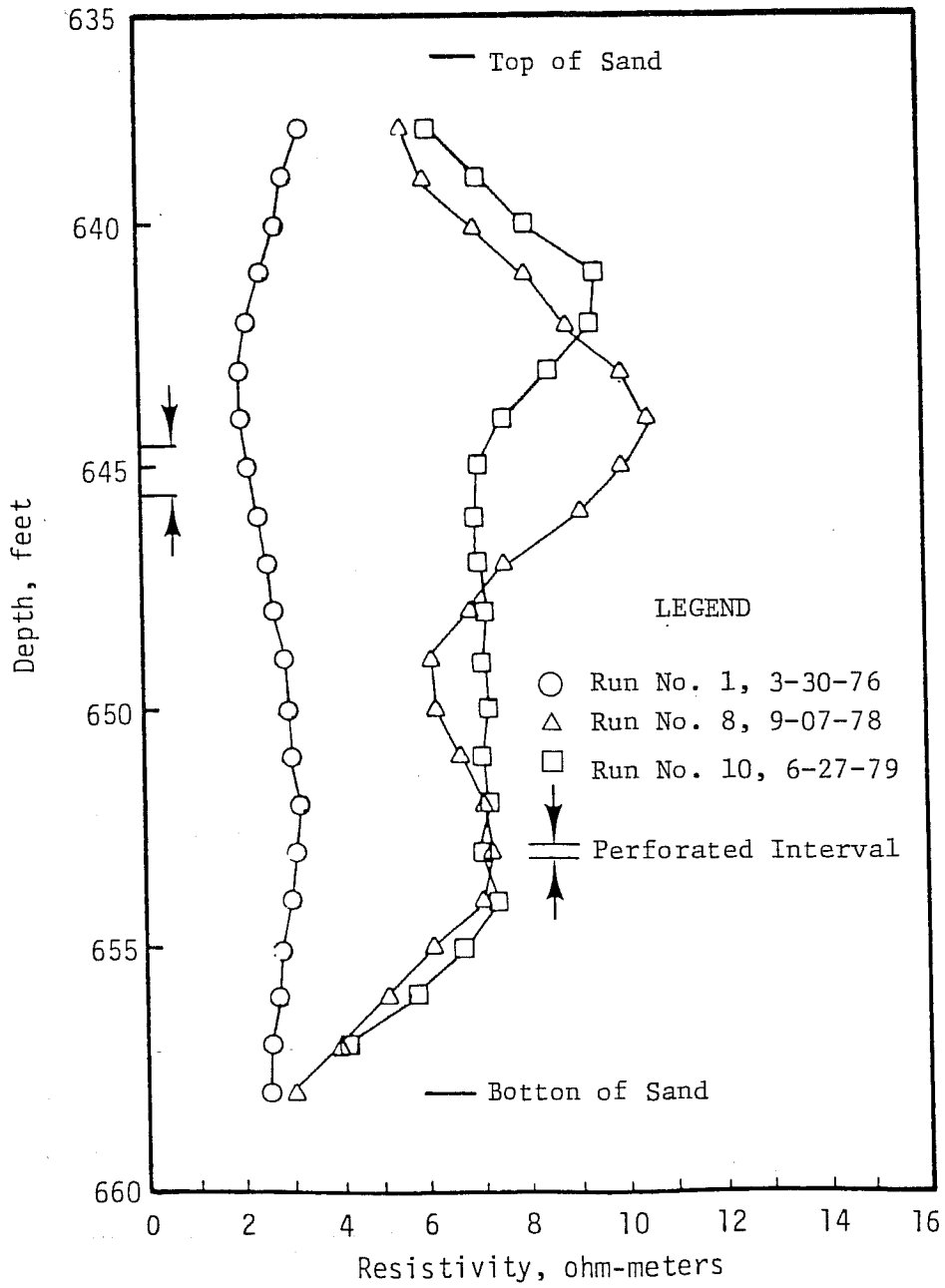


FIGURE 22

SELECTED LOG RESPONSES FOR WELL MP-132

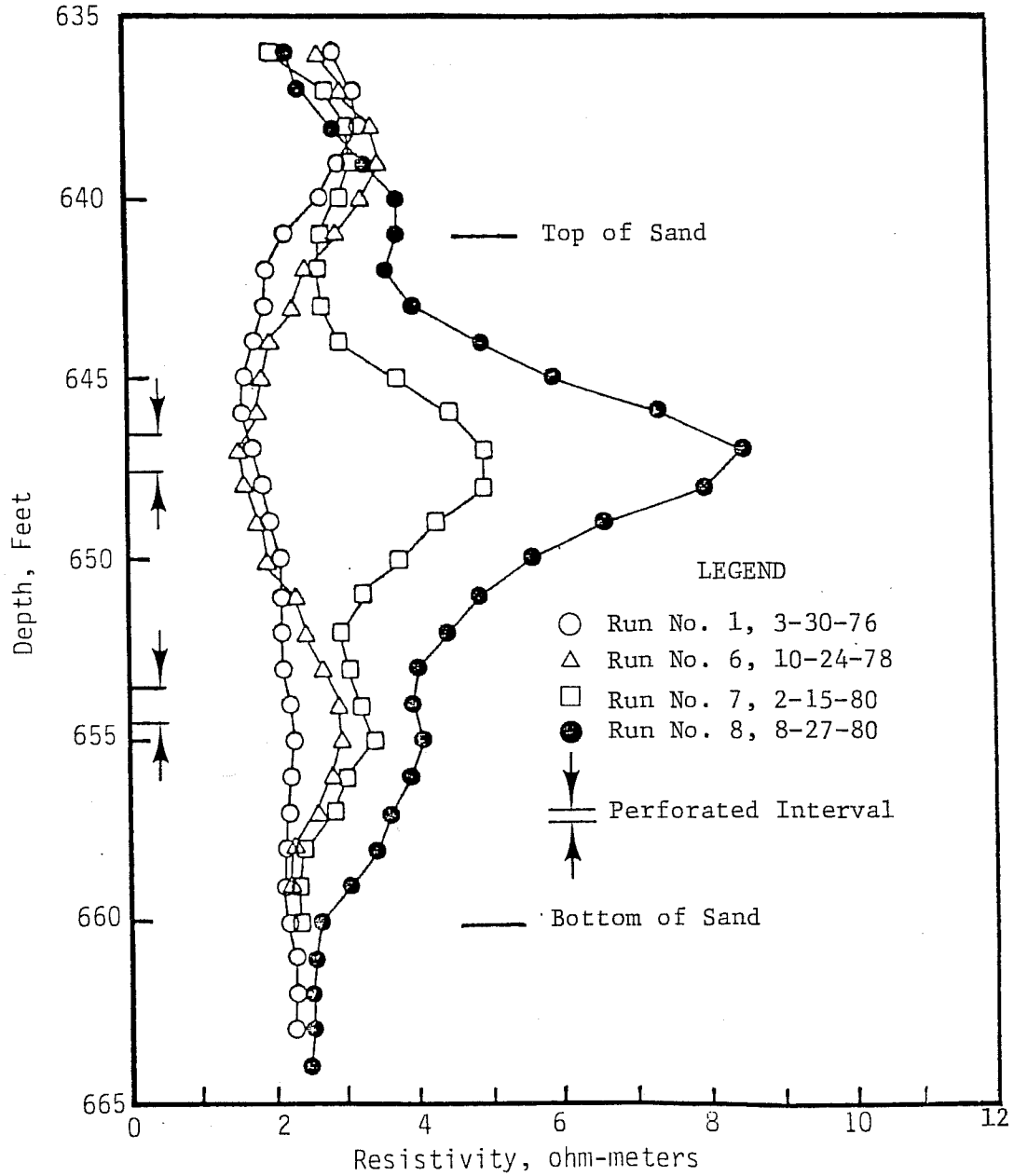


FIGURE 23

CORE FLOOD RESULTS USING CHEMICAL
SLUG FOR SOUTH PATTERN

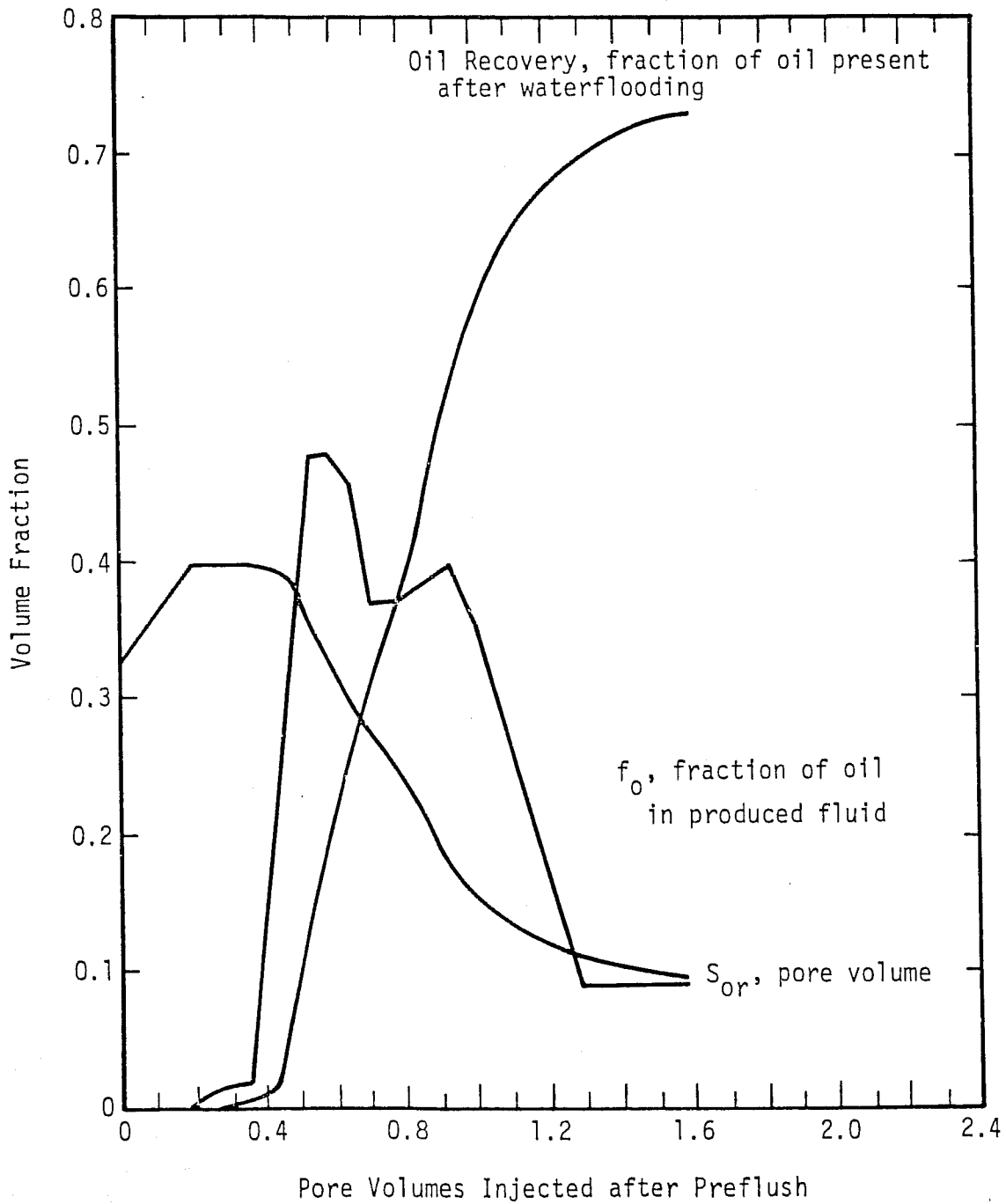


FIGURE 24

OIL DISPLACEMENT RESULTS IN BEREA AND EL DORADO
CORES USING UNION OIL PROCESS

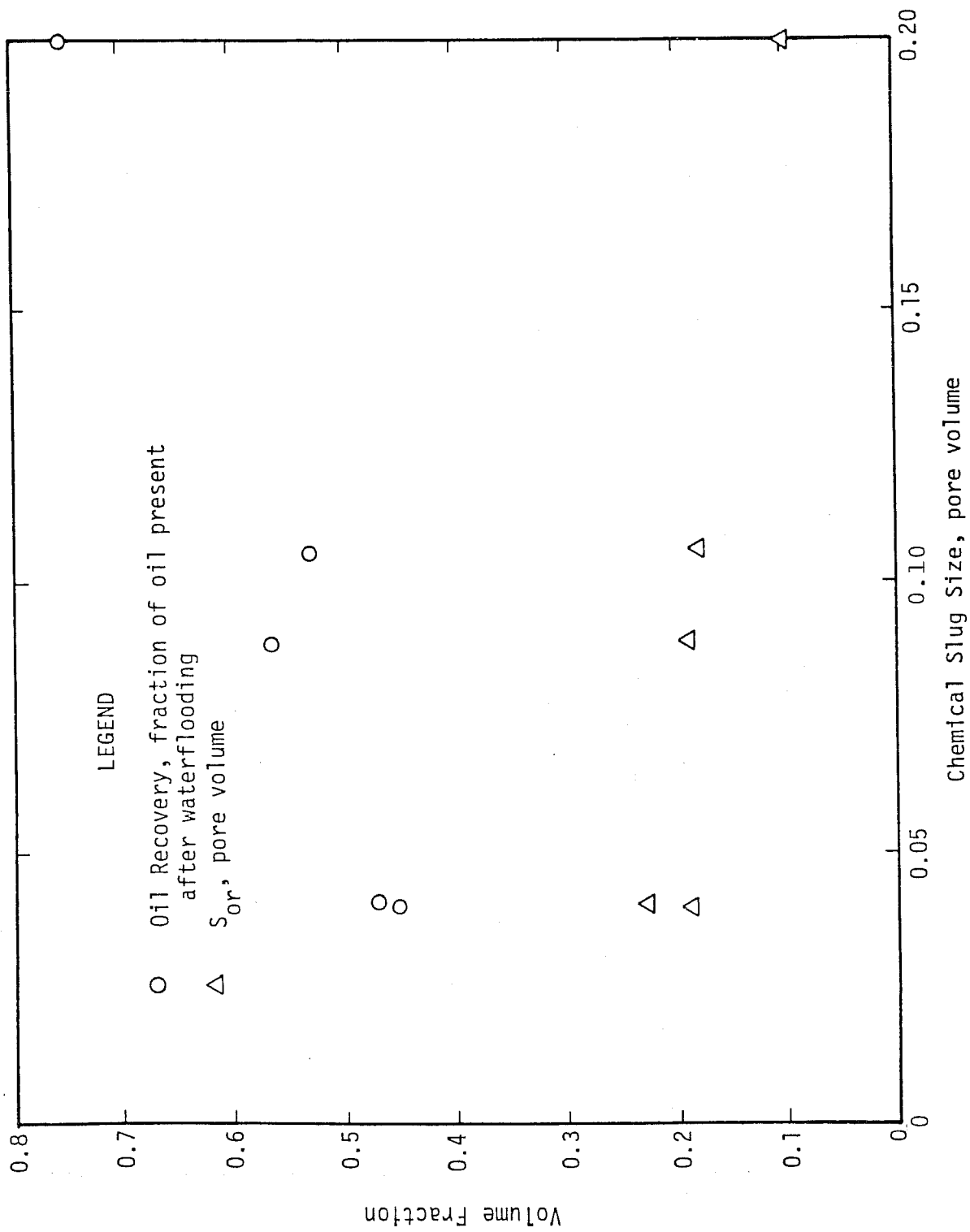


FIGURE 25

PRODUCED FLUIDS
HEGBERG LEASE
PROJECT TOTALS

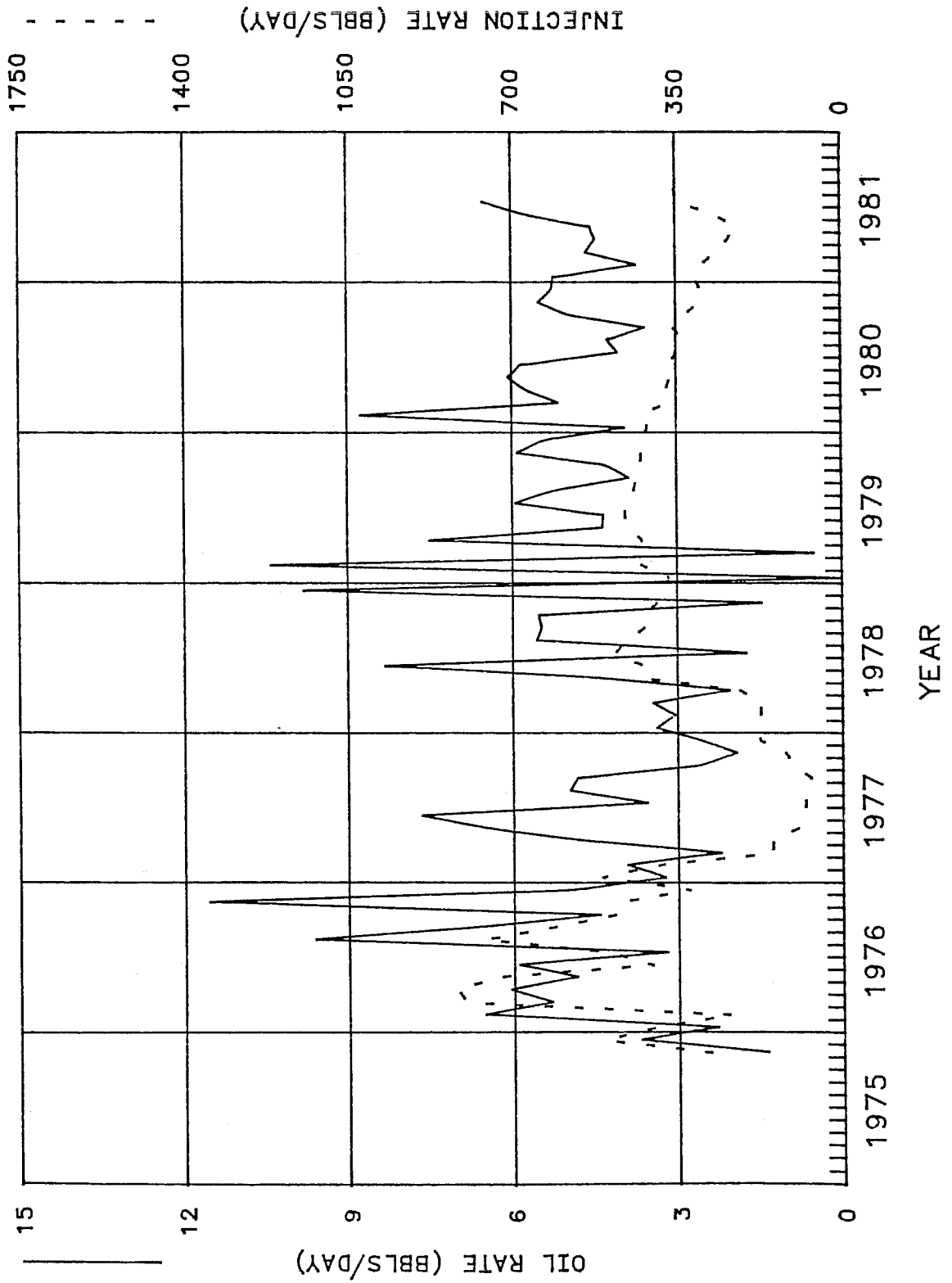


FIGURE 26

PRODUCED FLUIDS
HEGBERG LEASE
PROJECT TOTALS

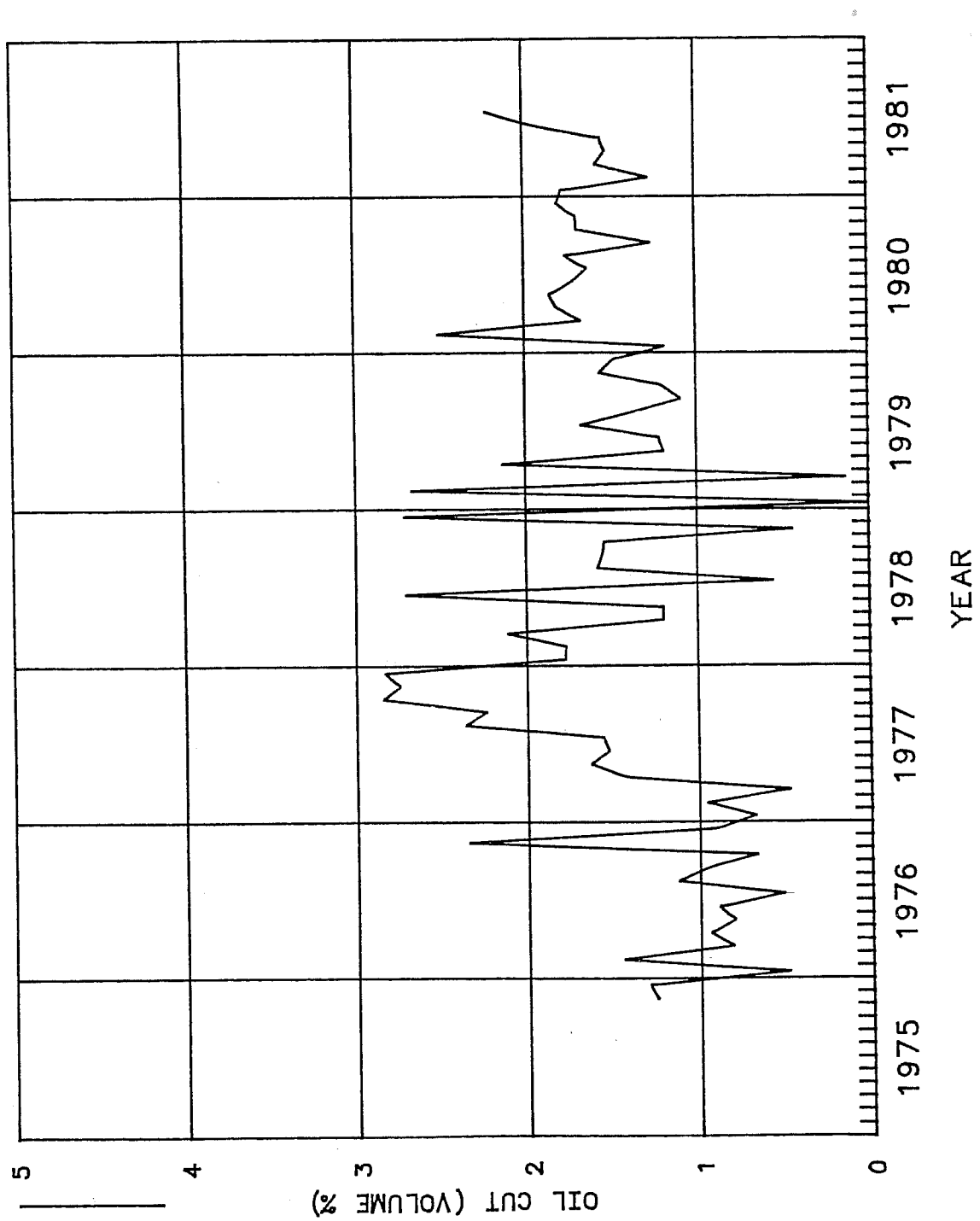


FIGURE 27

PRODUCED FLUIDS
HEGBERG LEASE
WELL MP-227

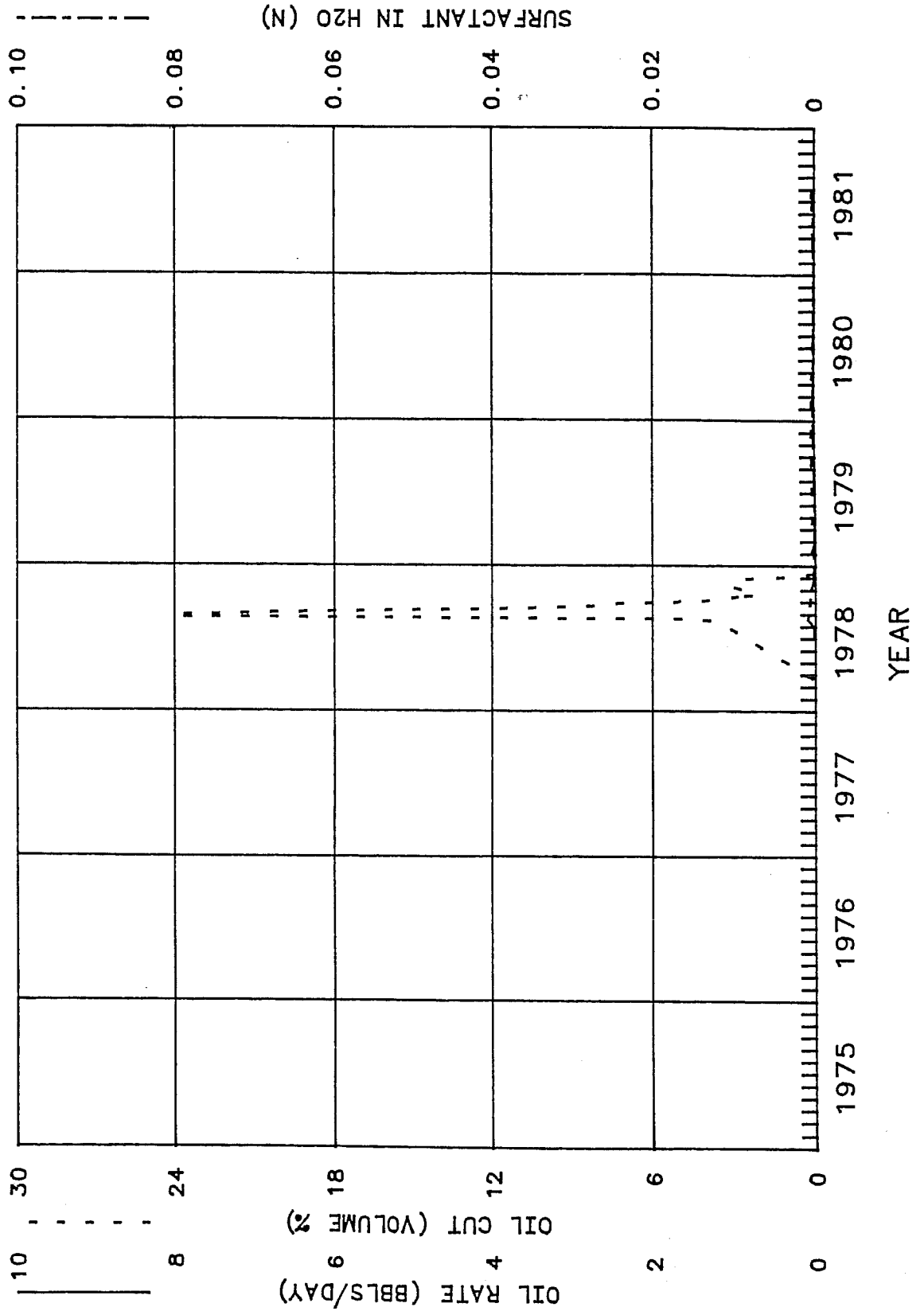


FIGURE 28

PRODUCED FLUIDS
 HEGBERG LEASE
 WELL MP-227

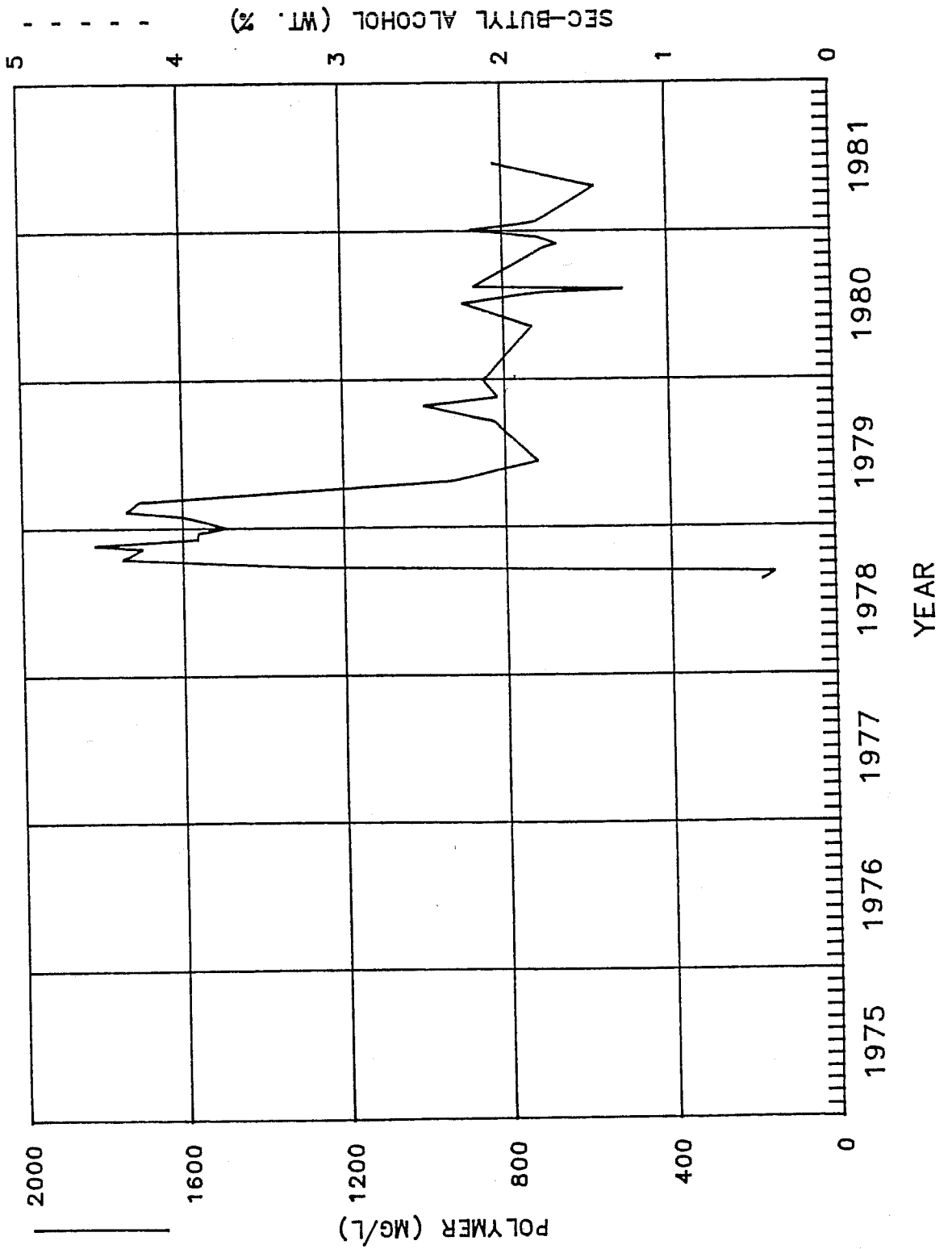


FIGURE 29

PRODUCED FLUIDS
HEGBERG LEASE
WELL MP-227

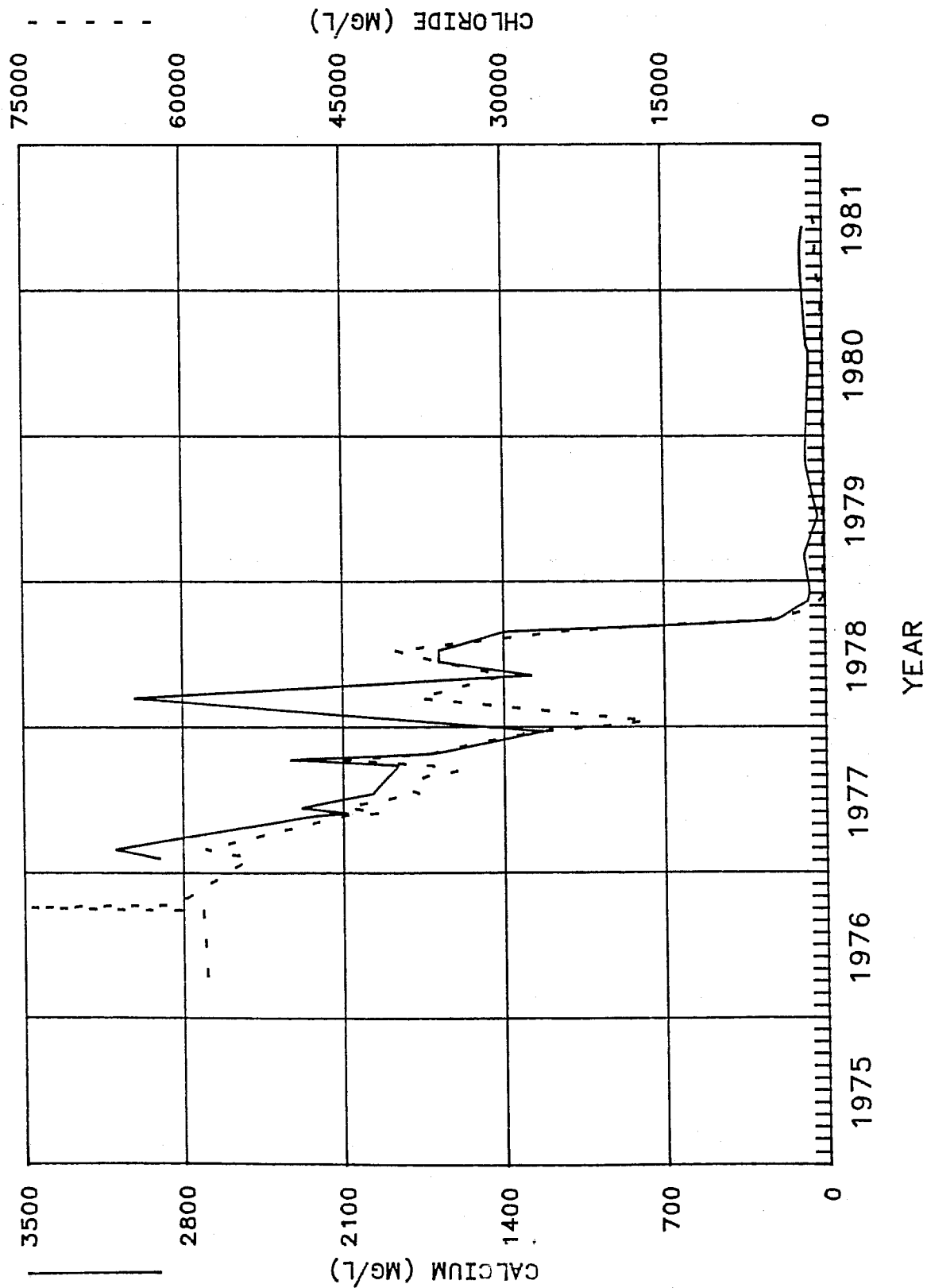


FIGURE 30

PRODUCED FLUIDS
 HEGBERG LEASE
 WELL MP-228

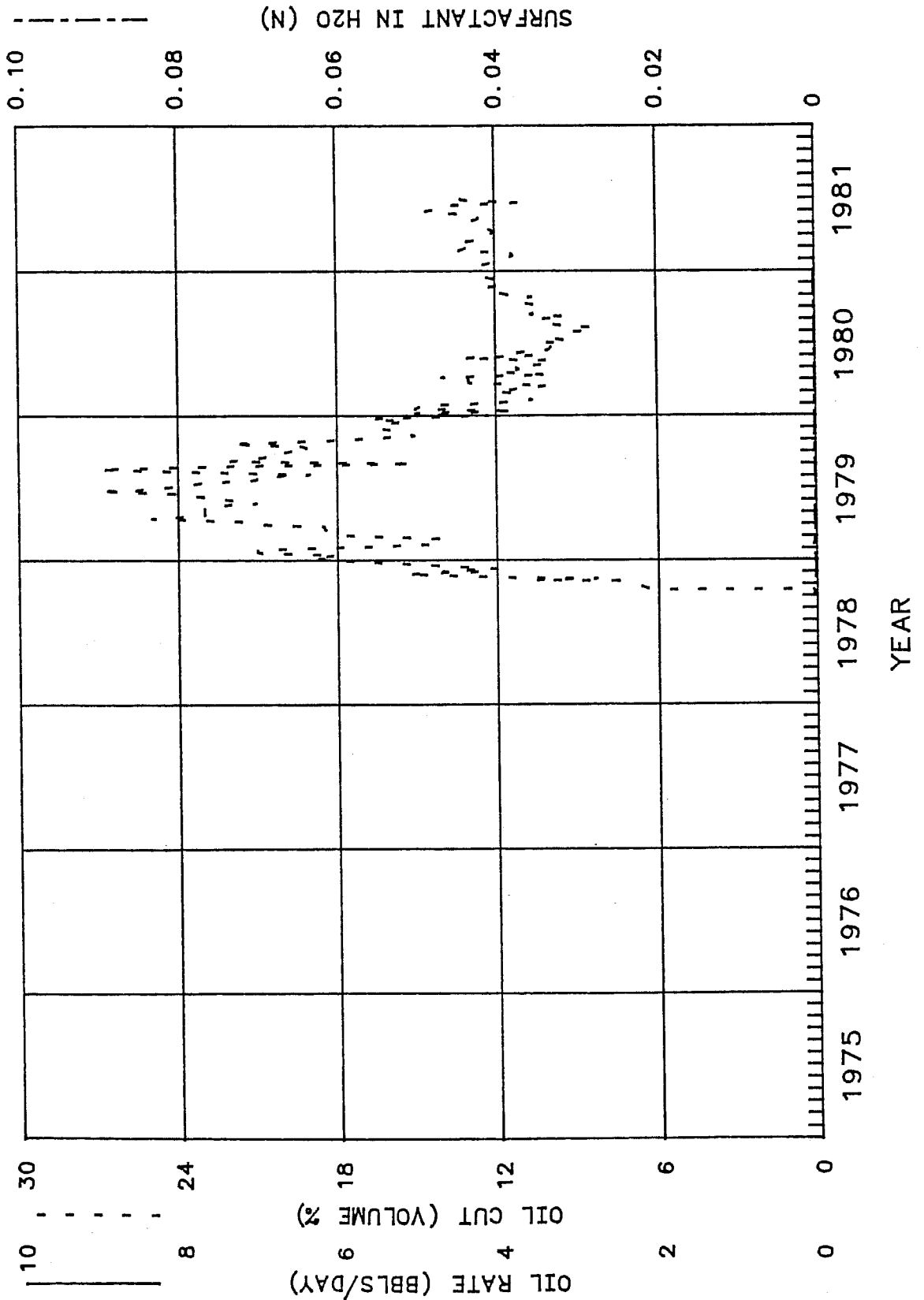


FIGURE 31

PRODUCED FLUIDS
 HEGBERG LEASE
 WELL MP-228

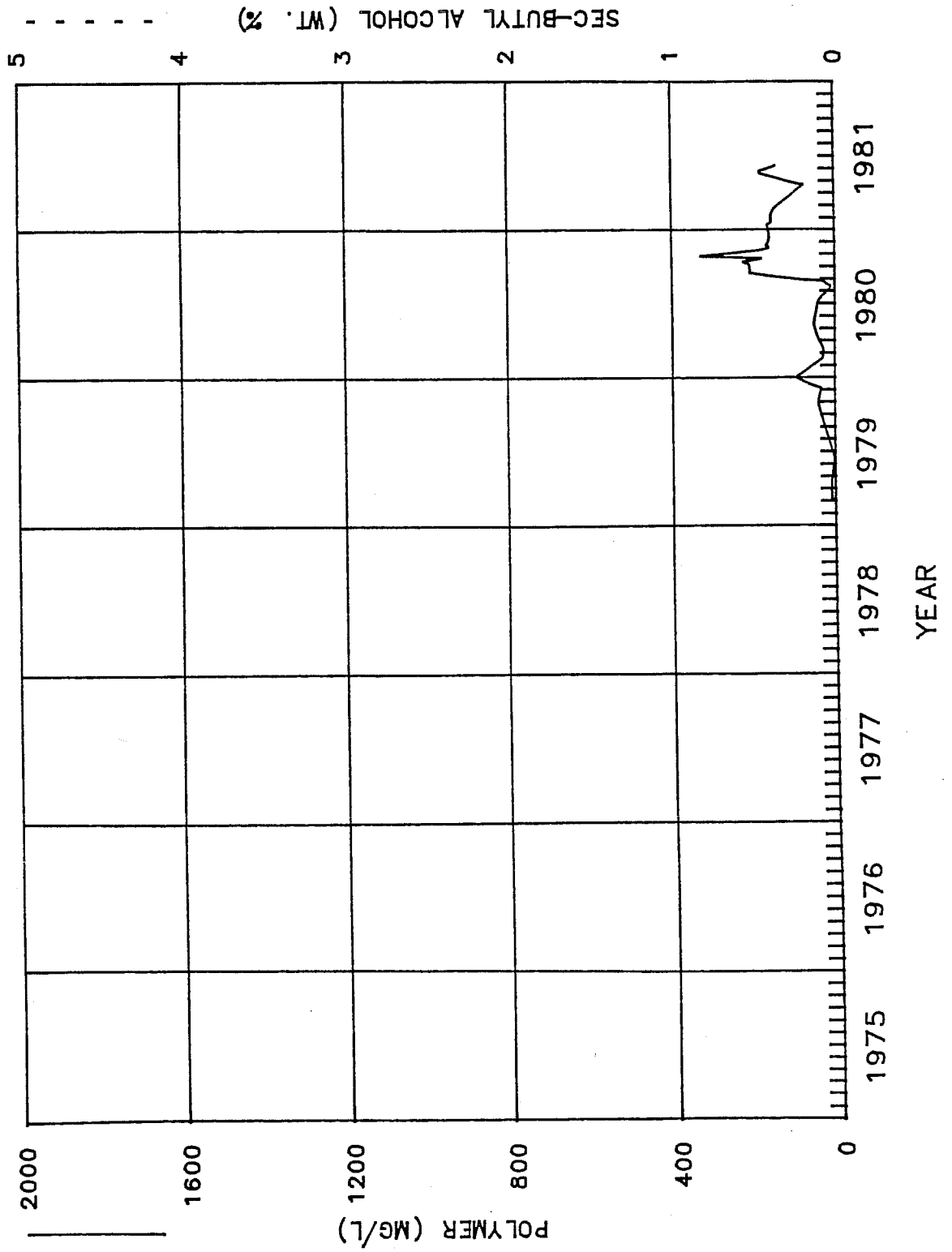


FIGURE 32

PRODUCED FLUIDS
HEGBERG LEASE
WELL MP-228

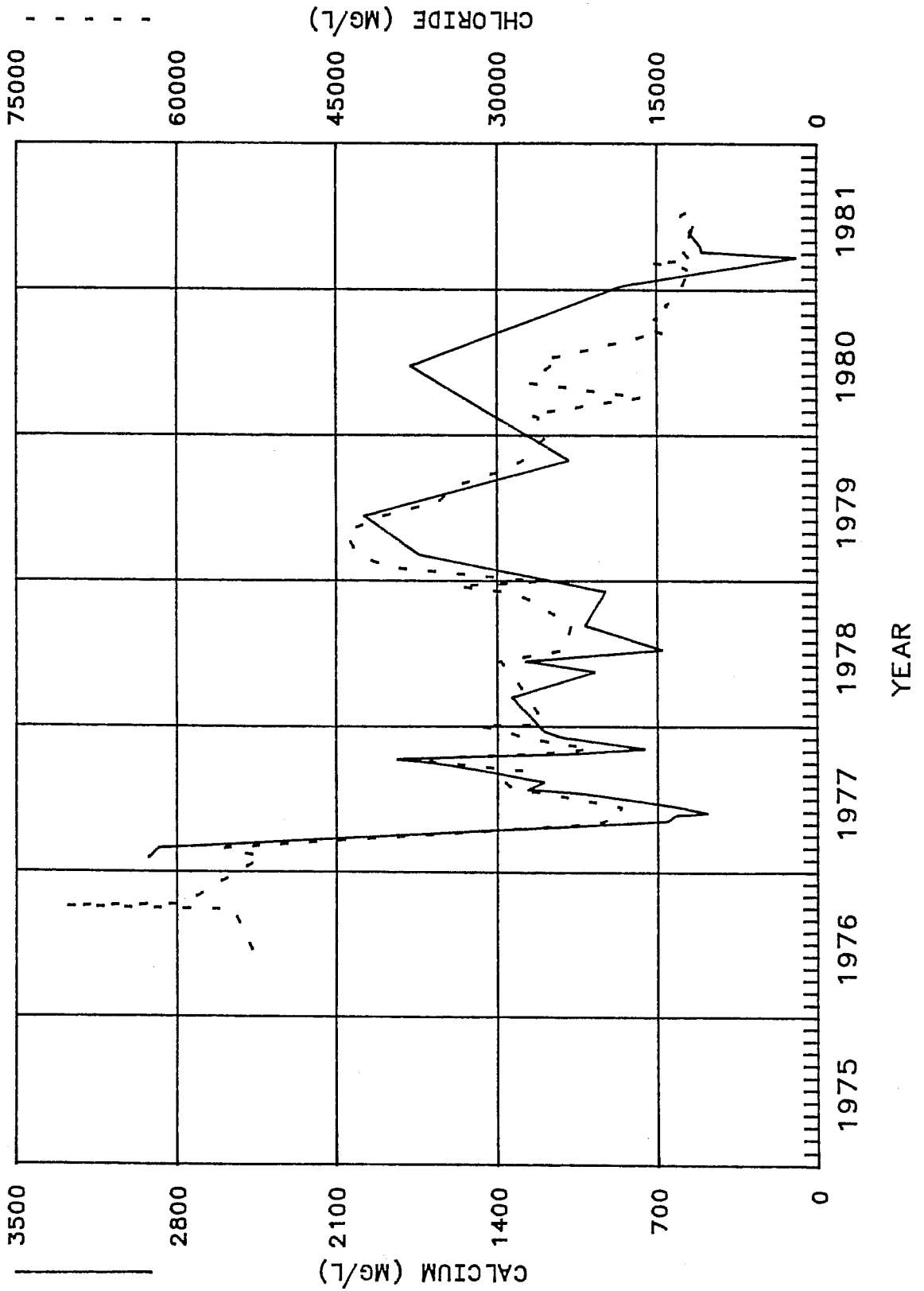


FIGURE 33

PRODUCED FLUIDS
 HEGBERG LEASE
 WELL MP-219

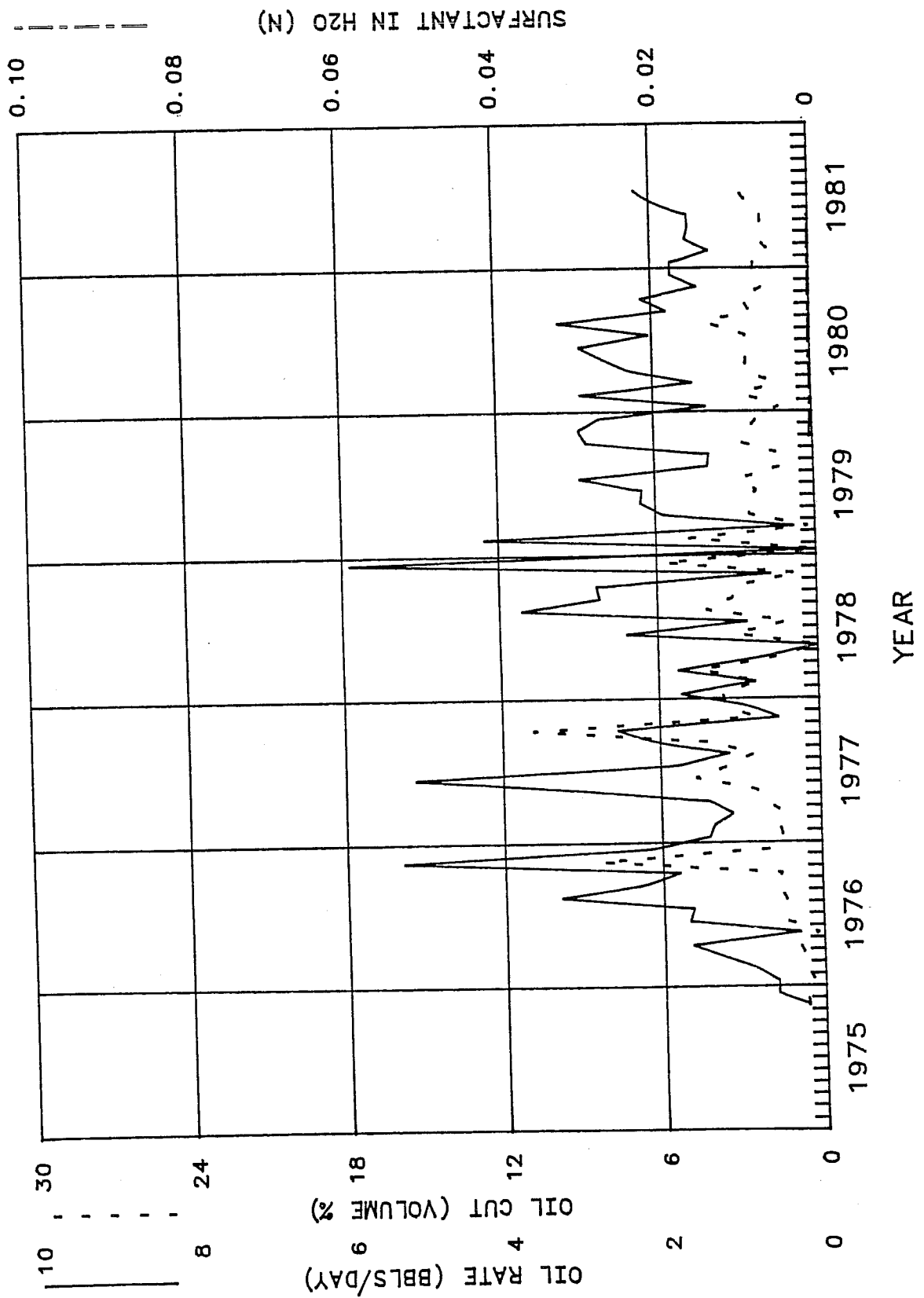


FIGURE 34

PRODUCED FLUIDS
 HEGBERG LEASE
 WELL MP-219

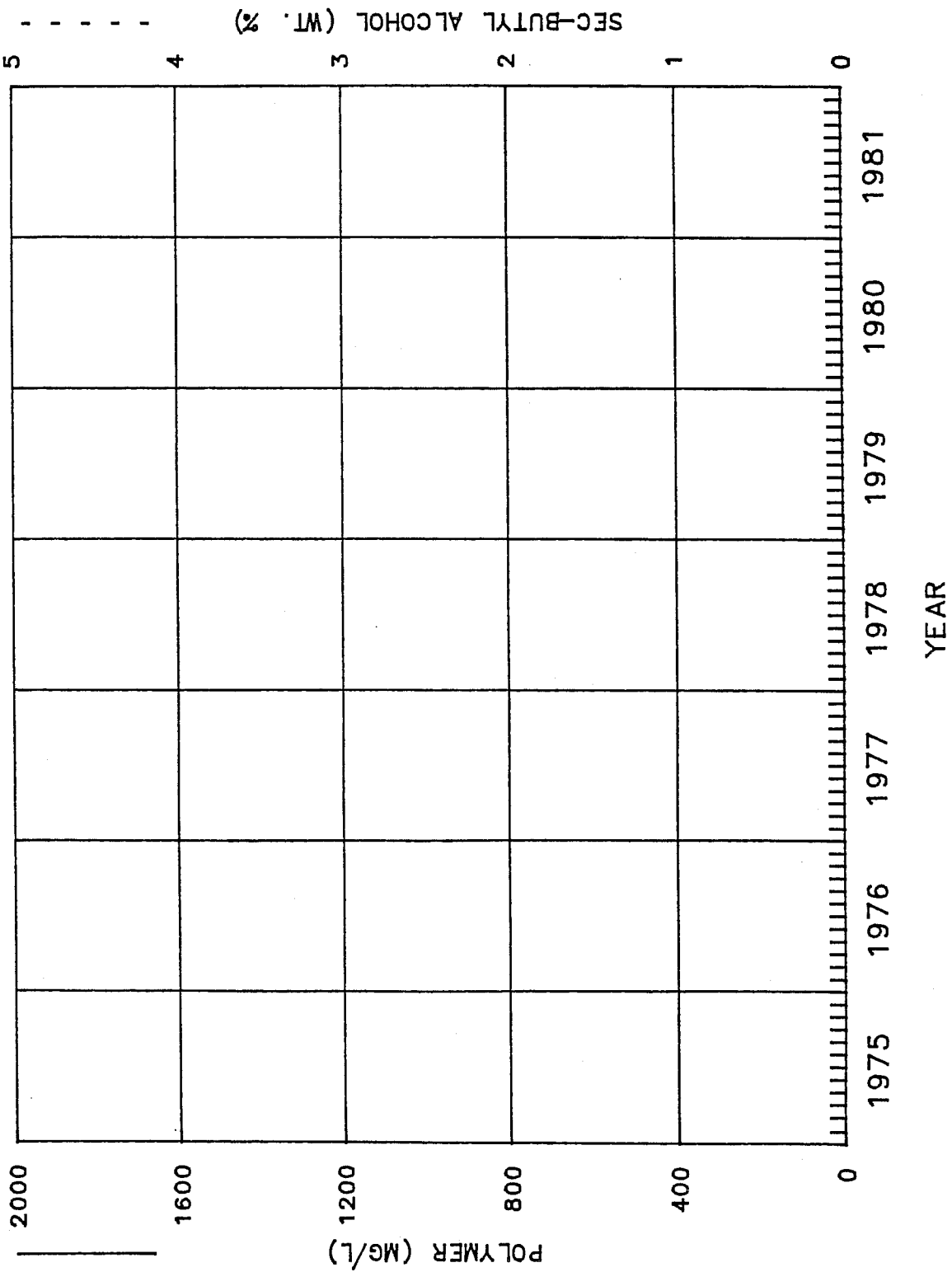
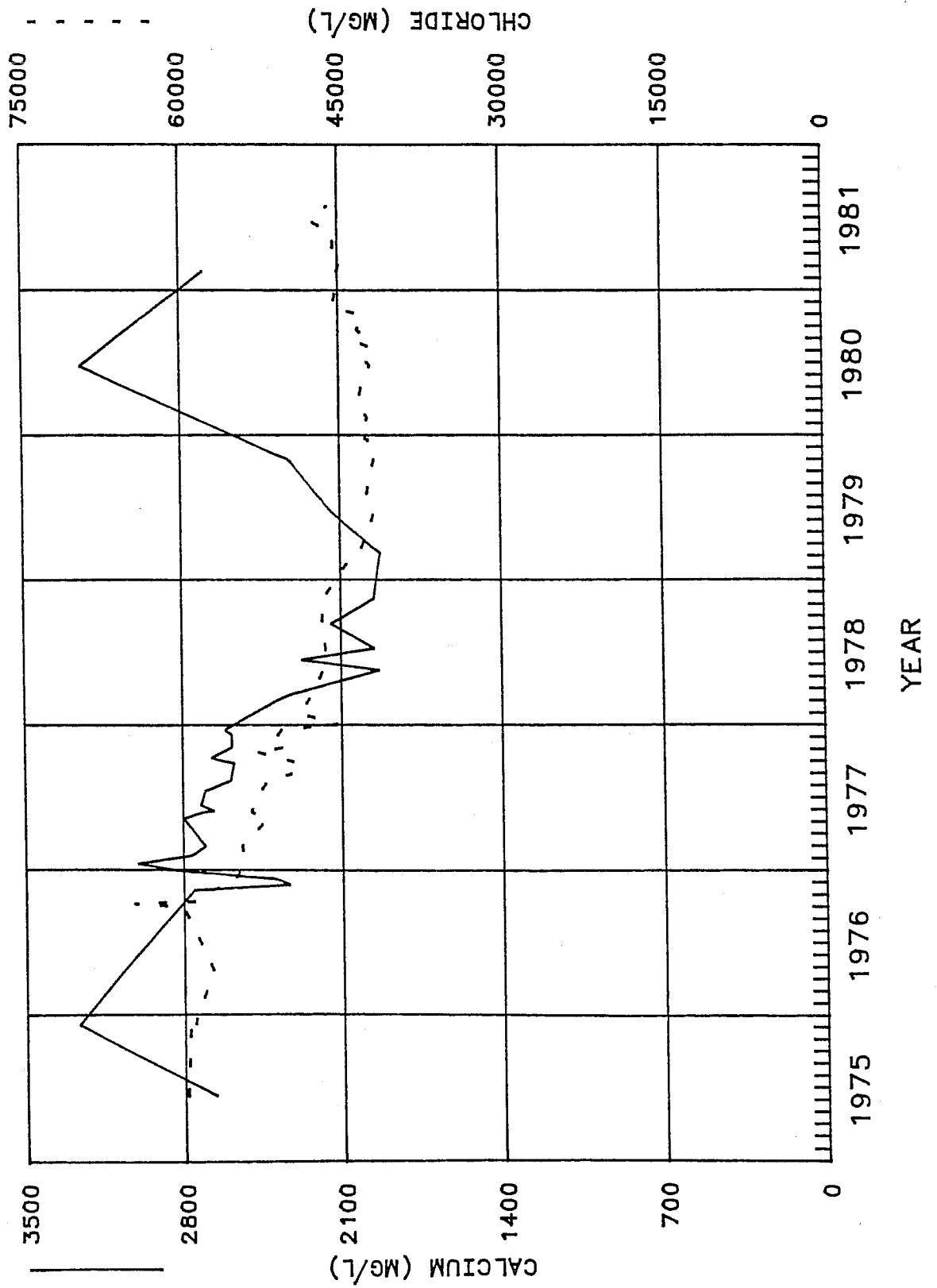


FIGURE 35

PRODUCED FLUIDS
HEGBERG LEASE
WELL MP-219



PRODUCED FLUIDS
 HEGBERG LEASE
 WELL MP-229

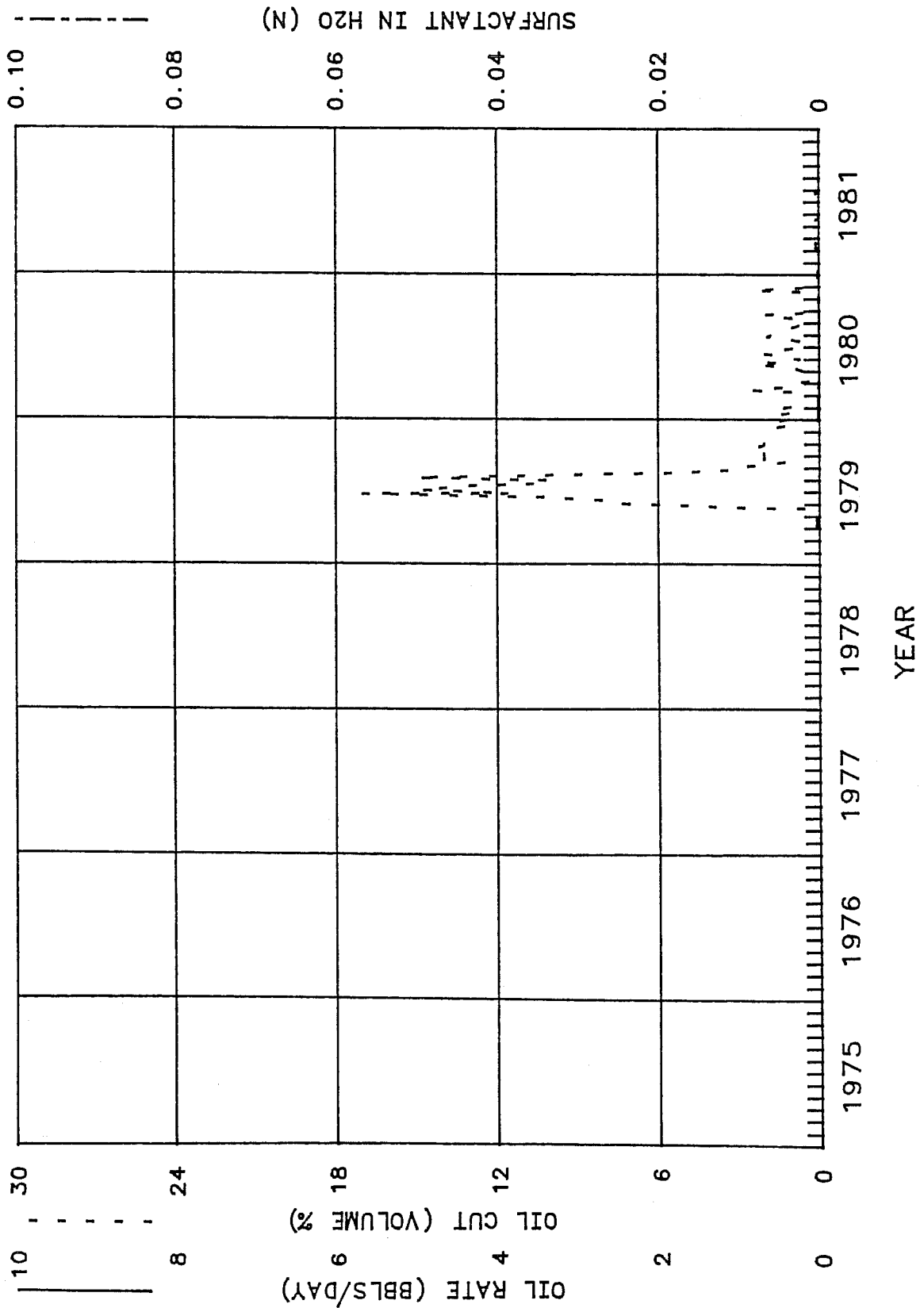
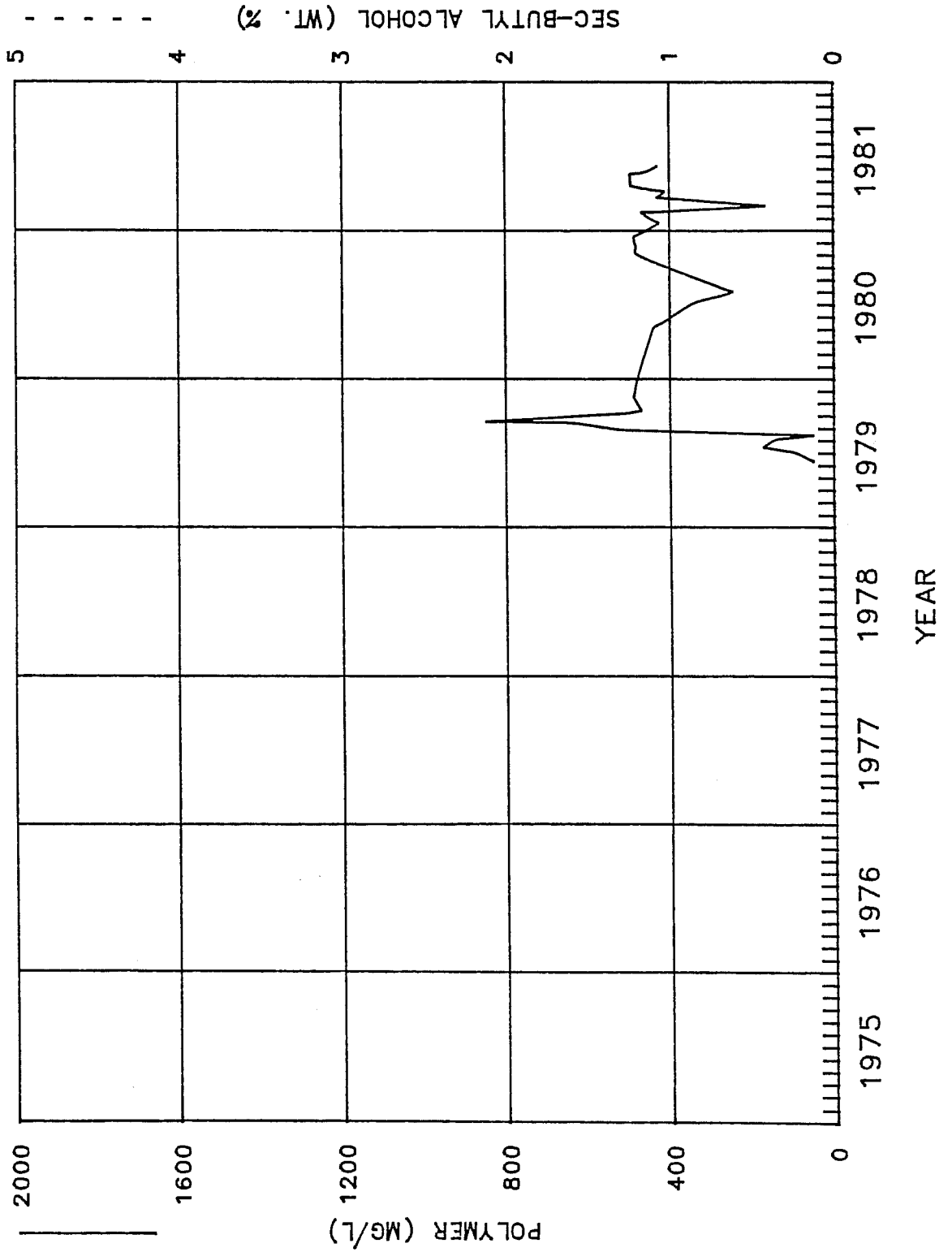


FIGURE 37

PRODUCED FLUIDS
 HEGBERG LEASE
 WELL MP-229



PRODUCED FLUIDS
 HEGBERG LEASE
 WELL MP-229

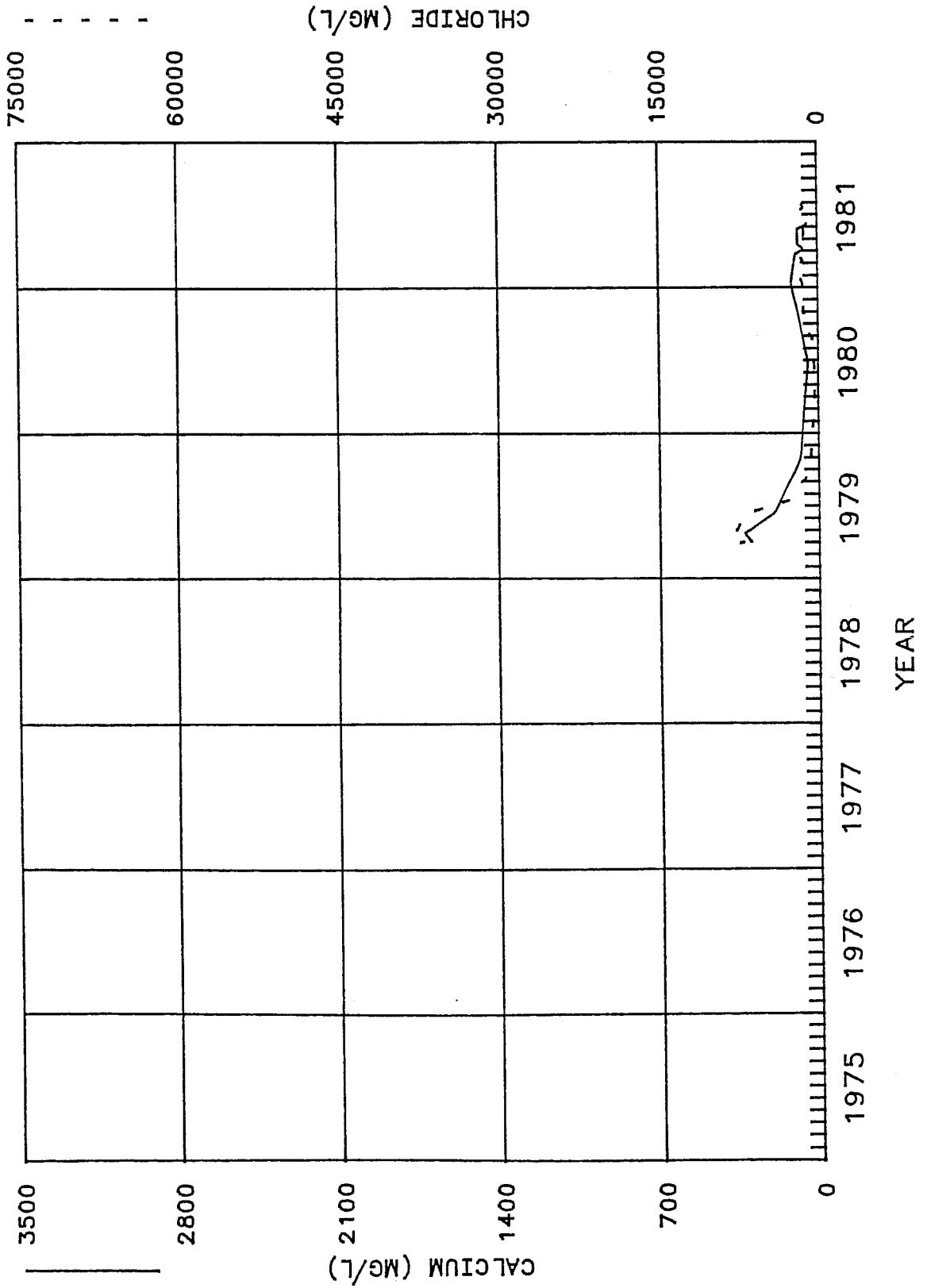
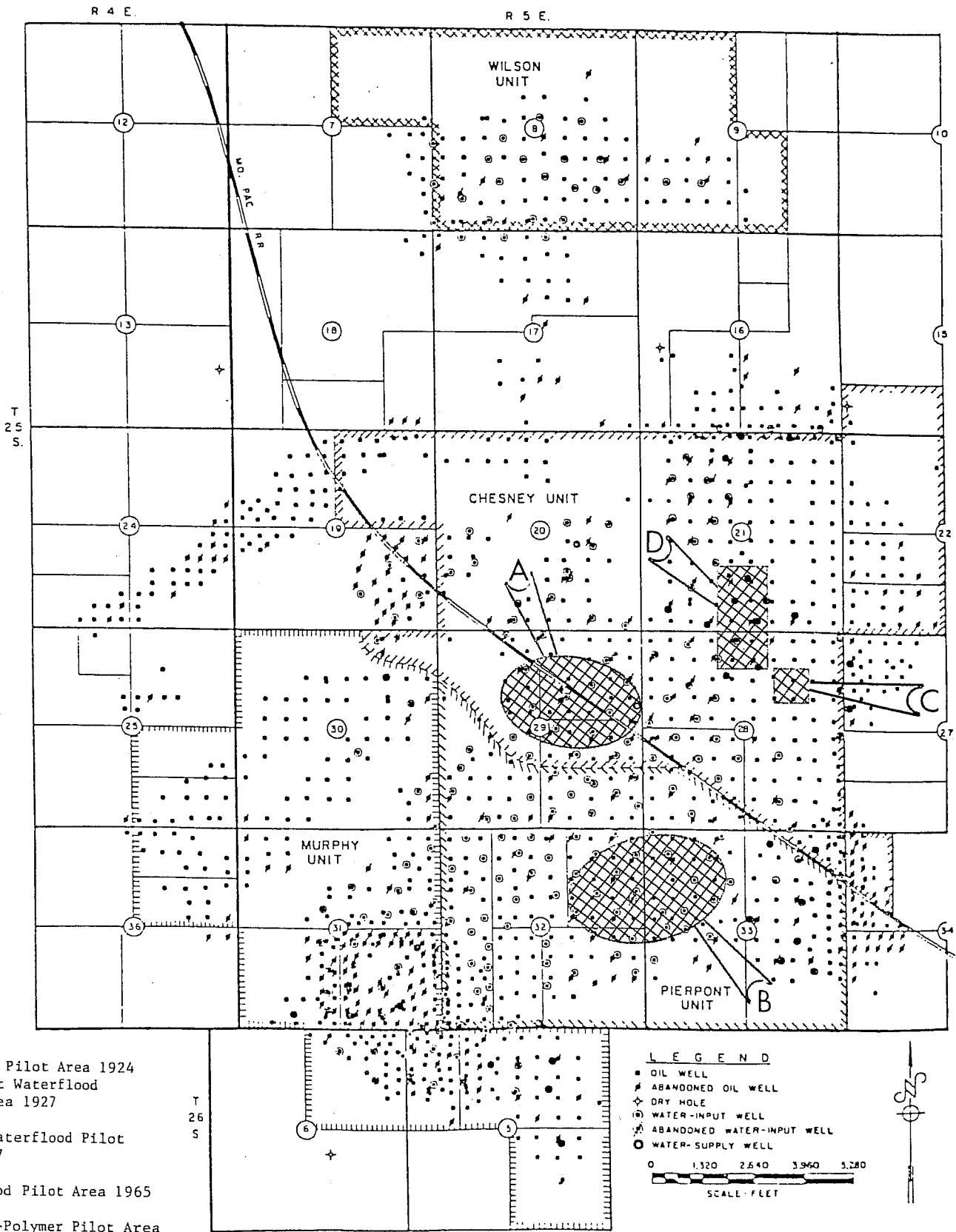


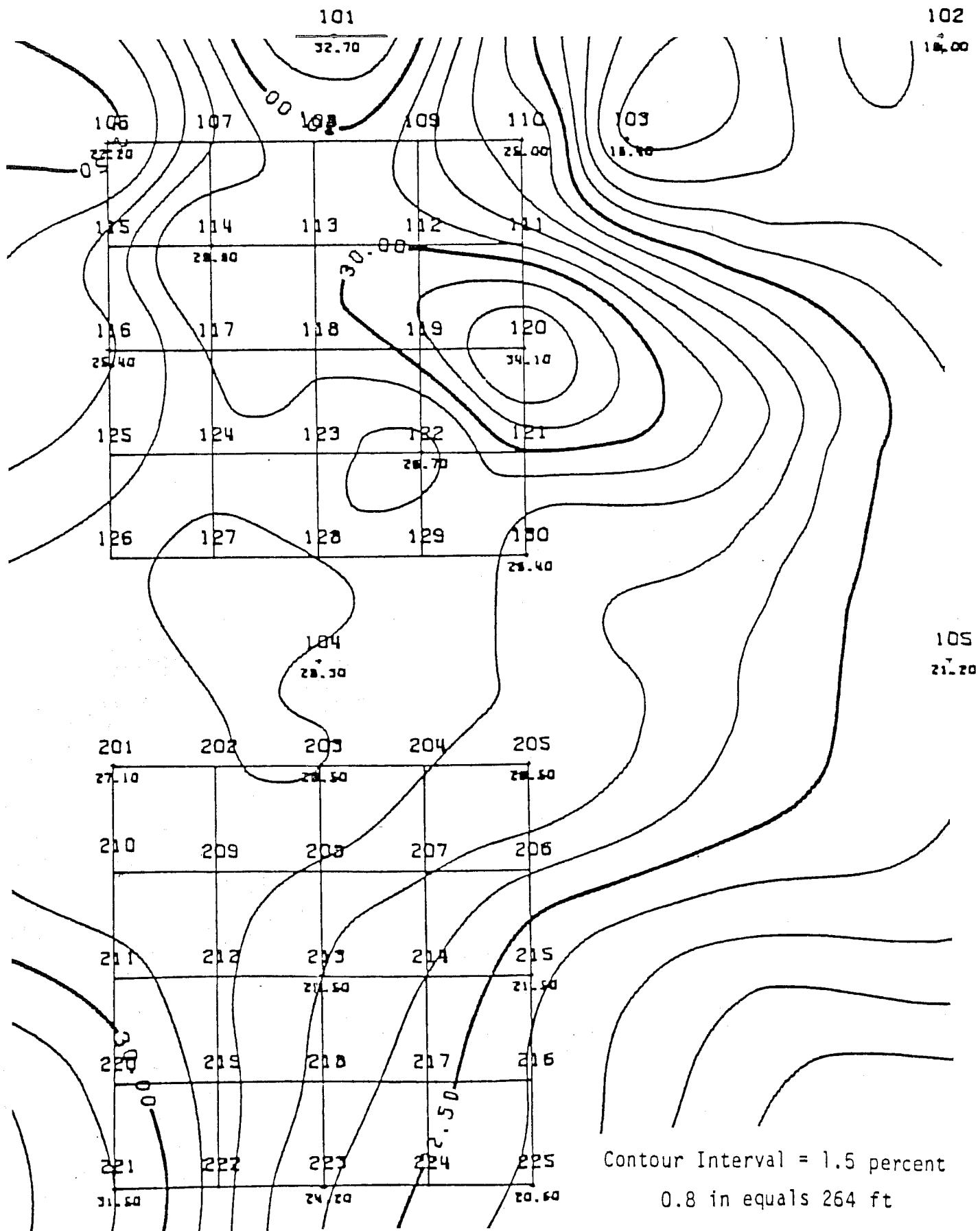
FIGURE 39

EOR PROJECTS IN THE EL DORADO FIELD



- A - Airflood Pilot Area 1924 and First Waterflood Pilot Area 1927
- B - Second Waterflood Pilot Area 1947
- C - Steamflood Pilot Area 1965
- D - Micellar-Polymer Pilot Area

OIL SATURATION DISTRIBUTION FROM CORE ANALYSIS



CAPACITY DISTRIBUTION USING CORE ANALYSIS DATA

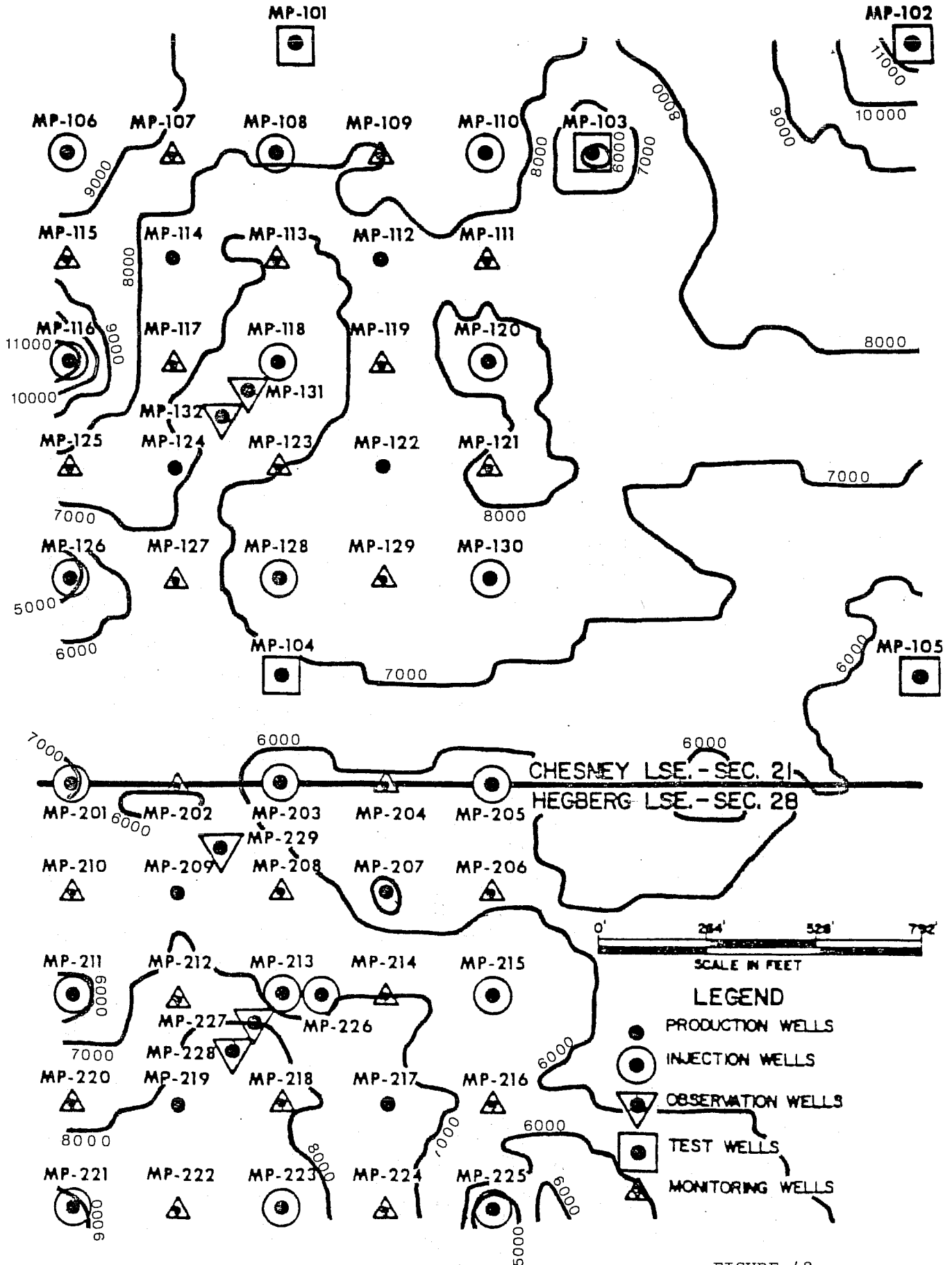


FIGURE 42

OIL SATURATION DISTRIBUTION FROM WELL LOGGING

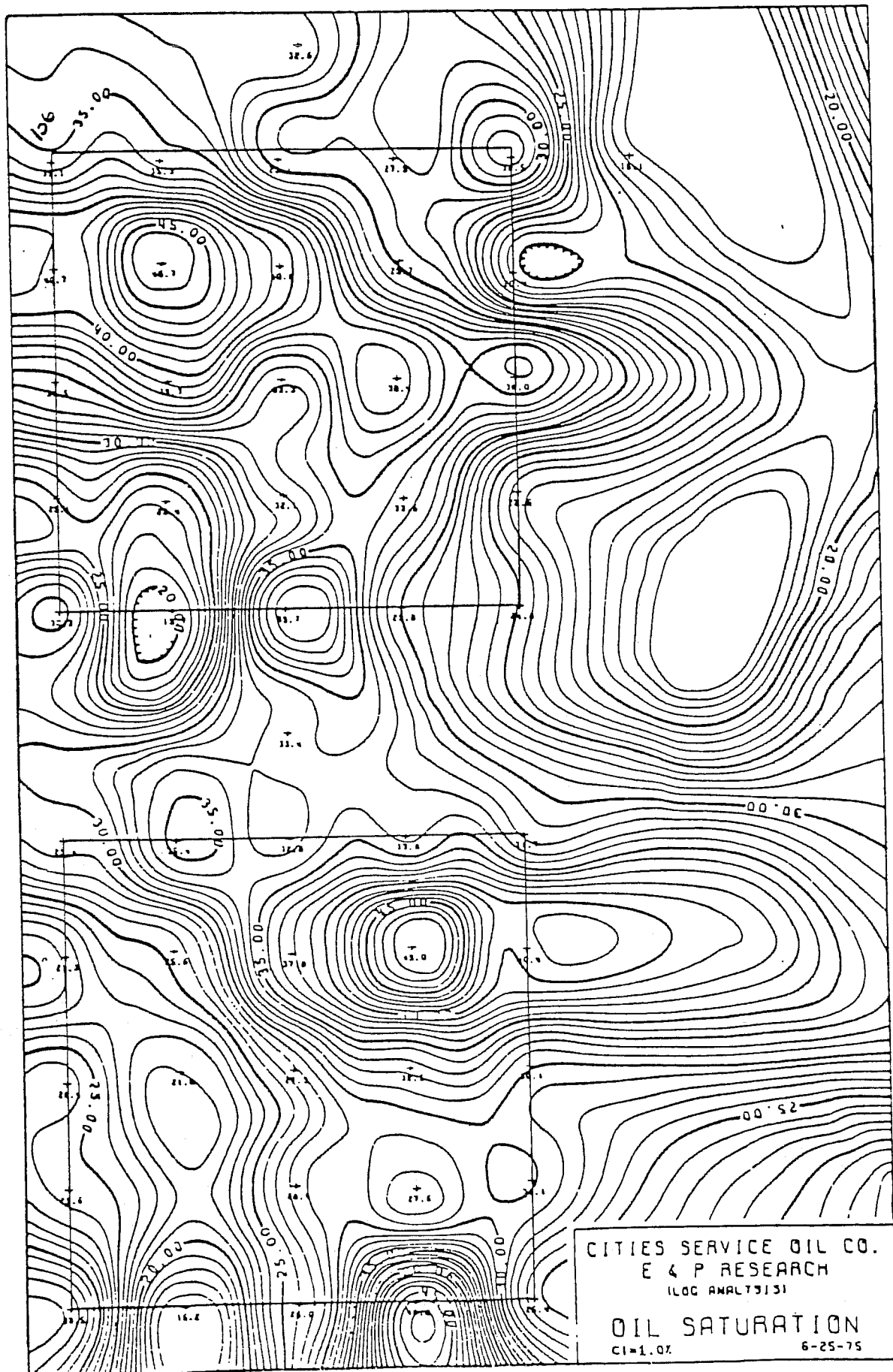
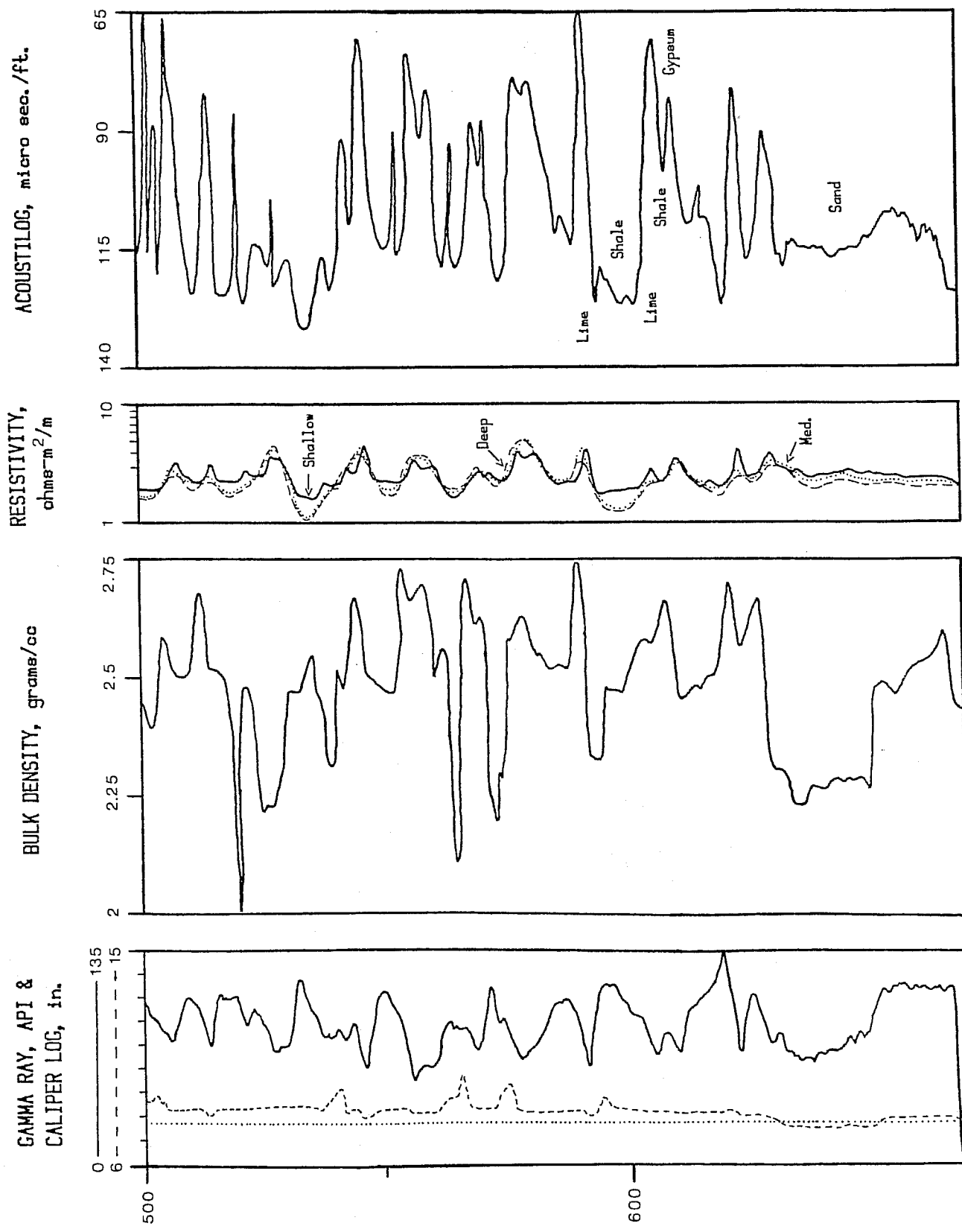
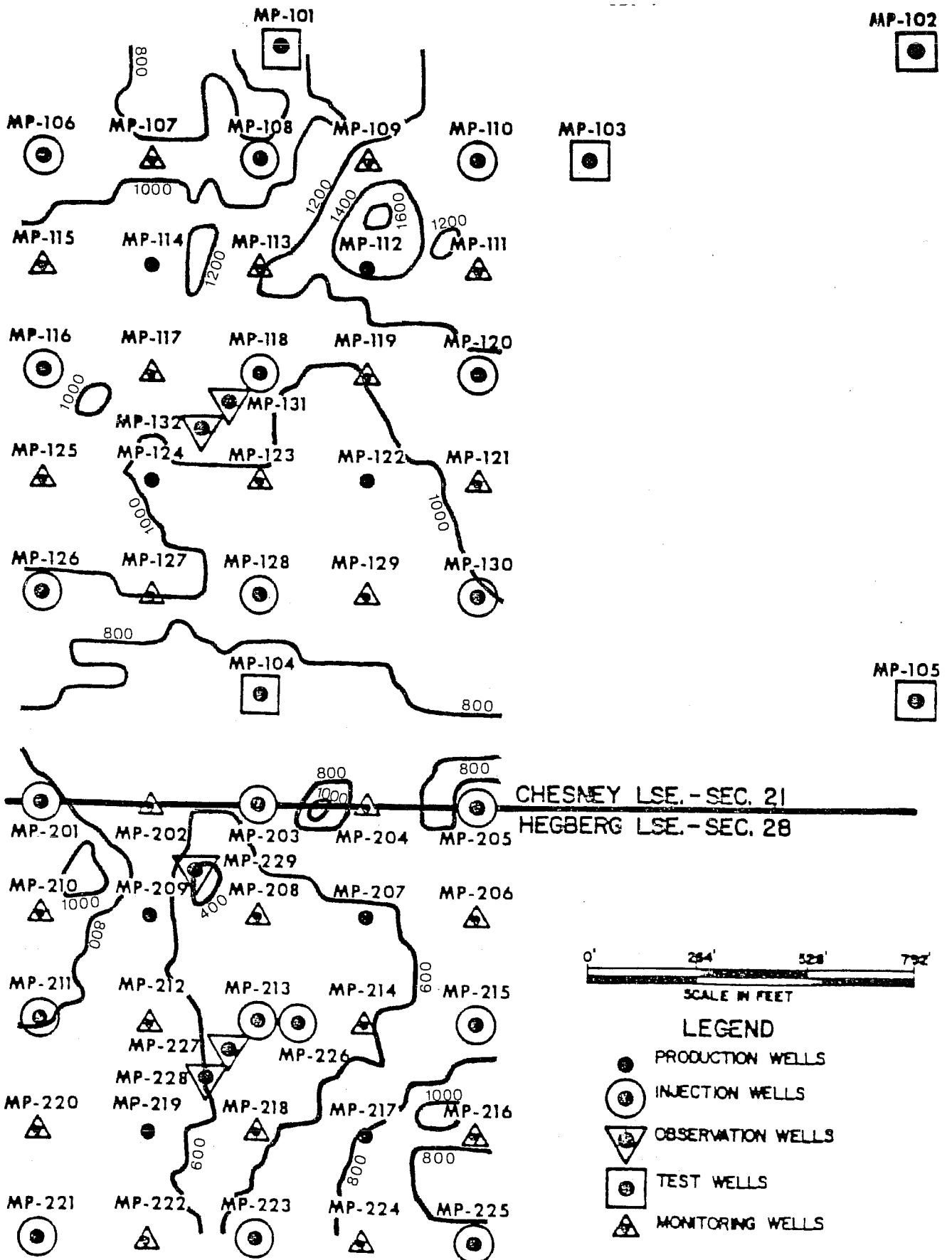


FIGURE 43

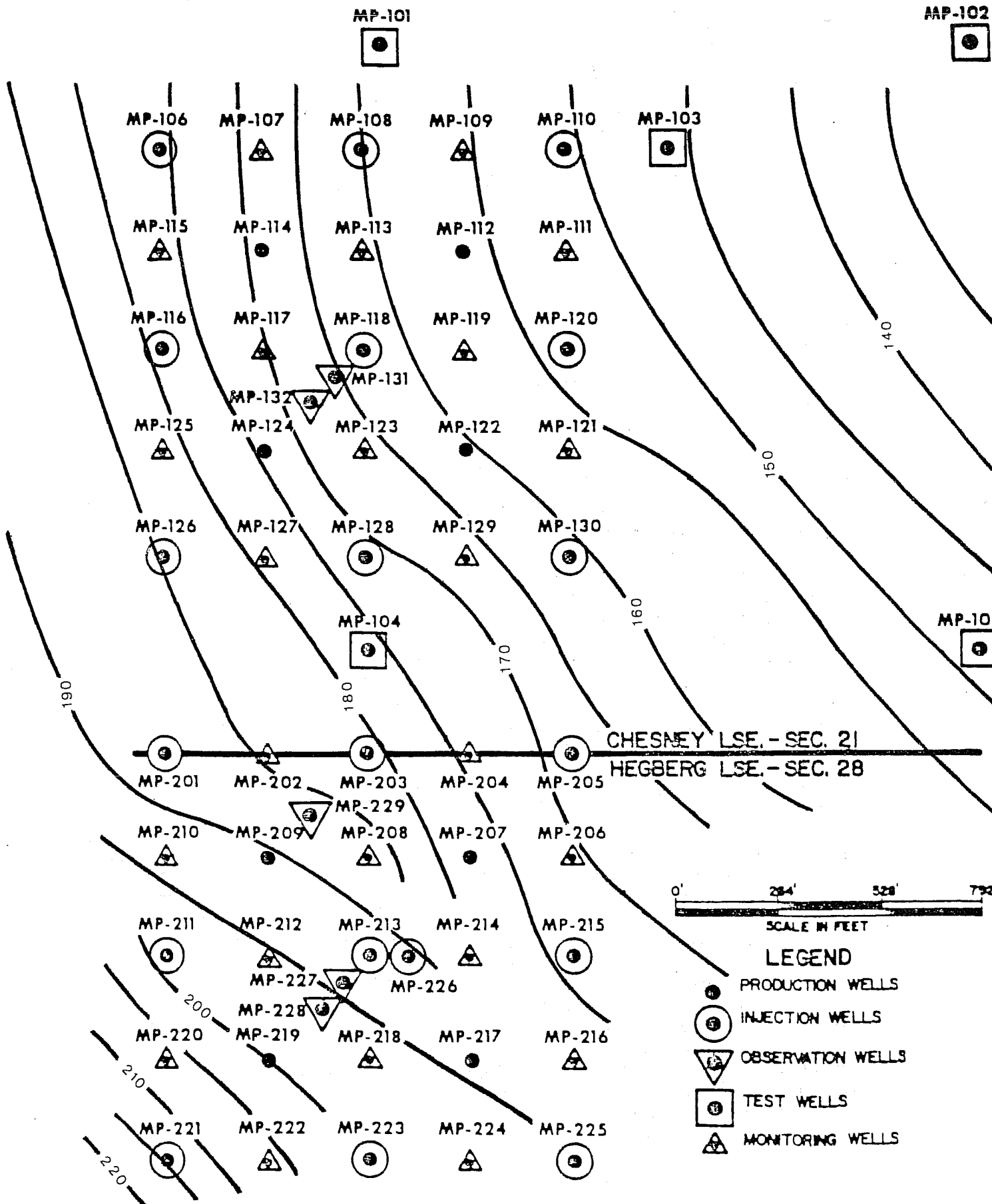
COMPOSITE LOG RESPONSE WELL MP-130



CAPACITY DISTRIBUTION USING PRESSURE TRANSIENT DATA



PRESSURE DISTRIBUTION MAP



APPENDIX A

GEOLOGICAL DESCRIPTION

Strata of the Admire Group (Wolfcampian Stage, Permian System) within Butler County, Kansas, are composed of an interbedded sequence of shales, limestones, siltstones, and sandstones. These sediments were deposited within a predominantly shallow marine environment which includes both shallow water carbonate and shale deposits as well as deltaic sediments. The source areas for Admire clastic deposits include the Nemaha Ridge, the Ouachita Uplift, and the Ozark Dome.

The Admire 650 Foot Sandstone, which contains the producing intervals within the El Dorado Field pilot area, was deposited within a progradational deltaic sequence of interbedded sandstones, siltstones, and shales. The deltaic deposits are overlain by limestones and shales which indicate a decline in the influx of clastics followed by subsidence and the subsequent transgression of the inland sea. A total of nine depositional facies are recognized within the Admire 650 Foot Sandstone based upon sedimentological analyses performed by Cities Service Company personnel.⁶ The main sedimentological characteristics for each of these depositional facies are summarized below.

Interdistributary Bay Silty Shale Facies

The interdistributary bay silty shale facies comprises the basal interval of the Admire 650-Foot Sandstone throughout the pilot area. Thickness estimates for the strata included within this facies average about 20 feet based upon gamma ray logs. The facies is dominated by laminated silty shales with asymmetrical siltstone ripples together with minor amounts of horizontally bedded silt and shale as well as some deformed bedding. The interval is burrowed, with the number of burrows decreasing up-section. The poor diversification of burrow types suggests possible brackish water conditions, while the decrease in abundance of burrows within the upper portions of the interval is probably related to an increase in the volume of coarse clastics entering the bay environment.

Interbedded Interdistributary Bay, Splay Channel, and Beach Sandstone Facies

This interval (henceforth described as the interbedded facies) comprises the basal reservoir facies throughout the entire project area. The average thickness of the interbedded facies is approximately 8 feet and ranges up to a maximum thickness of more than 20 feet. The interbedded facies is composed of splay channel sandstone deposits (generally ranging from 2 to 3 feet thick) alternating with interdistributary bay silts and shales (averaging 1 to 2 feet thick). Some reworking of the splay channel deposits is evidenced by thin, discontinuous beach deposits (average thickness 0.1 to 0.5 feet). The beach sandstones are recognized on the basis of contrasts in the sedimentary bedform structure relative to the splay channel deposits. The beach sandstones are characterized by planar laminated low angle cross bedding while splay channel sandstones display moderate-to-low angle trough cross

bedding and ripple bedding. Splay channel deposits are formed due to the breaching of distributary channel margins and the subsequent deposition of sand within the adjoining interdistributary bay. As a consequence, splay channel deposits display a great deal of similarity to distributary channel sands. These similarities include comparable sand fractions and sedimentary structures. Splay channel deposits are differentiated from distributary channel sandstones on the basis of thickness, geometry, the presence or absence of intercalated bay muds, and lateral extent. Splay channel sandstones are generally thin lobate deposits oriented at a high angle relative to the flow direction of the distributary channel system. The splay sands typically thin rapidly away from the distributary margin, resulting in a wedge shaped distribution in cross section. The limited areal extent of these sandstones, coupled with the lateral fluctuations in thickness, preclude effective correlation of individual splay channel deposits. The porosity and permeability characteristics for the splay channel sandstones are excellent, with average porosity values of 28 percent and average air permeabilities of 628 md.

Distributary Channel Sandstone Facies

Sandstones of the distributary channel facies comprise the main reservoir interval within the Admire 650-Foot Sandstone. The distributary channel sandstones are divided into low and high energy subfacies on the basis of contrasts in sand/shale ratios and sedimentary structures. Sandstones grouped within the low energy subfacies contain a larger shale fraction (greater than 10 percent) and a predominance of ripple bedding relative to the high energy subfacies. High energy distributary channel deposits are characterized by a predominance of trough-cross stratification and small quantities of siltstone and shale. Low energy channel sandstones were deposited along the margins of the distributary channel system, while high energy channel sands were preferentially deposited in the more hydraulically competent or active portions of the distributary channel system. Paleocurrent analysis, performed on three oriented cores from the project area were interpreted to indicate a northerly flow direction (centered along the western margin of the Hegberg and Chesney pilot areas) with branching flow to the east-northeast near the central portion of the project area (Well MP-210). Average thickness for the high energy channel subfacies is 8 feet, while low energy channel sandstones average 5.5 feet thick. Isopach maps illustrating the distribution for both of the distributary channel subfacies are presented in Figures A1 and A2.

Distributary channel sandstones range from very fine to fine grained and display a variety of sedimentary structures including asymmetric ripple bedding, trough-cross stratification, and subhorizontal bedding. Rip-up clasts of siltstone and shale, and deformation structures indicating slumping along channel margins are common. Routine core analysis data (based on whole core analyses) indicate average porosity values of 29.05 percent and 27.50 percent, respectively, for the high and low energy channel subfacies, while air permeability averages 447.6 md and 410.0 md respectively. It should be noted that the slightly higher porosity and permeability data reported for the interbedded facies relative to the

distributary channel sandstones is attributed to the scarcity of silt and mud within the splay channel deposits. The rapid pulse of sand associated with splay channel deposition is less likely to incorporate fine-grained suspended sediment relative to the channel sandstones which experienced episodic fluctuations in flow rate and volume.

Inactive Channel Fill Facies

The inactive channel fill facies is comprised of fine grained overbank and levee deposits formed during the terminal stage of distributary channel sedimentation. The channel fill sediments are poorly sorted mixtures of sand, silt, and clay which are typically less than 2 feet thick. The principal sedimentary structures include ripple bedding and deformation structures resulting from slumping of channel margins. Vertical burrows and root casts are common. This interval typically contains a significant volume of carbonaceous debris. The preservation of the organic matter indicates the presence of abundant vegetation, as well as anaerobic conditions within the abandoned channels at the time of deposition.

Lignite Shale Facies

Thin (0.1 to 0.5 feet) deposits of lignitic shale commonly overlie the inactive channel fill deposits, and represent the final stage in the filling of the abandoned distributary channel. The interval is comprised of gray to black silty shale enriched with respect to macerated organic matter. The lignitic shale facies displays a gradational basal contact and a sharp upper contact.

Protected Bay Biomicrite Facies with Local Lagoonal Shale

Sediments within this facies are comprised of burrow mottled calcareous siltstone gradationally overlain by argillaceous biomicrite (or fossiliferous wackestone). The biomicrite facies unconformably overlies the lignitic shale facies sediments. The fossil assemblage is comprised of a diverse assemblage of marine fauna including fragments of gastropods, pelecypods, ostracodes, foraminifers, echinoderms, and trilobites. The unabraded fossil assemblage, organic-rich argillaceous matrix, and the stratigraphic position above a marsh or channel fill were cited as evidence of deposition within a near shore, low energy (protected) bay. The diversity and type of marine fauna present precludes the existence of hypersaline conditions within bay environment which argues for good current circulation between the bay and open marine shelf.

Protected Bay Claystone and Shale Facies

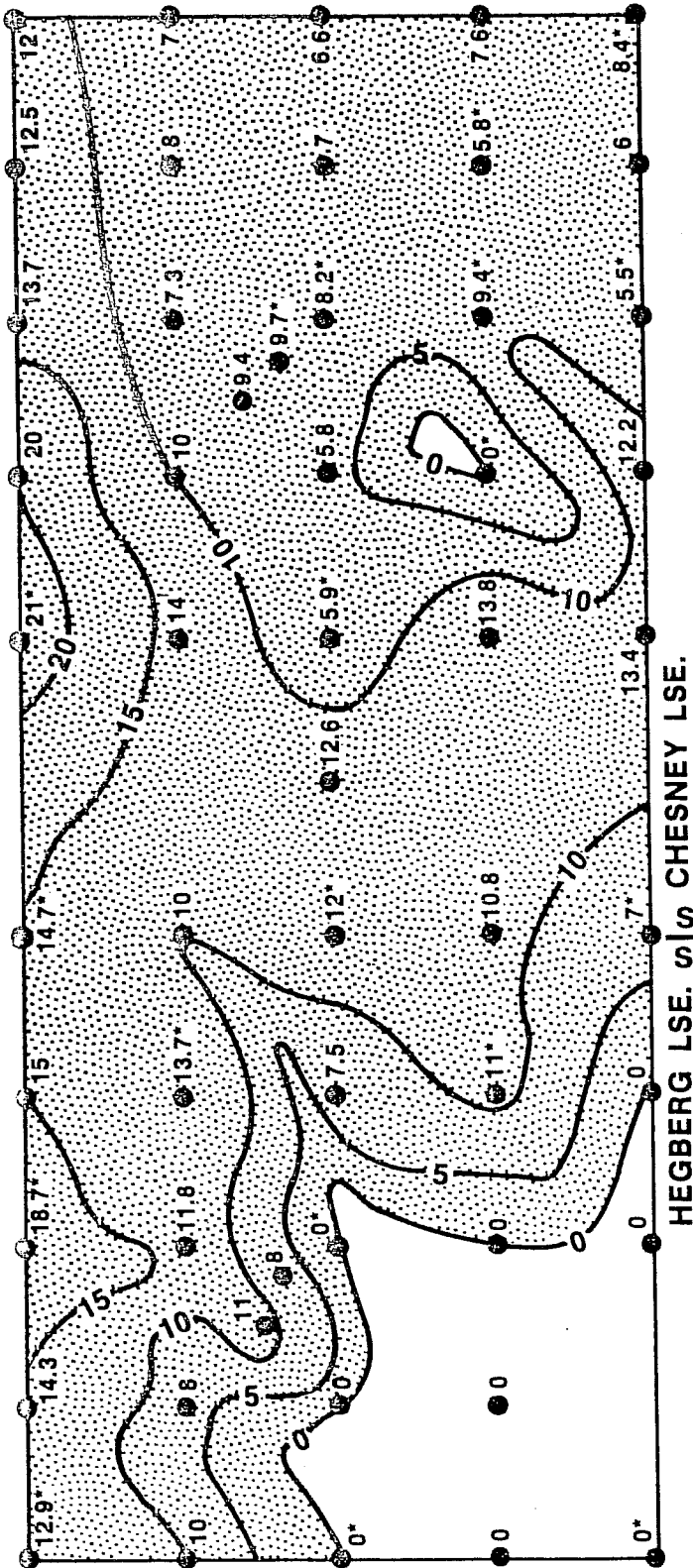
This facies is composed of interbedded gray shaly claystone, silty shale, and shale. Horizontally stratified to rippled interbeds of fossil hash are also present within this facies. The fossiliferous interbeds are composed of abraded fragments of marine organisms similar to the assemblage present within the protected bay biomicrite facies, and probably reflect deposition from storm generated currents. The claystone is described as massive, organic rich, burrowed, and probably

root mottled, with plant debris, pyrite and siderite nodules commonly present. These characteristics coupled with the absence of in situ carbonate-secreting fossils suggests a protected bay with a toxic substrate which received sporadic pulses of fossil debris from the nearly biomicrite facies sediments.

Open Marine Limestone Facies

The open marine limestone facies is composed of abraded pelecypod and echinoderm shell fragments within an argillaceous matrix. An open marine shelf dominated by wave action is postulated for this facies as indicated by the abundance of abraded fossil fragments.

ISOPACH MAP OF THE DISTRIBUTION CHANNEL
SANDSTONE FACIES (HIGH ENERGY)

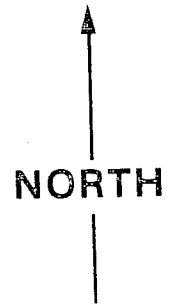
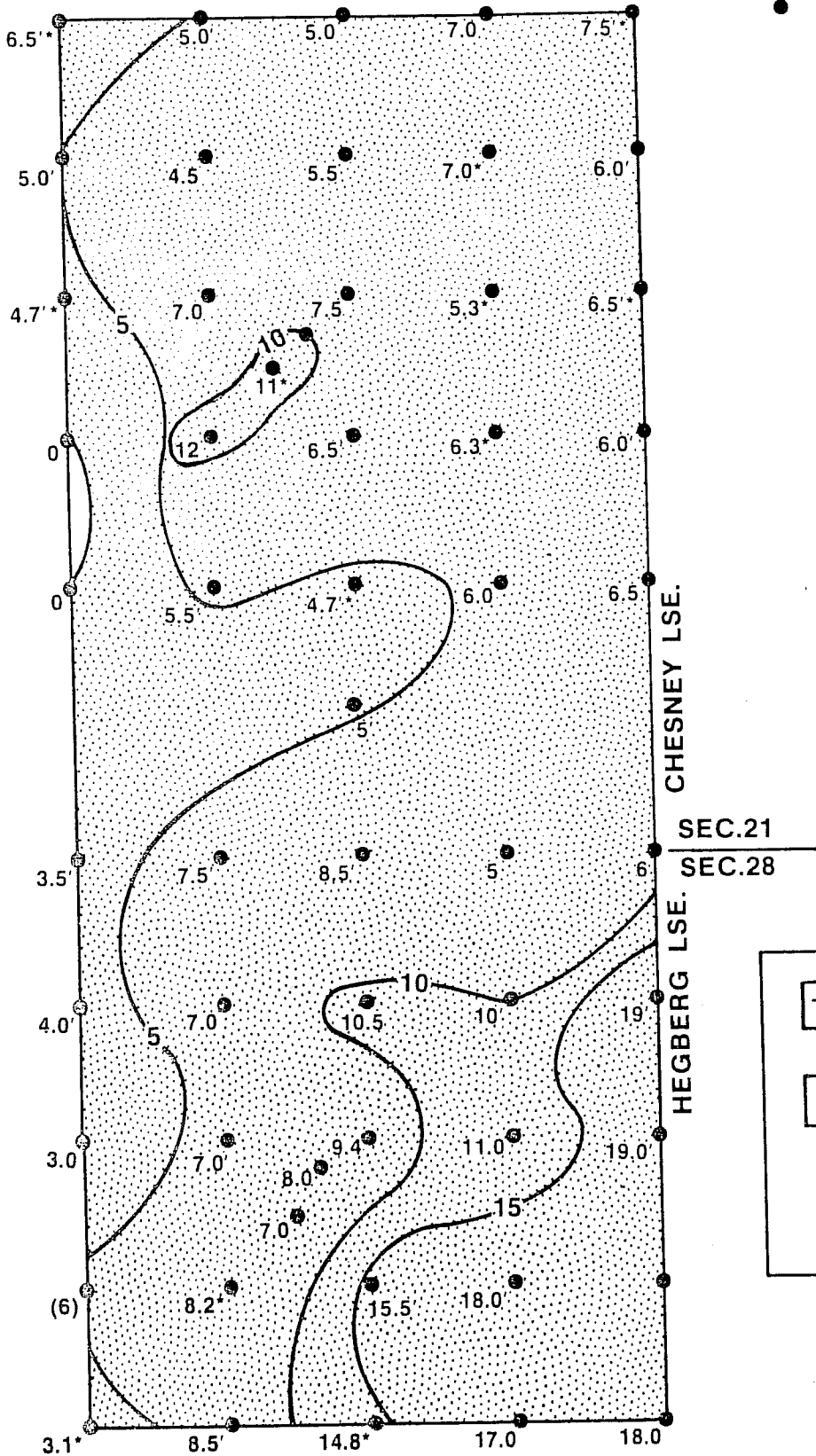


LEGEND

10*	THICKNESS BASED ON CORE DATA
10	THICKNESS BASED ON LOG DATA
CONTOUR INTERVAL : 5 ft.	
 264 ft. SCALE	

FIGURE A1

ISOPACH MAP OF THE DISTRIBUTARY CHANNEL
SANDSTONE FACIES (LOW ENERGY)



LEGEND

10*	THICKNESS BASED ON CORE DATA
10	THICKNESS BASED ON LOG DATA
CONTOUR INTERVAL: 5ft.	
 SCALE	